





This is to certify that the  
dissertation entitled

ANALYSIS OF THE SUBCHLOROPLASTIC DISTRIBUTION  
OF GENOMES UNCOUPLED 4 AND MAGNESIUM  
CHELATASE

presented by

NEIL D. ADHIKARI

has been accepted towards fulfillment  
of the requirements for the

Ph.D. degree in Genetics

A handwritten signature in black ink, appearing to read "Robert M. Lyle". The signature is written over a horizontal line.

Major Professor's Signature

6/30/2010

Date





**ANALYSIS OF THE SUBCHLOROPLASTIC DISTRIBUTION OF GENOMES  
UNCOUPLED 4 AND MAGNESIUM CHELATASE**

**By**

**Neil D. Adhikari**

**A DISSERTATION**

**Submitted to  
Michigan State University  
in partial fulfillment of the requirements  
for the degree of**

**DOCTOR OF PHILOSOPHY**

**Genetics**

**2010**

AN:

Chloropl

and man

contrib

Tight reg

of their p

species (l

oxygen. T

referred t

binding th

product. t

magnesi

chloroph

channel p

on chlor

we predic

chloropl

participa

magnesi

porphyrin

## ABSTRACT

### ANALYSIS OF THE SUBCHLOROPLASTIC DISTRIBUTION OF GENOMES UNCOUPLED 4 AND MAGNESIUM CHELATASE

By

Neil D. Adhikari

Chlorophyll is the primary light harvesting pigment for photosynthesis in higher plants and many other organisms that perform oxygenic photosynthesis. Twenty three enzymes contribute to chlorophyll metabolism at different stages of plant growth and development. Tight regulation of chlorophyll biosynthesis is important because chlorophylls and some of their precursors are strong photosensitizers that can produce toxic reactive oxygen species (ROS) if porphyrins that are exposed to bright light collide with molecular oxygen. The GENOMES UNCOUPLED 4 protein from *Arabidopsis thaliana* (hereafter referred to as GUN4) stimulates magnesium chelatase by a mechanism that involves binding the ChlH subunit of magnesium chelatase and its porphyrin substrate and product, the photosensitizing chlorophyll intermediates protoporphyrin IX and magnesium protoporphyrin IX, respectively. We hypothesized that GUN4 stimulates chlorophyll biosynthesis not only by activating magnesium chelatase but also by helping channel protoporphyrin IX into complexes of enzymes that drive chlorophyll biosynthesis on chloroplast membranes—the site of chlorophyll biosynthesis. From this hypothesis, we predicted that the porphyrin-bound form of GUN4 would more stably associate with chloroplast membranes by interacting with chloroplast membrane lipids or enzymes that participate in chlorophyll biosynthesis. Also, by binding protoporphyrin IX and magnesium protoporphyrin IX, GUN4 was previously hypothesized to shield these porphyrins from collisions with molecular oxygen thereby contributing to photooxidative

stress

conser

shown

stimula

acid sut

GUN4 ε

that allo

protoper

versions

previousl

in vivo. I

chloropla

Additional

inhibit the

transform

GUN4 ex

Based on

biosynthe

Mg-chelat

stress toler

significant

in vivo.

stress tolerance. To test these hypotheses, I used site-directed mutagenesis to change conserved amino acid residues of GUN4. These amino acid substitutions were previously shown to cause deficiencies in the porphyrin-binding activity and the Mg-chelatase-stimulatory activity of a *Synechocystis* relative of GUN4. I found that some of the amino acid substitutions that cause porphyrin-binding defects in the *Synechocystis* relative of GUN4 also cause porphyrin-binding defects in GUN4. I also developed a binding assay that allowed me to show for the first time that GUN4 binds its natural ligands—protoporphyrin IX and Mg-protoporphyrin IX. I used these porphyrin-binding deficient versions of GUN4 to test whether the porphyrin-binding activity of GUN4 that was previously demonstrated for cyanobacterial relatives of GUN4 in vitro is also significant in vivo. I found that porphyrins promote the association of GUN4 and ChlH with chloroplast membranes and induce Mg-chelatase activity on chloroplast membranes. Additionally, I found that defects in porphyrin binding and defects in ChlH function inhibit the association of GUN4 with chloroplast membranes. Finally, I found that stably transformed *Arabidopsis* plants that express porphyrin-binding-deficient versions of GUN4 exhibit higher expression levels of ROS-inducible genes compared to wild type. Based on these results, I conclude that GUN4 helps channel porphyrins into chlorophyll biosynthesis by binding porphyrins and ChlH on chloroplast membranes and stimulating Mg-chelatase activity. I further conclude that these activities contribute to photooxidative stress tolerance. These findings indicate that the porphyrin-binding activity of GUN4 significantly contributes to chlorophyll biosynthesis and photooxidative stress tolerance in vivo.

Berond

would e

project

highly

Erp. Hi

graduat

strong

## ACKNOWLEDGEMENTS

I would like to thank all my committee members, Drs. Gregg Howe, Jianping Hu, Beronda Montgomery, John Ohlrogge and Robert Larkin for their support and guidance. I would especially like to thank Dr. Larkin for letting me work on this very interesting project and providing excellent guidance.

I would like to thank Dr. John Froehlich and Robert Orlor for an excellent and highly productive collaboration during this entire project.

I would like to thank all my friends from Michigan State, especially Harrie van Erp, Hiroshi Maeda, Mike Ruckle and Hong Luo for their friendship and making graduate school life a fun and enjoyable experience.

Lastly, I would like to thank Kaori Ando and my family for their continued strong support along this journey, which made all the difference.

LIST

LIST

LIST

CHAP

CHAP

Mg-ch

CHAP

interac

CHAP

REFER

## TABLE OF CONTENTS

LIST OF TABLES.....	vi
LIST OF FIGURES.....	vii
LIST OF ABBREVIATIONS.....	x
CHAPTER 1: Introduction	
Tetrapyrrole biosynthesis in higher plants.....	1
Regulation of tetrapyrrole biosynthesis.....	18
Impact of chlorophyll metabolism on other cellular processes.....	27
<i>GENOMES UNCOUPLED 4</i> .....	30
CHAPTER 2: Porphyrins promote the association of <i>GENOMES UNCOUPLED 4</i> and a Mg-chelatase subunit with chloroplast membranes.	
Abstract.....	39
Introduction.....	40
Materials and methods.....	42
Results.....	52
Discussion.....	94
CHAPTER 3: The porphyrin-binding activity of GUN4 promotes GUN4-ChlH interactions and photooxidative stress tolerance in <i>Arabidopsis thaliana</i> .	
Abstract.....	106
Introduction.....	107
Materials and methods.....	111
Results.....	115
Discussion.....	139
CHAPTER 4: Conclusions and future perspectives.....	150
REFERENCES.....	156

7  
2

Table 2-

Table 2-2  
substituti

Table 2-3

Table 2-4  
indicated

Table 2-5  
chloroplas

Table 3-1

Table 3-2  
compated

Table 3-3  
following

## LIST OF TABLES

<b>Table 2-1.</b> Oligonucleotides used for site-directed mutagenesis.....	44
<b>Table 2-2.</b> Solubilities of GST-GUN4 $\Delta$ 1-69 containing the indicated amino acid substitutions when expressed in <i>E. coli</i> .....	68
<b>Table 2-3.</b> Quantitation of porphyrin binding by GUN4.....	70
<b>Table 2-4.</b> Quantitation of DPIX and Mg-DPIX binding by GUN4 containing the indicated amino acid substitutions.....	76
<b>Table 2-5.</b> Quantitation of Mg-chelatase activity in supernatants prepared from lysed chloroplasts.....	92
<b>Table 3-1.</b> SSLP and CAPS markers used for mapping <i>gun5-101</i> .....	113
<b>Table 3-2.</b> Percent decrease in the membrane association of ChlH in untreated samples compared to WT.....	130
<b>Table 3-3.</b> Percent increase in GUN4 protein in the membrane-containing pellet fraction following PPIX feeding.....	134

## LIST OF FIGURES

<b>Figure 1-1.</b> Tetrapyrrole biosynthesis pathway in higher plants.....	3
<b>Figure 2-1.</b> Distribution of GUN4, Tic40, and SS in fractionated chloroplasts.....	54
<b>Figure 2-2.</b> Subchloroplasmic distribution of PPIX, Mg-PPIX, and GUN4 after ALA feeding.....	56
<b>Figure 2-3.</b> Subchloroplasmic distribution of Tic40, SS, and total protein after ALA feeding.....	58
<b>Figure 2-4.</b> Analysis of GUN4-chloroplast membrane interactions in chloroplasts that were fed or not fed ALA.....	60
<b>Figure 2-5.</b> Subchloroplasmic distribution of GUN4 following post-import ALA feeding.....	62
<b>Figure 2-6.</b> Distribution of GUN4 in the chloroplast envelope, thylakoid, and stroma fractions after ALA feeding.....	64
<b>Figure 2-7.</b> Subchloroplasmic distribution of pea GUN4 and porphyrin levels after ALA feeding.....	65
<b>Figure 2-8.</b> Quantitative analysis of GUN4-binding DPIX and Mg-DPIX.....	71
<b>Figure 2-9.</b> Quantitative analysis of GUN4 binding PPIX, Mg-PPIX, and Mg-PPIX ME.....	73
<b>Figure 2-10.</b> Quantitative analysis of GUN4 binding uroporphyrin III, coproporphyrin III, heme, and pheophorbide <i>a</i> .....	74
<b>Figure 2-11.</b> Quantitative analysis of V123A, F191A, and R211A binding DPIX and Mg-DPIX.....	77
<b>Figure 2-12.</b> Subchloroplasmic distribution of porphyrin-binding-deficient GUN4 after ALA feeding.....	80
<b>Figure 2-13.</b> Mg-chelatase activity associated with chloroplast membranes after ALA feeding.....	81
<b>Figure 2-14.</b> Characterization of affinity-purified anti-ChlH $\Delta$ 1-823 antibodies.....	83
<b>Figure 2-15.</b> Subchloroplasmic distribution of pea ChlH after ALA feeding.....	85

7  
7  
Figure  
type a

Figure  
Subbel

Figure  
type c

Figure  
Mg-c

Figure  
porp

Figure

Figure  
trans

Figure  
diff

Figure

Figure  
shift

Figure

Figure  
850

Figure  
puri

Figure  
from

Figure  
deriv

Figure  
puri

<b>Figure 2-16.</b> Characterization of affinity-purified anti-ChlI $\Delta$ 1-60 antibodies. <i>A</i> , Wild type and <i>cs</i> mutants.....	86
<b>Figure 2-17.</b> Subchloroplastic distribution of ChlI and ChlD after ALA feeding. <i>A</i> , Subchloroplastic distribution of ChlI after ALA feeding.....	88
<b>Figure 2-18.</b> Characterization of affinity-purified anti-ChlD $\Delta$ 1-516 antibodies. <i>A</i> , Wild-type and <i>chlD</i> mutants.....	89
<b>Figure 2-19.</b> Solubility of pea GUN4 and pea ChlH in chloroplast-membrane-depleted Mg-chelatase assays.....	93
<b>Figure 2-20.</b> Subchloroplastic distribution of GUN4 after feeding with ALA or various porphyrins.....	95
<b>Figure 2-21.</b> Analysis of leaf senescence in <i>gun4-1</i> .....	102
<b>Figure 3-1.</b> Analysis of stably transformed Arabidopsis plants containing <i>GUN4</i> -related transgenes.....	117
<b>Figure 3-2.</b> Analysis of chlorophyll levels in <i>gun4</i> and <i>chlH/gun5</i> mutants grown under different fluence rates.....	119
<b>Figure 3-3.</b> Images of seedlings grown in $100 \mu\text{mol m}^{-2} \text{s}^{-1}$ white for 7d.....	120
<b>Figure 3-4.</b> Images of seedlings grown in $100 \mu\text{mol m}^{-2} \text{s}^{-1}$ white light for 4d and then shifted to $850 \mu\text{mol m}^{-2} \text{s}^{-1}$ white light for 3d.....	121
<b>Figure 3-5.</b> Positional cloning and sequence analysis of <i>gun5-101</i> .....	123
<b>Figure 3-6.</b> Analysis of GUN4 and Mg-chelatase subunit levels in $100 \mu\text{mol m}^{-2} \text{s}^{-1}$ and $850 \mu\text{mol m}^{-2} \text{s}^{-1}$ white light.....	124
<b>Figure 3-7.</b> Distribution of GUN4 in lysed and fractionated chloroplasts that were purified from <i>gun4</i> and <i>chlH/gun5</i> mutants and were either fed or not fed with PPIX...	126
<b>Figure 3-8.</b> Statistical analysis of GUN4 in membrane-containing pellet fractions derived from purified and fractionated chloroplasts.....	127
<b>Figure 3-9.</b> Distribution of GUN4 in soluble and membrane-containing pellet fractions derived from wild type, <i>gun5</i> , and <i>cs</i> chloroplasts.....	129
<b>Figure 3-10.</b> Distribution of ChlH/GUN5 in lysed and fractionated chloroplasts that were purified from <i>gun4</i> and <i>chlH/gun5</i> mutants and were either fed or not fed with PPIX...	133

15  
7  
2

Figure 3-11.  
 $\mu\text{mol m}^{-2} \text{s}^{-1}$

Figure 3-12.  
shift.....

Figure 3-13.  
light.....

<b>Figure 3-11.</b> Analysis of chlorophyll levels in <i>gun4</i> and <i>chlH/gun5</i> mutants grown in 10 $\mu\text{mol m}^{-2} \text{s}^{-1}$ white light.....	136
<b>Figure 3-12.</b> Induction of <i>WRKY40</i> and <i>ZAT10</i> expression during a fluence-rate shift.....	138
<b>Figure 3-13.</b> Analysis of <i>WRKY40</i> and <i>ZAT10</i> expression in diurnal and continuous light.....	140

GUN4

ROS

ALA

PPIX

Mg-PPIX

Mg-PPIX-

POR

RCC

PAO

CAO

$^1O_2$

$H_2O_2$

$OH^{\cdot}$

$O_2^{\cdot-}$

Lhcb

## LIST OF ABBREVIATIONS

GUN4	Genomes Uncoupled 4
ROS	Reactive Oxygen Species
ALA	5-aminolevulinic acid
PPIX	Protoporphyrin IX
Mg-PPIX	Magnesium protoporphyrin IX
Mg-PPIX-ME	Magnesium protoporphyrin IX monomethyl ester
POR	Protochlorophyllide oxidoreductase
RCC	Red chlorophyll catabolite
PAO	Pheophorbide <i>a</i> oxygenase
CAO	Chlorophyllide <i>a</i> oxygenase
$^1\text{O}_2$	Singlet oxygen
$\text{H}_2\text{O}_2$	Hydrogen peroxide
$\text{OH}^\bullet$	Hydroxyl radical
$\text{O}_2^{\bullet-}$	Superoxide
Lhcb	Light harvesting chlorophyll a/b binding protein



joined p  
compou  
develop  
biosynth  
chloroph  
bacteria.  
which are  
contribute  
NADPH c  
cofactor in  
of inorgan  
for photosy  
of photorec  
synthesizin  
simultaneou  
synthesize f  
chlorophylls  
All te  
acid (ALA).

CHAPTER 1  
INTRODUCTION

**TETRAPYRROLE BIOSYNTHESIS IN HIGHER PLANTS**

Chlorophylls are tetrapyrroles; tetrapyrroles are compounds consisting of four joined pyrrole rings which can either be linear or cyclic. Tetrapyrroles are essential compounds for all organisms and perform many functions during growth and development. They form a large and diverse family of molecules that are biosynthetically related. Examples of tetrapyrroles found in nature include heme, chlorophyll, bilins, phycobilins, siroheme, vitamin B<sub>12</sub>, and factor F<sub>430</sub> of methanogenic bacteria. These molecules serve as the prosthetic groups in many proteins, most of which are essential. For example, heme is the prosthetic group in proteins that contribute to respiration (cytochrome), oxygen metabolism (catalase, peroxidase and NADPH oxidase) and oxygen binding (leghemoglobin). Siroheme is an important cofactor in enzymes such as nitrite and sulfite reductases, which function in assimilation of inorganic nitrogen and sulphur. Chlorophylls are the major light harvesting pigments for photosynthesis. Phytychromobilin is the chromophore for phytychromes—a family of photoreceptors that perceive red and far-red light. No organism is capable of synthesizing all tetrapyrroles, but many synthesize two or more major products either simultaneously or at different stages in development (Beale, 1999). Plants can synthesize four classes of tetrapyrroles: siroheme, hemes, phytychromobilin, and chlorophylls.

All tetrapyrroles are synthesized from a common precursor,  $\delta$ -aminolevulinic acid (ALA). ALA can be synthesized by two different pathways. ALA synthase



catalyzes

eukaryote

(Gibson et

alpha-prote

utilizes glu

Castelfranc

glutamate, g

tRNA (Kann

by glutamyl

semialdehyd

glutamate 1-s

1978: Hoobe

Steps conserv

Three enz

molecule of u

1999). First, A

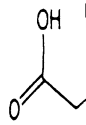
molecules of

porphobilinog

catalyzes ALA biosynthesis in organisms belonging to the alpha-proteobacteria and all eukaryotes that lack chloroplasts by condensing glycine and succinyl-coenzyme A (Gibson et al., 1958; Kikuchi et al., 1958). Plants, algae and all bacteria besides the alpha-proteobacterial group, utilize an entirely distinct ALA biosynthetic pathway that utilizes glutamate rather than glycine and succinyl-coenzyme A (Beale and Castelfranco, 1974; Beale et al., 1975; Meller et al., 1975). To synthesize ALA from glutamate, glutamyl tRNA synthetase activates glutamate by ligating it to glutamyl tRNA (Kannangara et al., 1984). The glutamyl tRNA is committed to ALA biosynthesis by glutamyl tRNA reductase, which converts the glutamyl tRNA to glutamate 1-semialdehyde (GSA) (Pontoppidan and Kannangara, 1994). GSA is transaminated by glutamate 1-semialdehyde aminotransferase yielding ALA (Kannangara and Gough, 1978; Hooper et al., 1988) (Figure 1-1).

#### Steps conserved in biosynthesis of all tetrapyrroles (the 'common pathway')

Three enzymes perform the sequential conversion of eight ALA molecules into one molecule of uroporphyrinogen III—the first closed macrocyclic tetrapyrrole (Beale, 1999). First, ALA dehydratase performs an asymmetric condensation that converts two molecules of ALA into porphobilinogen (Jordan and Sehra, 1980). Next, porphobilinogen deaminase polymerizes four molecules of porphobilinogen yielding



Glucose

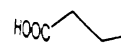


Figure 1-1.  
Numbers in  
synthetase.  
aminotransf  
Uroporphor  
(7c) Sirohe  
Coproporph  
chelataze. (1  
Mg-prorop  
oxidoreduct  
(15b) Chlor  
reductase. (1  
substance. (1  
catabolite re

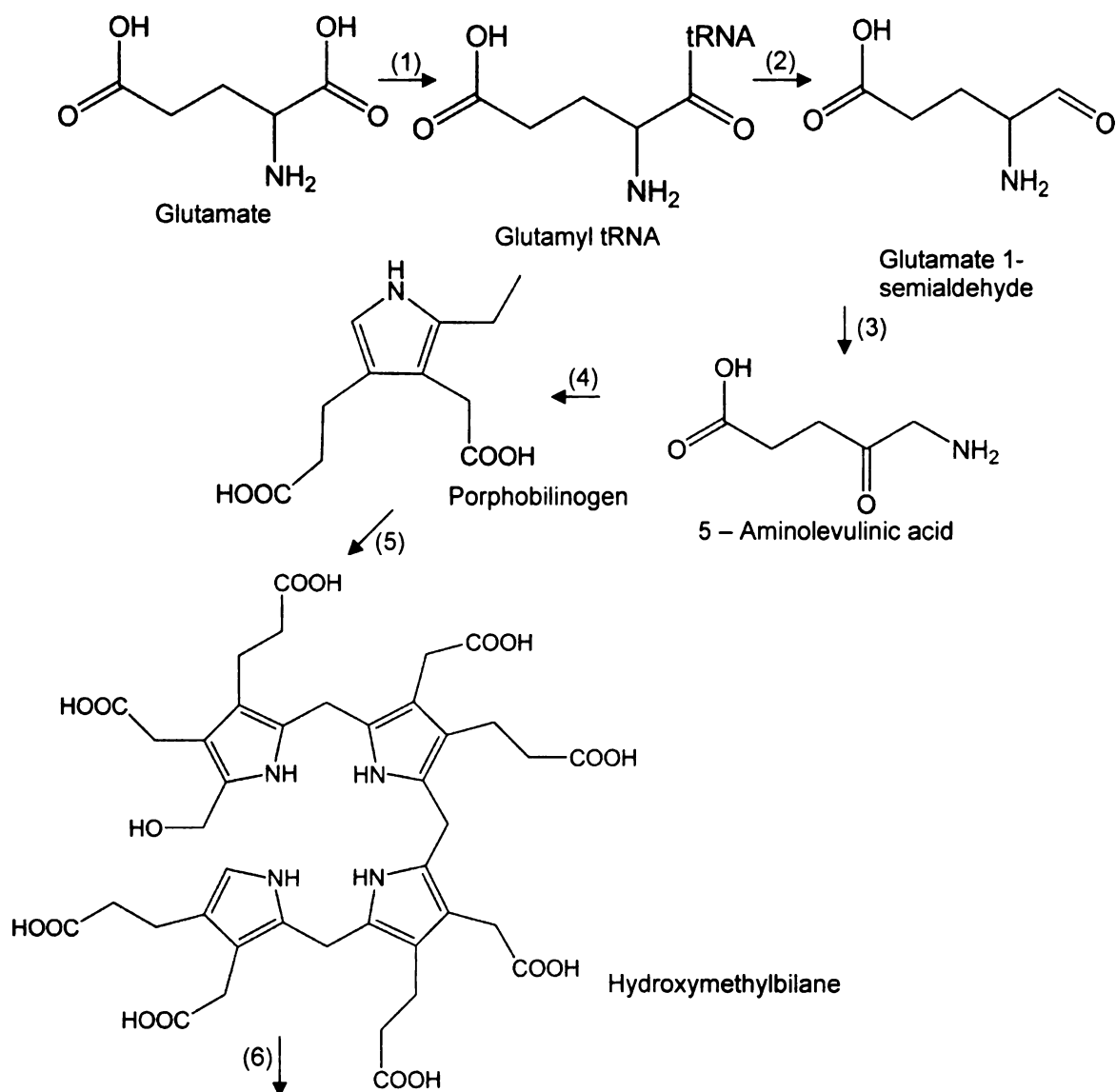


Figure 1-1. Tetrapyrrole biosynthesis pathway in higher plants.

Numbers indicate enzymes that catalyze each reaction as follows: (1) Glutamyl t-RNA synthetase, (2) Glutamyl t-RNA reductase, (3) Glutamate 1-semialdehyde aminotransferase, (4) ALA dehydratase, (5) Porphobilinogen deaminase, (6) Uroporphyrinogen III synthase, (7a) Uroporphyrinogen III methylase, (7b) Oxidase, (7c) Siroheme ferrochelatase, (7d) Uroporphyrinogen III decarboxylase, (8) Coproporphyrinogen III decarboxylase, (9) Protoporphyrinogen IX oxidase, (10a) Mg-chelatase, (10b) Ferrochelatase, (11) Mg-protoporphyrin IX methyltransferase, (12) Mg-protoporphyrin IX monomethylester oxidative cyclase, (13) Protochlorophyllide oxidoreductase, (14) Divinyl chlorophyllide reductase, (15a) Chlorophyll synthase, (15b) Chlorophyllase, (16) Hydroxymethyl chlorophyllide *a*, (17) Chlorophyll *b* reductase, (18) 7-Hydroxymethyl chlorophyll *a* reductase, (19) Mg-dechelating substance, (20) Pheophytinase, (21) Pheophorbide *a* oxygenase, (22) Red chlorophyll catabolite reductase.



H<sub>3</sub>

H<sub>2</sub>

Fig

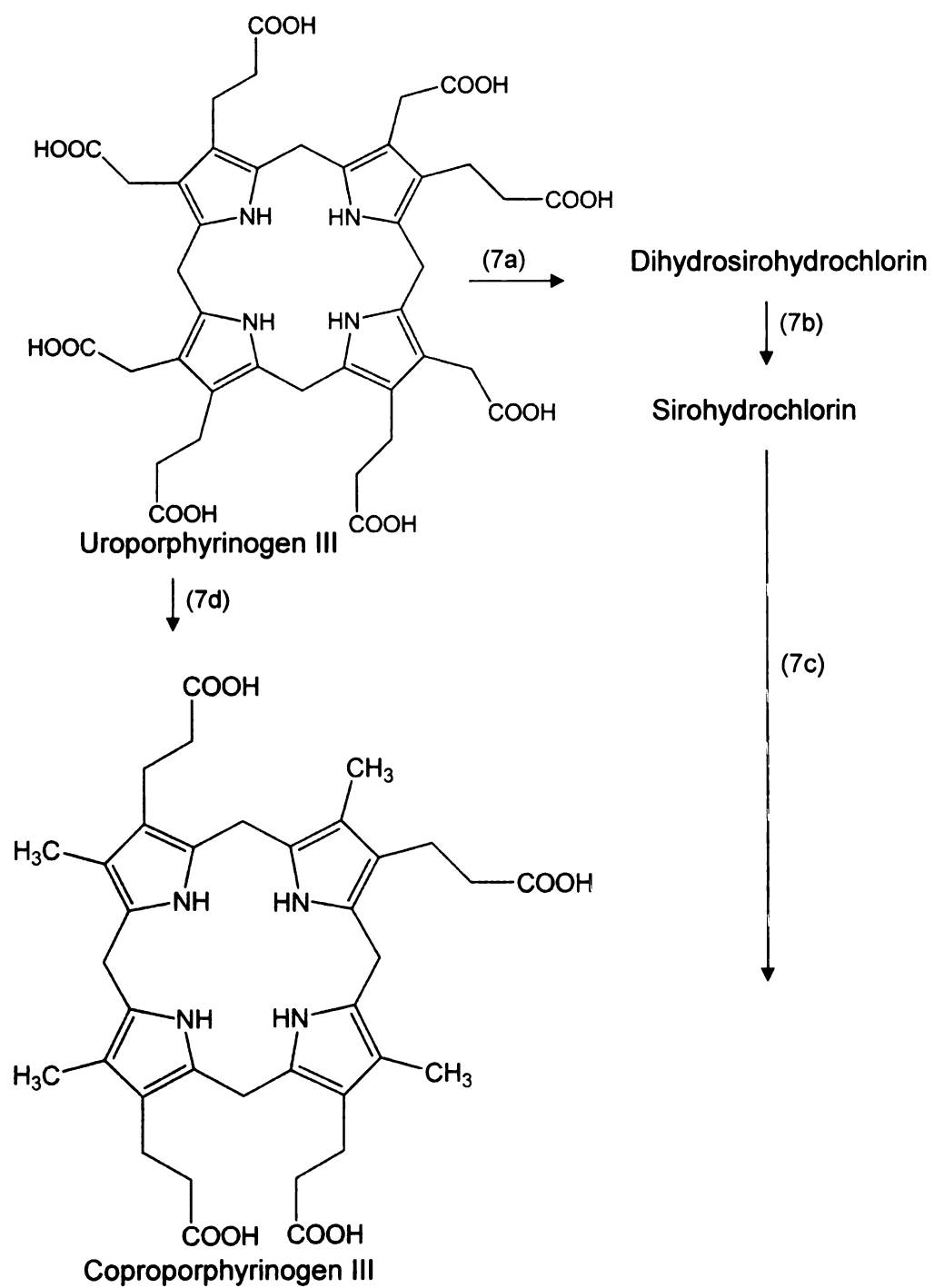


Figure 1-1 Tetrapyrrole biosynthesis pathway in higher plants (continued).

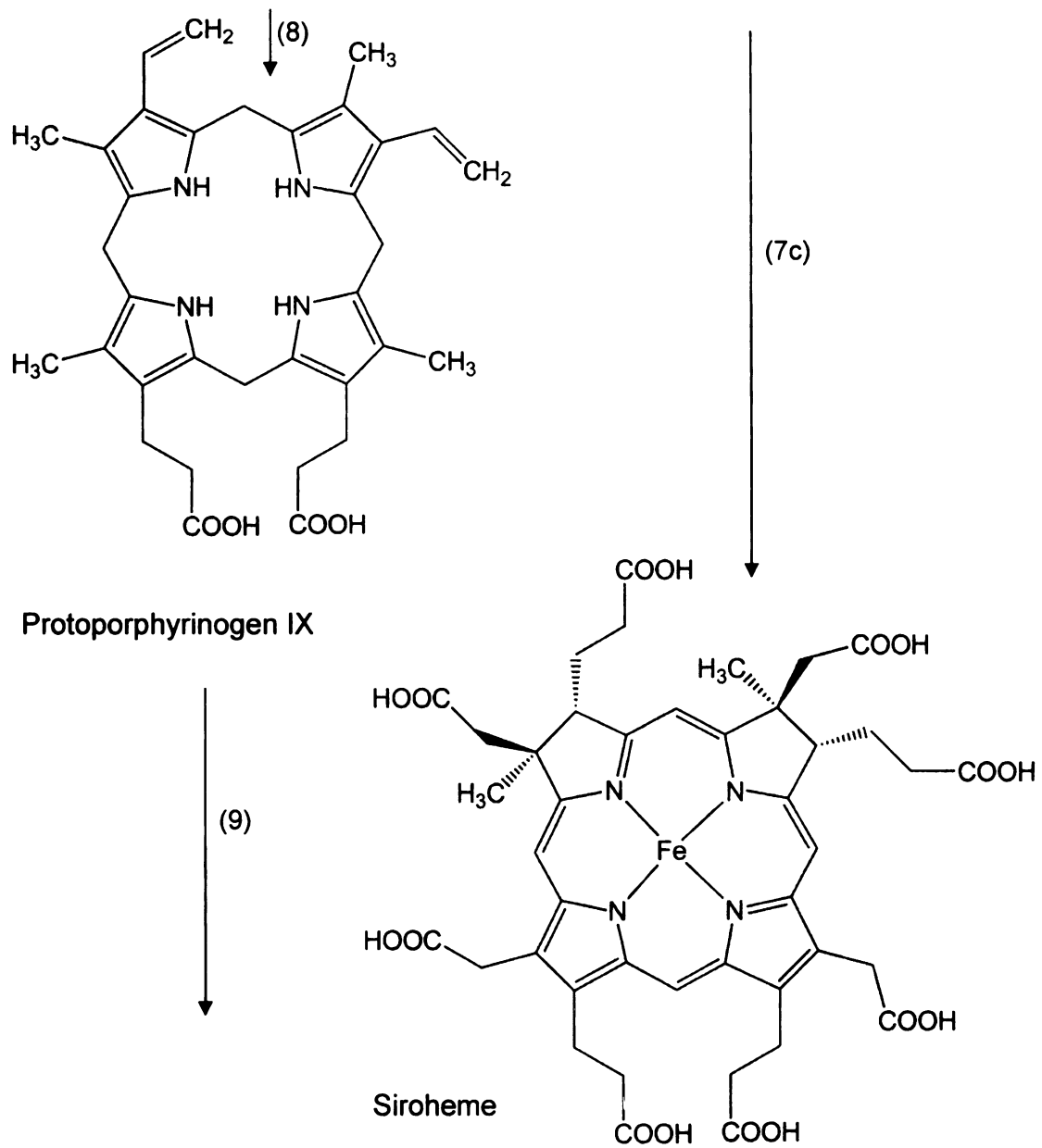


Figure 1-1 Tetrapyrrole biosynthesis pathway in higher plants (continued).

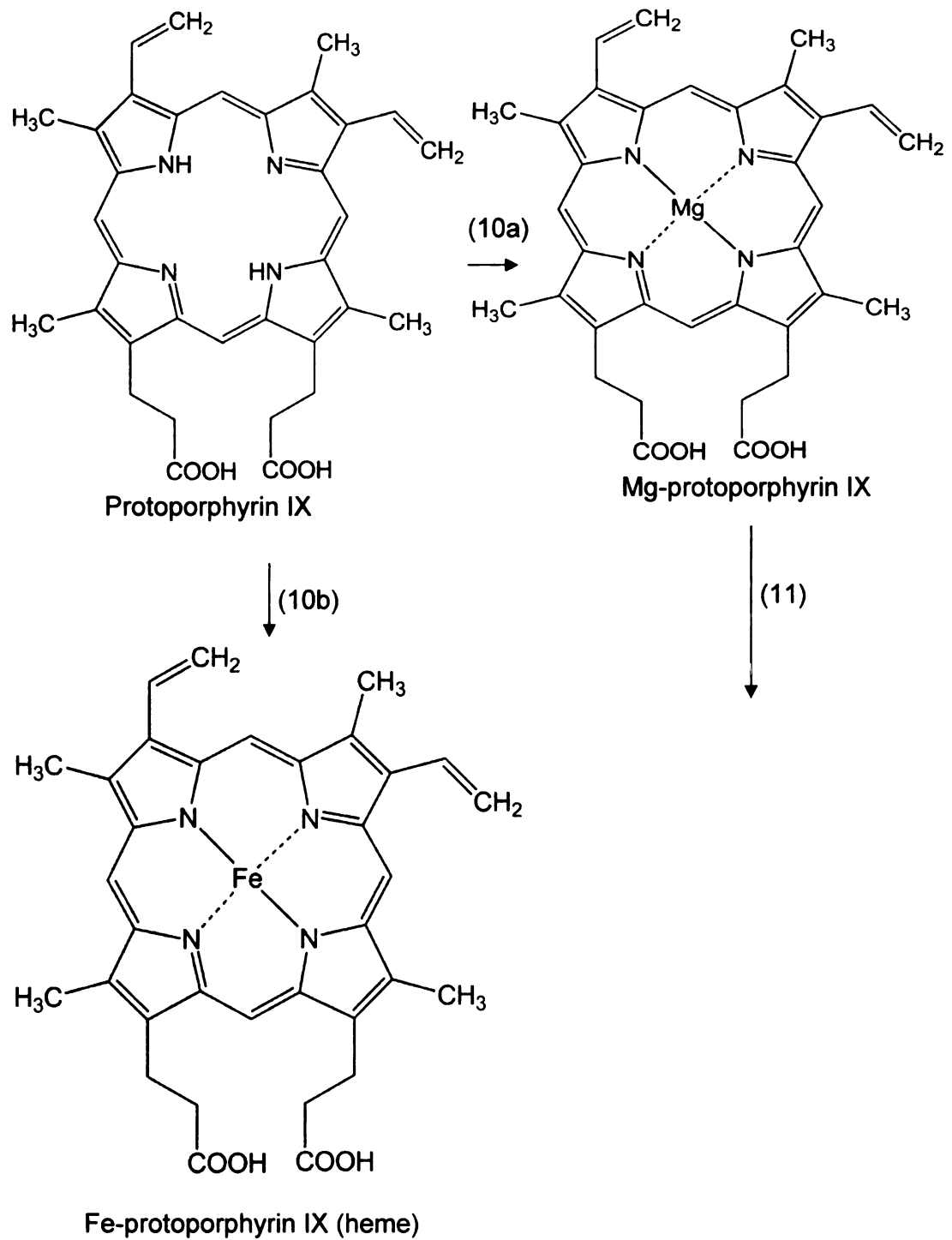


Figure 1-1 Tetrapyrrole biosynthesis pathway in higher plants (continued).

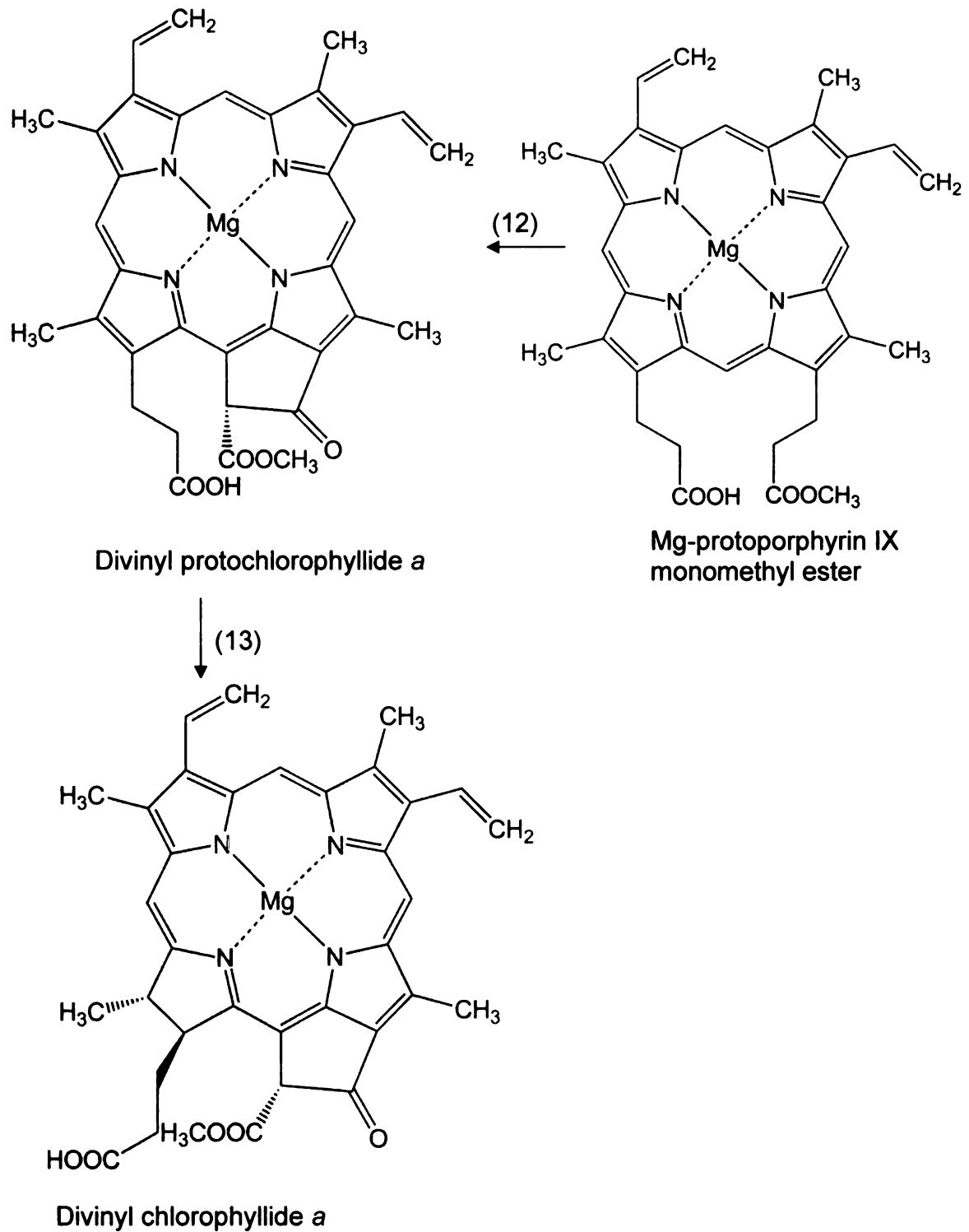


Figure 1-1 Tetrapyrrole biosynthesis pathway in higher plants (continued).

THE  
7  
201



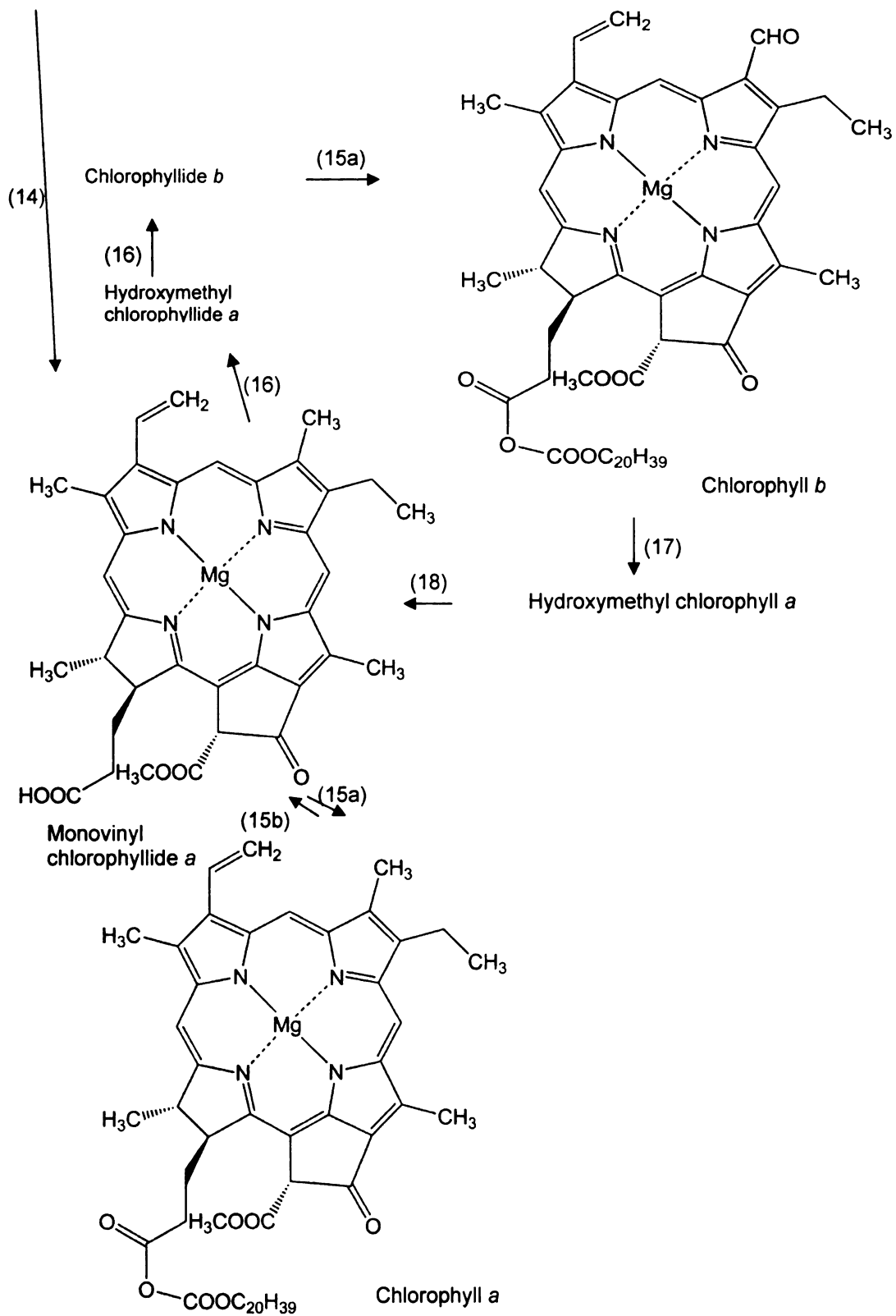


Figure 1-1 Tetrapyrrole biosynthesis pathway in higher plants (continued).

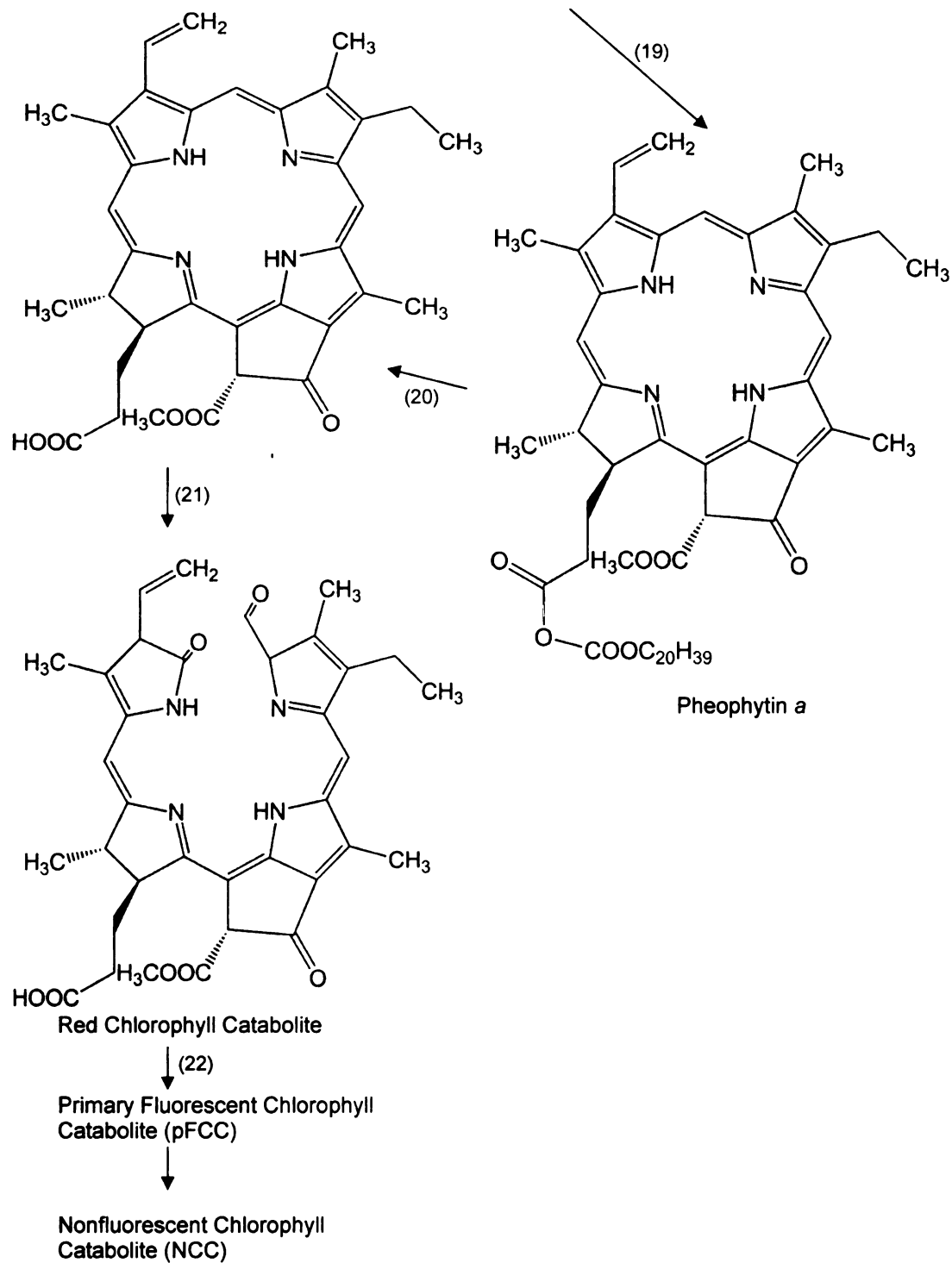


Figure 1-1 Tetrapyrrole biosynthesis pathway in higher plants (continued).

hydroxymethylbilane, the first linear tetrapyrrole. Free hydroxymethylbilane rapidly undergoes a spontaneous and irreversible cyclization that yields uroporphyrinogen I, a biologically non-relevant product (Battersby et al., 1979). Uroporphyrinogen III synthase, directs the conversion of hydroxymethylbilane to the correct isomer—uroporphyrinogen III—either during or immediately after the formation of hydromethylbilane (Hart and Battersby, 1985; Tsai et al., 1987).

Uroporphyrinogen III is a branch-point substrate that can serve as a precursor for either siroheme or protoporphyrin IX. For the biosynthesis of siroheme, uroporphyrinogen III methylase converts uroporphyrinogen III to dihydrosirohydrochlorin (Leustek et al., 1997), which is then converted to sirohydrochlorin by an oxidase; the gene that encodes this oxidase has not yet been identified (Tanaka and Tanaka, 2007). Siroheme ferrochelatase then inserts  $\text{Fe}^{2+}$  into the porphyrin ring of sirohydrochlorin yielding siroheme (Raux-Deery et al., 2005).

For the biosynthesis of protoporphyrin IX, uroporphyrinogen III decarboxylase catalyzes the stepwise decarboxylation of uroporphyrinogen III yielding coproporphyrinogen III (Luo and Lim, 1993). Coproporphyrinogen III oxidative decarboxylase catalyzes the oxidative decarboxylation of two of the four propionate residues on rings A and B of coproporphyrinogen III, yielding protoporphyrinogen IX (Cavaleiro et al., 1974), which is then converted to protoporphyrin IX by protoporphyrinogen IX oxidase (Klemm and Barton, 1987).

Uroporphyrinogen III is hydrophilic, exhibits a low affinity for metals, and is photochemically unreactive. By contrast, protoporphyrin IX is hydrophobic, exhibits a much higher affinity for metals than uroporphyrin III, and is photochemically reactive.

THE  
7  
201

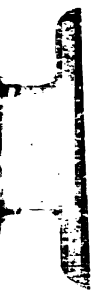


In fact, diphenyl ether herbicides cause lethal photooxidative stress by causing the buildup of protoporphyrin IX (Witkowski and Halling, 1988, 1989). Additionally, Arabidopsis mutants that exhibit misregulated porphyrin metabolism suffer from potentially lethal photooxidative damage (Kim et al., 2008). Thus, porphyrins are thought to be synthesized from porphyrinogens at the last possible moment to guard against photooxidative stress (Beale, 1999). The photosensitizing effects of porphyrins are not limited to plants. In humans, porphyric diseases cause severe blistering of the skin on exposure to light (Kauppinen, 2005; Puy et al., 2010).

### Chlorophyll biosynthesis

In plants, protoporphyrin IX is a branch-point substrate that can be utilized for the biosynthesis of either hemes or chlorophylls (Figure 1-1). Ferrochelatase inserts  $\text{Fe}^{2+}$  into protoporphyrin IX yielding heme; Mg-chelatase commits protoporphyrin IX to chlorophyll biosynthesis by inserting  $\text{Mg}^{2+}$  into protoporphyrin IX, yielding Mg-protoporphyrin IX. Mg-chelatase is an ATP-dependent enzyme that contains three subunits, ChlH, ChlI and ChlD (Willows, 2003). In contrast, ferrochelatase consists of a single subunit and does not require ATP (Loeb, 1995). The difference in ATP requirements between ferrochelatase and Mg-chelatase are thought to be related to the distinct energy requirements for inserting  $\text{Mg}^{2+}$  and  $\text{Fe}^{2+}$  into protoporphyrin IX. Inserting  $\text{Mg}^{2+}$  into protoporphyrin IX requires more energy than inserting  $\text{Fe}^{2+}$  because removal of water molecules coordinated to  $\text{Mg}^{2+}$  is an energy-intensive process (Fleischer et al., 1964; Hambright, 1975).

THE  
7  
201



Mg-protoporphyrin IX methyltransferase methylates the carboxyl group of the ring C propionate side chain of Mg-protoporphyrin IX, yielding the next intermediate, Mg-protoporphyrin IX monomethyl ester (Yee et al., 1989; Block et al., 2002). Next, the Magnesium protoporphyrin IX monomethyl ester oxidative cyclase catalyzes an oxygen-dependent reaction that yields divinyl protochlorophyllide by synthesizing a fifth ring to magnesium protoporphyrin IX monomethyl ester. This oxidative cyclase is a multisubunit enzyme that contains a non-heme iron (Bollivar and Beale, 1996).

Protochlorophyllide oxidoreductase (POR) reduces ring D of divinyl protochlorophyllide, yielding divinyl chlorophyllide. POR is a light-dependent enzyme in angiosperms. In contrast, cyanobacteria and algae encode a light-independent POR that shares no sequence similarity with POR. Gymnosperms have both light-dependent as well as light-independent PORs (Masuda et al., 2003; Bollivar, 2006).

The vinyl group on ring B of divinyl chlorophyllide is reduced by divinyl chlorophyllide reductase yielding monovinyl chlorophyllide *a* (Nagata et al., 2005; Nakanishi et al., 2005). In the final step of chlorophyll *a* biosynthesis, chlorophyll synthase esterifies monovinyl chlorophyllide *a* with phytol-pyrophosphate, yielding chlorophyll *a*.

#### The chlorophyll cycle

A portion of chlorophyll *a* pool is converted to chlorophyll *b* by the action of chlorophyllide *a* oxygenase. The phytol group from chlorophyll *a* is assumed to be removed by chlorophyllase, which then provides monovinyl chlorophyllide *a* as a substrate for chlorophyllide *a* oxygenase (Figure 1-1). Chlorophyll *a* oxygenase then

converts monovinyl chlorophyllide *a* to chlorophyllide *b* in a two-step reaction (Oster et al., 2000). Chlorophyllide *b* is then phytylated by chlorophyll synthase yielding chlorophyll *b* (Oster et al., 2000; Eggink et al., 2004). Thus, plants can increase the chlorophyll *b* pool without de novo synthesis of chlorophyllide *a*—for example, in the dark. Chlorophyll *b* is reversibly inter-converted to chlorophyll *a* via the intermediate 7-hydroxymethyl chlorophyll *a* by the enzymes chlorophyll *b* reductase (Horie et al., 2009; Sato et al., 2009) and 7-hydroxymethyl chlorophyll *a* reductase, respectively (Scheumann et al., 1996; Nagane et al., 2010). Plants use the chlorophyll cycle to adjust the stoichiometry of chlorophyll *a* and *b* for optimal light harvesting in various light environments. In addition, conversion of chlorophyll *b* to *a* is an important first step in the chlorophyll degradation pathway (Tanaka and Tanaka, 2007).

### Biosynthesis of hemes

Protoporphyrin IX is converted to heme by ferrochelatase. There are several biologically important hemes that are distinguished by modifications of protoheme (also referred to as heme or heme *b*). Following heme *b*, heme *a* and heme *c* are the most commonly observed forms of heme (Severance and Hamza, 2009). Heme *a* is synthesized by the substitution of a vinyl side chain with a 17-carbon isoprenoid side chain and the oxidation of a methyl side chain to a formyl group. Heme *c* belongs to the C-type hemoproteins such as cytochrome *c* in which the two vinyl side chains of heme *b* are covalently attached to the protein (Severance and Hamza, 2009). Heme oxygenase catalyzes the oxidation and ring opening of heme, resulting in the formation of the linear tetrapyrrole biliverdin IX $\alpha$ . Phytychromobilin synthase then converts this product

to the 3(*Z*) isomer of phytochromobilin (Terry et al., 1995; Kohchi et al., 2001). An isomerase, the molecular identity of which is still unclear, is implicated in the conversion of 3(*Z*) phytochromobilin to 3(*E*)-phytochromobilin, which assembles with the apophytochrome in the cytoplasm to form phytochrome (Terry et al., 1993).

#### Localization of tetrapyrrole biosynthesis

In metazoans, ALA is synthesized in the mitochondria and is then transported to the cytosol. Coproporphyrinogen III is synthesized from ALA in the cytosol. Coproporphyrinogen III is transported into the mitochondria by an unknown mechanism, and converted to heme (Severance and Hamza, 2009). In plants, tetrapyrrole biosynthesis is thought to take place exclusively in the plastids, although there have been conflicting reports about the localization of the heme branch. Some studies indicate that heme biosynthesis occurs solely in the plastids (Masuda et al., 2003) while others report partial heme biosynthesis takes place in the mitochondria (Jacobs and Jacobs, 1987; Cornah et al., 2002). Recent analyses of the mitochondrial proteome failed to detect either of the two isoforms of ferrochelatase in *Arabidopsis* and rice (Heazlewood et al., 2004; Huang et al., 2009), thus favoring the model of exclusive chloroplast-localization of tetrapyrrole biosynthesis in higher plants. Phytochromobilin synthesis takes place entirely in the plastids as well (Kohchi et al., 2001), but the phytochrome apoproteins bind the phytochromobilin in the cytosol, yielding the functional photoreceptor (Terry et al., 2002).

Within the plastids, biosynthesis of the hydrophilic precursors from glutamate to protoporphyrinogen IX takes place in the stroma. Biosynthesis of the hydrophobic

THE  
7  
201



tetrapyrroles protoporphyrin IX (Watanabe et al., 2001), heme (Suzuki et al., 2002), Mg-protoporphyrin IX (Fuesler et al., 1984; Nakayama et al., 1998), Mg-protoporphyrin IX monomethyl ester (Block et al., 2002), protochlorophyllide (Tottey et al., 2003), chlorophyllide (Barthelemy et al., 2000; Masuda et al., 2003) and chlorophyll (Eggink et al., 2004) is localized to the thylakoid and envelope membranes. Nonetheless, chlorophyll only accumulates in the thylakoid and not in the envelope membranes. The rationale for chlorophyll biosynthesis occurring in the both the thylakoid and envelope membranes is a matter of speculation. One hypothesis is that chlorophyll biosynthesis in the envelope facilitates the formation of pigment protein complexes as chlorophyll precursor- and chlorophyll-binding proteins are imported into the chloroplast (Reinbothe et al., 1995; Tottey et al., 2003; Kim et al., 2005). Another possibility is that the chlorophyll metabolism in the envelope could act as plastid-derived signals (Rodermeil and Park, 2003; Nott et al., 2006; Ankele et al., 2007; Koussevitzky et al., 2007).

### Degradation of chlorophyll

The long standing model for chlorophyll degradation is that the first step in the degradation of chlorophyll is the conversion of chlorophyll *b* to chlorophyll *a* (Eckhardt et al., 2004; Hortensteiner, 2006; Tanaka and Tanaka, 2007). The next step is removal of the phytol chain from chlorophyll *a* by chlorophyllase to yield chlorophyllide *a* (Jacob-Wilk et al., 1999; Tsuchiya et al., 1999; Hortensteiner, 2006), followed by the release of the Mg<sup>2+</sup> atom that is catalyzed by a low molecular weight magnesium dechelating substance (MCS). The molecular identity of MCS remains unknown, and



the exact mechanism of demetallation remains unclear (Suzuki et al., 2002; Pruzinska et al., 2003; Suzuki et al., 2005; Suzuki et al., 2005). Demetallation yields pheophorbide *a* from chlorophyllide *a*.

The recent discovery of a novel, plastid-localized pheophytinase encoded by the *PPH* gene indicates that the pathway of chlorophyll degradation to pheophorbide *a* is complex (Schelbert et al., 2009). Chlorophyll *a* can lose its  $Mg^{2+}$  yielding pheophytin *a*. In vitro, pheophytinase specifically dephytylates pheophytin *a* yielding pheophorbide *a*. *pph-1*, a knockout mutant, exhibits a stay-green phenotype and accumulates pheophytin *a* when senescence is induced by prolonged incubations of leaves in the dark—indicating a block in chlorophyll degradation. Based on these findings, PPH has been proposed to be an important component of the chlorophyll degradation pathway. Based on the observation that chlorophyll degradation can proceed at similar rates in wild type *Arabidopsis* and an *Arabidopsis* double knockout mutant that lacks both isoforms of chlorophyllase, chlorophyllase is no longer considered to be essential for the degradation of chlorophyll (Schenk et al., 2007). In the most recent model for the degradation of chlorophyll, removal of the  $Mg^{2+}$  atom from chlorophyll *a* by MCS yielding pheophytin *a* is most likely the first step. Next, pheophytinase dephytylates pheophytin *a* yielding pheophorbide *a*. The fact that chlorophyllide is most likely not an intermediate of chlorophyll breakdown suggests that chlorophyll synthesis and breakdown are metabolically separated during leaf senescence, contrary to what was previously believed (Schelbert et al., 2009).

Pheophorbide *a* oxygenase (PAO) catalyzes another key step in chlorophyll degradation by opening the porphyrin macrocycle of pheophorbide *a* yielding the red

chlorophyll catabolite (RCC) (Hortensteiner, 1998; Pruzinská, 2003). RCC is subsequently reduced to primary fluorescent chlorophyll catabolite (pFCC) by red chlorophyll catabolite reductase (RCCR) (Rodoni et al., 1997; Hortensteiner et al., 2000). pFCCs then undergo further modifications in the vacuole, presumably by the acidic environment of the vacuole, to form nonfluorescent chlorophyll catabolites (NCC) (Krautler, 2008).

#### Subcellular localization of chlorophyll degradation

Chlorophyllase localization is unclear; some reports suggest its localization in the chloroplast inner envelope (Brandis et al., 1996; Matile et al., 1997; Tsuchiya et al., 1999) while others indicate an entirely non-plastidic localization (Hortensteiner, 2006; Schenk et al., 2007). Currently, the identity and localization of the magnesium dechelating substance is also unknown (Eckhardt et al., 2004; Hortensteiner, 2006). Pheophorbide a oxygenase (PAO) has been suggested to be localized in gerontoplast envelopes based on activity measured in purified barley gerontoplast envelope membranes (Matile and Schellenberg, 1996). The upregulation of *PAO* gene expression during the conversion of chloroplasts to gerontoplasts is an important mechanism that regulates the degradation of chlorophyll (Hortensteiner, 2006). Red chlorophyll catabolite reductase (RCCR) contains a predicted chloroplast transit peptide, can be imported into chloroplasts in vitro (Wuthrich et al., 2000), and is found in the stroma. In contrast to PAO, RCCR is constitutively expressed in chloroplasts as well as gerontoplasts (Rodoni et al., 1997; Matile et al., 1999; Yao and Greenberg, 2006). Localization of RCCR in the cell seems to depend on the developmental stage of the

plant. In young seedlings, it is localized in both plastids and mitochondria whereas in mature leaves it is present primarily in the chloroplasts (Mach et al., 2001). Upon induction of cell death by bacterial infection or protoporphyrin IX treatment, RCCR localization was observed to change from mostly localization in the chloroplast to localization in the chloroplast, mitochondria and cytosol (Yao and Greenberg, 2006). One explanation for this variation in subcellular localization of RCCR could be that during the induction of stress-inducing events such as bacterial infection or porphyrin accumulation, RCCR may bind and/or reduce porphyrins or porphyrin-related molecules in mitochondria and possibly chloroplasts, which could generate light-dependent reactive oxygen species. This could cause an alteration in organelle behavior and activate a cascade leading to programmed cell death (Yao and Greenberg, 2006).

## **REGULATION OF TETRAPYRROLE BIOSYNTHESIS**

### Developmental stage

Chloroplast biogenesis and function plays a major role in the regulation of tetrapyrrole biosynthesis. During chloroplast biogenesis, there is a massive demand for chlorophyll and a massive induction of tetrapyrrole biosynthesis. At this stage, inducing the expression of genes that encode proteins contributing to tetrapyrrole metabolism is a major mechanism driving this robust biosynthesis of tetrapyrroles. After chloroplast biogenesis is completed, the level of tetrapyrroles must be finely regulated for optimal chloroplast function. Regulated gene expression continues to be an important mechanism that coarsely regulates tetrapyrrole biosynthesis in mature chloroplasts. As

described in more detail below, feedback regulation at the posttranslational level is critical for the fine regulation of tetrapyrrole biosynthesis (Masuda and Fujita, 2008).

### Light

Light plays a major role in the development of photosynthetically active chloroplasts in angiosperms. When seedlings are grown in dark, chloroplast biogenesis is blocked. These dark grown seedlings contain etioplasts rather than chloroplasts. Etioplasts are prechloroplasts that form in the dark because many of the light-regulated genes that are required for proper chloroplast biogenesis are expressed at levels that are inadequate to support chloroplast biogenesis and because chlorophyll biosynthesis does not occur in the dark due to a lack of POR activity; POR is a light-dependent enzyme. In the dark, protochlorophyllide accumulates bound to POR in the prolamellar body of the etioplast. The accumulation of protochlorophyllide in dark indicates that all the enzymes participating in tetrapyrrole biosynthesis are synthesized and are active even in the dark in the early developmental stages of the seedling (Masuda and Fujita, 2008). Protochlorophyllide accumulates to a threshold level in the dark, and then protochlorophyllide biosynthesis is inhibited. This down regulation of protochlorophyllide biosynthesis is critical to the survival of plants; accumulation of excess amounts of protochlorophyllide that are not bound by POR can yield potentially lethal levels of reactive oxygen species when dark-grown seedlings are exposed to light (Meskauskiene et al., 2001). As described in more detail below, this buildup of protochlorophyllide inhibits the ALA synthesis by mechanisms that include feedback inhibition of glutamyl tRNA reductase and inhibition of *HEMA1* expression—the gene

that encodes glutamyl tRNA reductase. For further growth, the developing seedling has to synthesize increasing amounts of chlorophyll upon exposure to light. To do so, flux down the entire tetrapyrrole biosynthetic pathway has to be increased, especially so down the chlorophyll branch. At the same time, there has to be a tight coordination between chlorophylls and the chlorophyll binding proteins for assembly of the photosynthetic complexes.

#### Transcriptional regulation of chlorophyll synthesis during chloroplast biogenesis

The expression of several genes that encode enzymes required for chlorophyll biosynthesis are induced to very high levels during chloroplast biogenesis. Glutamyl tRNA reductase is a major target for the transcriptional regulation of chlorophyll biosynthesis. Glutamyl tRNA reductase is encoded by two genes in Arabidopsis, *HEMA1* and *HEMA2*. *HEMA1* is predominantly expressed in photosynthetic tissues, rapidly induced by light, and is thought to mostly contribute to chlorophyll biosynthesis. *HEMA2* isoform is ubiquitously and constitutively expressed and is thought to predominantly drive tetrapyrrole biosynthesis in nonphotosynthetic tissues (Ilag et al., 1994; Bougri and Grimm, 1996; Tanaka et al., 1996; Goslings et al., 2004; Matsumoto et al., 2004). *HEMA1*, *CHLH* (encoding the porphyrin-binding and Mg<sup>2+</sup> binding subunit of magnesium chelatase), *CHL27/CRD1* (encoding a subunit of magnesium protoporphyrin IX monomethylester cyclase), *CAO* (chlorophyll a oxygenase) belong to a cluster of genes that get rapidly upregulated by light within 1 hour of illumination during the onset of greening of etiolated seedlings and reaching a plateau after 3 hours, suggesting that these genes are key for regulating the biosynthesis and flux through the

chlorophyll branch (Matsumoto et al., 2004). *GENOMES UNCOUPLED 4*, a novel regulator of magnesium chelatase, also follows a similar expression pattern (Stephenson and Terry, 2008). Genes encoding the rest of the enzymes in the common tetrapyrrole pathway and most of the chlorophyll branch belong to a separate cluster based on expression pattern. They are slowly upregulated after seedlings are exposed to light. Their expression reaches a maximum, approximately 9 to 12 hours after de-etiolation begins (Matsumoto et al., 2004). *PORA* and *PORB* genes, which encode protochlorophyllide oxidoreductase, are regulated very differently by light under the above conditions compared to rest of the genes in the chlorophyll branch. The levels of the mRNAs that encode *PORA* and *PORB* accumulate in the dark to relatively high levels, but are reduced to much lower levels within 3 to 6 hours after dark-grown seedlings are exposed to light (Armstrong et al., 1995; Matsumoto et al., 2004). This may be a mechanism by which flow through the chlorophyll branch is regulated so as to prevent an abnormally high accumulation of chlorophyllide or chlorophyll, which could be phototoxic to the seedlings. The expression pattern of *HEMA1*, *CHLH*, *GUN4*, *CRD1* and *CAO* matches that of *Lhcb1*, suggesting that these genes are important for coordinating chlorophyll biosynthesis to a functional photosynthetic apparatus during de-etiolation (Matsumoto et al., 2004; Stephenson and Terry, 2008).

#### Feedback regulation of glutamyl tRNA reductase

Negative feedback regulation of enzymes is another important mechanism that regulates chlorophyll biosynthesis. Glutamyl tRNA reductase is a major target of feedback regulation. Heme regulates ALA biosynthesis by feedback inhibition of

glutamyl tRNA reductase, the enzyme that converts glutamyl tRNA to ALA (Pontoppidan and Kannangara, 1994; Vothknecht et al., 1996). Additionally, the FLU protein inhibits glutamyl tRNA reductase if excess protochlorophyllide accumulates. FLU was first identified from an Arabidopsis conditional *fluorescence* (*flu*) mutant and has been localized to the chloroplast membranes. Protochlorophyllide accumulates to higher than wild type levels in *flu* when grown in dark, and *flu* seedlings are photobleached on exposure to light. Repression of glutamyl tRNA reductase by FLU has been shown to occur independently of the feedback inhibition by heme (Meskauskiene et al., 2001; Goslings et al., 2004). Thus, FLU prevents excess protochlorophyllide from accumulating in the dark. Upon illumination, protochlorophyllide levels decrease as it gets converted to chlorophyll, and so do levels of heme thereby relieving the feedback inhibition of glutamyl tRNA reductase and stimulating ALA synthesis. FLU has been shown to interact directly and specifically with glutamyl tRNA reductase encoded by *HEMA1*, which is expressed in photosynthetically active tissues, using a yeast two hybrid system. *ulf3*, a suppressor of the *flu* mutation was identified. This suppressor reduces ALA synthesis and protochlorophyllide accumulation, and is allelic to *hyl*, the gene encoding heme oxygenase. This data supports a model in which heme antagonizes the effect of the *flu* mutation by independently inhibiting glutamyl tRNA reductase (Goslings et al., 2004).

#### Regulation of chlorophyll in mature chloroplasts

In mature chloroplasts, synthesis of new chlorophyll is needed mainly to replace the chlorophyll that becomes degraded during photosynthesis, as compared to a massive

THES  
7  
2010

1

burst in chlorophyll biosynthesis that is required during greening. Maintenance of the photosynthetic apparatus is very important for sustaining the photoautotrophic growth of higher plants. Light and circadian clock are major regulators of chlorophyll biosynthesis and the accumulation of chlorophyll-binding proteins (Beator and Kloppstech, 1993). In addition, the demand for chlorophyll in the cell varies depending on the photosynthetic activity. Similar to regulation of chlorophyll biosynthesis during chloroplast biogenesis, regulating ALA biosynthesis is one major mechanism for regulating chlorophyll synthesis in mature chloroplasts. Both diurnal cycle and circadian clock were found to influence *HEMA1* expression (Kruse et al., 1997; Matsumoto et al., 2004) and activity (Kruse et al., 1997). Similar to *HEMA1* upregulation, *CHLH*, *CRD1*, *CAO* and *Lhcb1* genes, which were found to be rapidly upregulated during chloroplast biogenesis, also get rapidly upregulated in mature green leaves following dark to light shift. In contrast to their expression pattern during chloroplast biogenesis, *PORA* and *PORB* genes also get upregulated following a dark to light shift, although their expression levels peak slower than *HEMA1*, *CHLH*, *CRD1* and *CAO*. In addition to regulation by the diurnal cycle, all of these genes are also regulated by the circadian clock (Matsumoto et al., 2004). The remaining genes encoding enzymes that contribute to the common part of the tetrapyrrole pathway and the chlorophyll branch are under a diurnal regulation but not the circadian clock (Matsumoto et al., 2004). These data suggest that regulating the expression of *HEMA1*, *CHLH*, *CRD1* and *CAO* are important for coordinating chlorophyll biosynthesis with assembly of a functional photosynthetic apparatus in mature green leaves, while *PORA* and *PORB* may function in maintaining chlorophyll biosynthesis (Matsumoto et al.,



2004). These data also indicate that light and circadian rhythm regulates the synthesis of chlorophyll and chlorophyll-binding proteins, as has been proposed before (Beator and Kloppstech, 1993).

Other regulators of chlorophyll-biosynthesis-related gene expression.

Phytochrome interacting factors: Phytochrome interacting factors (PIFs) belong to the basic helix-loop-helix (bHLH) family of transcription factors that are capable of activating or repressing gene expression (Castillon et al 2007). PIF1 and PIF3 play roles as critical modulators by which plants coordinate chlorophyll biosynthesis in response to light conditions and developmental stage (Huq et al., 2004). PIF1 is a negative regulator of chlorophyll biosynthesis in the dark because *pif1* mutant seedlings accumulate protochlorophyllide when grown in the dark and are photobleached when transferred to the light (Huq et al., 2004). Negative regulation by PIF1 is in turn at least partially attenuated by light, which would allow plants to perform higher rates of chlorophyll biosynthesis in light. In contrast to PIF1, PIF3 positively regulates chlorophyll biosynthesis in the initial hours of de-etiolation (Kim et al., 2003; Monte et al., 2004). However, recent reports indicate that *pif1*, *pif3* and *pif1pif3* double mutants accumulate protochlorophyllide when grown in the dark. These mutants also accumulate more chlorophyll than wild type in the initial 2 hours following de-etiolation, suggesting a model in which both PIF1 and PIF3 act similarly and are negative regulators of chlorophyll biosynthesis in the dark (Stephenson et al., 2009).



Golden2-like: *Golden2-like (GLK)* genes belong to the GARP family of transcription factors (Riechmann et al., 2000) that were originally identified in maize and have been shown to promote chloroplast biogenesis in Arabidopsis, maize and *Physcomitrella patens* (Rossini et al., 2001; Fitter et al., 2002; Yasumura et al., 2005). Arabidopsis has two *GLK* genes, *GLK1* and *GLK2*. *glk1 glk2* double mutants have reduced transcript and protein levels derived from genes participating in chlorophyll biosynthesis and light harvesting. These mutants are significantly pale green and have poorly developed chloroplasts (Fitter et al., 2002). Transcriptome analysis of transgenic plants containing transgenes that inducibly express *GLK1* and *GLK2* indicates that a major function of GLKs is to induce the expression of genes that encode enzymes in chlorophyll biosynthesis (e.g., *HEMA1*, *CHLH*, *CRD1* and *CAO*) and other processes related to the light reactions of photosynthesis (Waters et al., 2009). Overexpression of *GLK1* and *GLK2* in stably transformed plants causes an increase in chlorophyll levels (Waters et al., 2008; Waters et al., 2009). Based on these findings the GLKs have been proposed to help co-regulate gene expression that is related to the light reactions of photosynthesis.

#### Regulation of Mg-chelatase

Mg-chelatase consists of three subunits that are conserved in all organisms that perform photosynthesis. These subunits are often named BchI, BchD, and BchH in organisms that synthesize bacteriochlorophyll, and ChlI, ChlD, and ChlH in organisms that synthesize chlorophyll. In Arabidopsis, their masses are approximately 40 kDa, 80 kDa and 140 kDa, respectively (Willows et al., 2003). ChlH is the porphyrin-binding and Mg<sup>2+</sup>-binding subunit of this enzyme whereas ChlI and ChlD belong to the AAA

THE  
7  
201



(ATPases Associated with a variety of Activities) class of proteins (Fodje et al., 2001; Willows et al., 2004). ChlI and ChlD provide the energy that drives the metalation reaction.

Circadian regulation: Like many other genes involved in tetrapyrrole biosynthesis, *CHLH* transcript levels oscillate significantly during the diurnal cycle and are regulated by the circadian clock (Gibson et al., 1996; Nakayama et al., 1998; Matsumoto et al., 2004). Mg-chelatase activity mirrors the expression of the ChlH subunit (Papenbrock et al., 1999). Timing Of CAB expression 1 (TOC1), a key component of circadian regulation, binds the promoter of the *CHLH* gene and controls its circadian expression (Legnaioli et al., 2009).

Magnesium and ATP:  $Mg^{2+}$  and ATP are two substrates for Mg-chelatase. The concentration of  $Mg^{2+}$  in the chloroplast stroma and the ATP/ADP ratio in the chloroplast fluctuates during the diurnal cycle.  $Mg^{2+}$  binding promotes the cooperative binding of both ATP and porphyrins (Reid and Hunter, 2004).  $Mg^{2+}$  was previously reported to affect the subchloroplastic distribution of Mg-chelatase. When chloroplasts are lysed and fractionated in the presence of 5 mM  $Mg^{2+}$ , ChlH localizes predominantly to the chloroplast envelopes. When chloroplasts are lysed and fractionated in 1mM  $Mg^{2+}$ , ChlH localizes to the soluble fraction. Possible interpretations of this data are that a  $Mg^{2+}$ -induced conformational change in ChlH promotes the association of ChlH with chloroplast envelope membranes (Gibson et al., 1996; Nakayama et al., 1998) or that  $Mg^{2+}$  causes the enzyme to pellet. ATP has also been reported to affect the competition between Mg-chelatase and ferrochelatase because ATP is essential for Mg-chelatase activity (Jensen et al., 1999; Reid and Hunter, 2004), but ATP inhibits the activity of



ferrochelatase (Cornah et al., 2002). Thus, changes in the ATP/ADP ratios in the day/night cycle have been proposed to affect the channeling of protoporphyrin IX into the heme or the chlorophyll branch (Cornah et al., 2003).

Redox: Activities of a number of enzymes involved in photosynthesis are coupled to the photosynthetic electron transport via the thioredoxin system (Buchanan and Balmer, 2005). Similarly, the ChII subunit of Mg-chelatase is a target for thioredoxin (Balmer et al., 2003; Ikegami et al., 2007). The ATPase activity of ChII from *Arabidopsis* is fully inactivated by oxidation but readily reactivated by a thioredoxin-assisted reduction (Ikegami et al., 2007). Also, the ATPase activity of ChII was inhibited by N-ethylmaleimide, a thiol-modifying reagent (Ikegami et al., 2007), which was shown to bind ChII specifically, (Jensen et al., 2000). Based on these data, ChII is proposed to be regulated by thioredoxin (Ikegami et al., 2007; Masuda and Fujita, 2008).

## **IMPACT OF CHLOROPHYLL ON OTHER CELLULAR PROCESSES**

In addition to its role in the light harvesting reactions of photosynthesis, recent reports have indicated the involvement of chlorophyll metabolism in the regulation of particular physiological processes in plants such as (1) regulating the size of photosystem antenna, (2) chloroplast senescence, and (3) plastid-to-nucleus signaling (Tanaka and Tanaka, 2006).

In green plants, antenna size is determined by the amount of chlorophyll that is associated with the photosystems. For example, in response to high light intensity, plants decrease the size of the antenna complexes that surround the photosystems and

vice versa. However, chlorophyll *a* oxygenase (*CAO*)-overexpressing plants are unable to decrease the size of their antenna complexes in response to high light intensity, in contrast to wild type. Additionally, the chlorophyll *a/b* ratio increased in wild type plants acclimated from low light to high light, but in transgenic plants overexpressing *CAO*, chlorophyll *a/b* ratios remained low under high light conditions, and the antenna proteins Lhcb1, Lhcb3 and Lhcb6 proteins accumulated compared to wild type under these same conditions. On the other hand, a defect in chlorophyll *b* biosynthesis in the *chl-1* mutant is correlated with a decrease in the accumulation of Lhcb 1, 3 and 6. Based on these data, chlorophyll *b* biosynthesis was suggested to play a role in regulating antenna size of photosystem II (Tanaka and Tanaka, 2005).

Evidence that chlorophyll metabolism can affect senescence comes from an analysis of the maize *pao* mutant, which has defects in chlorophyll catabolism. Slower rates of degradation were reported for the chlorophyll-binding light harvesting complex protein II (Lhcb II) relative to other proteins in *pao* relative to wild type (Pruzinska et al., 2003). Similar reports have shown that pheophorbide *a* oxygenase (*PAO*) knockout mutants of *Arabidopsis* show a stay-green phenotype after dark-induced senescence compared to wild type in both maize and *Arabidopsis* (Pruzinska et al., 2003; Pruzinská et al., 2005).

The chlorophyll precursors Mg-protoporphyrin IX (Mg-PPIX) and Mg-Protoporphyrin IX monomethyl ester (Mg-PPIX ME) have been suggested to affect plastid-to-nucleus signaling. Feeding Mg-PPIX to *Arabidopsis* protoplasts in dim light causes Lhcb levels to decrease. In this same report, treating chlorophyll precursors with norflurazon caused Mg-PPIX levels to increase and repress the expression of a large

number of nuclear genes, most of which are involved in photosynthesis (Strand et al., 2003). Consistent with this model, Arabidopsis mutants with defects in Mg-PPIX and Mg-PPIX ME biosynthesis have defects in the plastid regulation of nuclear gene expression (Mochizuki et al., 2001; Strand et al., 2003). Buildup of Mg-PPIX is controversial; using sensitive methods such as liquid chromatography-mass spectrometry, recent reports find no buildup of Mg-PPIX, Mg-PPIX ME or any other chlorophyll biosynthetic intermediate under conditions in which nuclear gene expression is repressed (Mochizuki et al., 2008; Moulin et al., 2008). The mechanism by which the metabolism of Mg-PPIX and Mg-PPIX ME might affect nuclear gene expression remains an open question (Voigt et al., 2009).

In green algae, it was observed that direct feeding of either Mg-protoporphyrin IX or Mg-protoporphyrin IX monomethyl ester, but not protoporphyrin IX or protochlorophyllide or chlorophyllide, induced expression of *Heat Shock Protein 70* (*HSP70*) genes whose product is involved in protecting photosystem II from high light induced damage (Kropat et al 1997).

Mg-PPIX has been shown to activate nuclear DNA replication via the A-type cyclin dependent kinase (CDKA), which is a regulatory component of the eukaryotic cell cycle in the red alga *Cyanidioschyzon merolae* and in tobacco cell cultures (Kobayashi et al., 2009). For such a system to work, it seems logical that a cytosolic component has to be present to perceive a tetrapyrrole signal. These findings suggest a link between tetrapyrrole metabolism in the plastid and the regulation of the cell cycle.



## ***GENOMES UNCOUPLED 4 (GUN4)***

In Arabidopsis, the expression of many nuclear genes that encode photosynthesis-related proteins requires the biogenesis of functional chloroplasts (Nott et al., 2006; Larkin and Ruckle, 2008; Woodson and Chory, 2008). To identify these “plastid signals” and plastid signaling mechanisms, Joanne Chory and her colleagues developed a screen for Arabidopsis mutants that have defects in the plastid regulation of photosynthesis-related nuclear genes. These mutants were named *genomes uncoupled* (*gun*) because the coordinated expression of the plastid and nuclear genomes is disrupted in these mutants (Susek and Chory, 1992; Susek et al., 1993). The *gun4-1* mutant was isolated from the first *gun* mutant screen (Susek et al., 1993; Mochizuki et al., 2001). The *gun4-1* allele was cloned by map-based cloning. As summarized below, GUN4 encodes a novel positive regulator of chlorophyll biosynthesis (Larkin et al., 2003).

In Arabidopsis, leaky *gun4* mutants are partially chlorophyll deficient and knockout mutants are albino under normal growth conditions. However, knockout mutants can accumulate readily observable quantities of chlorophyll in dim light (Larkin et al., 2003). Based on these data Larkin et al. (2003) concluded that *GUN4* encodes a positive regulator of chlorophyll biosynthesis that is not absolutely required for chlorophyll accumulation in vivo. GUN4 knockout mutants in *Synechocystis* sp. PCC 6803 were subsequently reported to not accumulate chlorophyll (Sobotka et al., 2008). Based on these data, the major biological function of GUN4 appears to be conserved between cyanobacteria and plants.



*GUN4* is a nuclear gene that encodes a chloroplast-localized protein in plants. After import into the chloroplast, GUN4 protein is 22 kDa. GUN4 is found mainly in the stroma of chloroplasts that are purified from rosette leaves of ca. one-month-old *Arabidopsis* plants. Lesser but readily detectable quantities of GUN4 are found in envelope and thylakoid membranes of these same leaves. GUN4 is monomeric in the chloroplast stroma, but GUN4 is part of large multisubunit complexes in solubilized thylakoid and envelope membranes. These complexes range in size from 500 kDa to greater than 1 MDa. A GUN4 complex was purified from solubilized chloroplast membranes and found to contain ChlH (aka, the 140 kDa subunit of Mg-chelatase). Based on these data and the chlorophyll-deficient phenotype of *gun4* mutants, GUN4 was hypothesized to stimulate chlorophyll biosynthesis by activating Mg-chelatase. Indeed, in quantitative enzyme assays, *Synechocystis* sp. PCC 6803 GUN4 (hereafter referred to as SynGUN4) was found to stimulate Mg-chelatase activity threefold. Porphyrin binding assays and qualitative enzyme assays provided evidence that SynGUN4 stimulates Mg-chelatase by a mechanism in which GUN4 binds both the porphyrin substrate and product of Mg-chelatase (Larkin et al., 2003). The ChlH subunit of Mg-chelatase was subsequently shown to associate with SynGUN4 (Sobotka et al., 2008).

Crystal structures are available for GUN4 relatives from *Synechocystis* sp. PCC 6803 (Verdecia et al., 2005) and *Thermosynechococcus elongatus* (Davison et al., 2005). The porphyrin-binding domain of GUN4 from SynGUN4 was identified using NMR and extensive-site-directed mutagenesis. This porphyrin-binding domain of SynGUN4 is conserved among all GUN4 relatives and is hereafter referred to as the

THE  
7  
2011



GUN4 core domain (Verdecia et al., 2005). Although GUN4 is encoded by single copy genes in plants and many cyanobacteria, particular cyanobacteria may contain multiple genes that encode the GUN4 core domain. Cyanobacteria may contain distinct amino-terminal domains fused to the GUN4 core domain. These amino-terminal domains may contain no sequence similarity to known proteins or may contain similarity to kinase, protease, or protein interaction domains. These findings are consistent with GUN4-related proteins performing diverse functions in particular cyanobacteria. In plants, chloroplast transit peptides are fused to the amino terminus of the GUN4 core domain and ca. 35 residues are fused to the carboxy-terminus of the GUN4 core domain (Larkin et al., 2003; Davison et al., 2005; Verdecia et al., 2005).

Based on genetic and biochemical data, GUN4 from cyanobacteria and plants is expected to bind the substrate and product of Mg-chelatase, PPIX and Mg-PPIX (Larkin et al., 2003; Wilde et al., 2004; Davison et al., 2005; Verdecia et al., 2005; Sobotka et al., 2008). There is no published data that provides compelling evidence that the GUN4 protein binds any porphyrin besides PPIX and Mg-PPIX in vivo. Because of the low water solubility of PPIX and Mg-PPIX, the porphyrin-binding activity of GUN4 has been studied using deuteroporphyrin IX (DPIX) and Mg-deuteroporphyrin IX (Mg-DPIX). DPIX and Mg-DPIX lack two vinyl groups found in PPIX and Mg-PPIX and are significantly more water-soluble than PPIX and Mg-PPIX (Larkin et al., 2003; Davison et al., 2005; Verdecia et al., 2005). The  $K_d^{\text{Mg-DPIX}}$  and the  $K_d^{\text{DPIX}}$  were found to be  $0.26 \pm 0.029 \mu\text{M}$  and  $2.2 \pm 0.3 \mu\text{M}$ , respectively (Larkin et al., 2003). Using different binding assays, essentially these same  $K_d^{\text{Mg-PPIX}}$  and  $K_d^{\text{PPIX}}$  values were

THE  
7  
201



obtained for SynGUN4 and *Thermosynechococcus elongatus* GUN4 (Davison et al., 2005; Verdecia et al., 2005).

Metalated porphyrins like heme and Mg-PPIX are rigidly planar whereas porphyrins that lack metals such as PPIX are more malleable and assume a more ruffled or puckered conformation. Structural studies with *Bacillus subtilis* ferrochelatase suggest that the conversion of the more malleable puckered PPIX to the rigid and planar heme drives the dissociation of heme from the product-binding site (Lecerof et al., 2000; Sigfridsson and Ryde, 2003). GUN4 and Mg-chelatase are different from ferrochelatase in that they bind Mg-DPIX and in the case of GUN4, bind Mg-DPIX with a higher affinity than DPIX (Karger et al., 2001; Larkin et al., 2003; Davison et al., 2005; Verdecia et al., 2005). Based on the much lower  $K_d^{\text{Mg-DPIX}}$  than  $K_d^{\text{DPIX}}$ , SynGUN4, was proposed to facilitate the dissociation of Mg-PPIX from the product-binding site of Mg-chelatase (Larkin et al., 2003). This model is supported by the observation that amino acid substitutions that specifically lower the affinity of SynGUN4 for Mg-DPIX but not DPIX also significantly reduce the Mg-chelatase stimulatory activity of SynGUN4 (Verdecia et al., 2005). The porphyrin-binding specificity of SynGUN4 was investigated using 6 artificial and natural porphyrins. The conclusion from this work is that SynGUN4 has a higher affinity for planar porphyrins than porphyrins with nonplanar conformations and that SynGUN4 has a higher affinity for porphyrins containing particular metals (Verdecia et al., 2005). Nonetheless, because of technical limitations, prior to the work published from this thesis, there was no report that compared the binding affinity of GUN4 from any species for the natural ligands PPIX and Mg-PPIX to other porphyrins. Such experiments are important

because results from these experiments would indicate whether GUN4 binds PPIX and Mg-PPIX and might suggest whether the interpretations of data obtained with DPIX and Mg-DPIX should be modified. Results from such experiments might help indicate whether GUN4 binds porphyrins other than PPIX and Mg-PPIX *in vivo*.

A proteinaceous cofactor that stimulates an enzyme by a mechanism that involves binding the enzyme as well as one of its substrates and products is novel enzymology. Mg-chelatase may require such a novel cofactor to protect itself from the ROS that are generated when O<sub>2</sub> collides with porphyrins that have been exposed to the light. O<sub>2</sub> in its ground state is a relatively stable molecule but can be converted to highly reactive and damaging forms such as singlet oxygen (<sup>1</sup>O<sub>2</sub>), hydrogen peroxide (H<sub>2</sub>O<sub>2</sub>), superoxide or hydroxyl radicals (OH<sup>•</sup>) upon energy transfer or by electron transfer reactions (Halliwell, 1999; Huq et al., 2004; Krieger-Liszkay, 2005). Absorbing a quanta of light excites chlorophyll. If long lived electronically excited states of chlorophyll known as triplet chlorophyll are not quenched by carotenoids, they may transfer energy to O<sub>2</sub> after colliding with O<sub>2</sub> yielding <sup>1</sup>O<sub>2</sub>. <sup>1</sup>O<sub>2</sub> can be converted into other ROS such as superoxide anion (O<sub>2</sub><sup>•-</sup>) and hydrogen peroxide (H<sub>2</sub>O<sub>2</sub>), the highly toxic hydroxyl radical (OH<sup>•</sup>) or perhydroxyl radicals (O<sub>2</sub>H<sup>•</sup>) (Gomes et al., 2005; Flors et al., 2006; Gadjev et al., 2006). Such ROS can lead to apoptotic and necrotic cell death (Kim et al., 2008). GUN4 may be necessary to prevent ROS stress by binding porphyrins and helping channel PPIX into chlorophyll biosynthesis. Additionally, by channeling PPIX into chlorophyll biosynthesis, GUN4 might also help Mg-chelatase compete with ferrochelatase for PPIX.



In addition to channeling PPIX into chlorophyll biosynthesis, GUN4 has been proposed to bind readily detectable pools of PPIX and Mg-PPIX. Plants perform a burst of PPIX and Mg-PPIX biosynthesis at dawn and readily detectable levels of these porphyrins accumulate throughout the day (Pöpperl et al., 1998; Papenbrock et al., 1999; Mochizuki et al., 2008; Moulin et al., 2008). GUN4 or a GUN4-ChlH complex has been hypothesized to bind the PPIX and Mg-PPIX that accumulates during the diurnal cycle and shield these porphyrins from collisions with O<sub>2</sub> thereby protecting plants from ROS-triggered apoptotic and necrotic cell death (Larkin et al., 2003). Indeed, a high-resolution crystal structure and extensive site-directed mutagenesis support a model in which GUN4 envelopes porphyrins thereby shielding them from collisions with O<sub>2</sub> (Verdecia et al., 2005).

The photosensitizing properties of PPIX were previously shown to inactivate Mg-chelatase in *Rhodobacter capsulatus* by driving the formation of covalent adducts between the *R. capsulatus* relative of ChlH and the PPIX it binds. This inactivation of Mg-chelatase appears to facilitate the rapid down regulation of bacteriochlorophyll biosynthesis and photosynthesis in *R. capsulatus*, which performs only anoxygenic photosynthesis (Willows et al., 2003). *Rhodobacter* species were found to lack a relative of GUN4 (Larkin et al., 2003). Thus, GUN4 was proposed to protect Mg-chelatase from forming covalent adducts with bound PPIX in the presence of bright light and O<sub>2</sub> in organisms that perform oxygenic photosynthesis (Verdecia et al., 2005). The observation that *GUN4* is required for the accumulation of chlorophyll only in bright light but not in dim light (Larkin et al., 2003), and the observation that *gun4* mutants exhibit greater sensitivity to light when grown in diurnal cycles that cause



PPIX and Mg-PPIX to accumulate at higher levels relative to continuous light (Peter and Grimm, 2009) are consistent with a role for GUN4 in photoprotection.

In this thesis, I report several conceptual advances for GUN4. (1) I report on a technical advance to porphyrin-binding assays that allows the first demonstration that GUN4 can bind PPIX and Mg-PPIX. Using this new binding assay, I compare the binding affinity of GUN4 for PPIX and Mg-PPIX to other natural and unnatural porphyrins. Based on these data and a review of published genetic and biochemical data, I conclude that the major and possibly only role of GUN4 in plants is stimulating Mg-chelatase and binding PPIX and Mg-PPIX in vivo. (2) I show that the porphyrin binding promotes the association of GUN4 with chloroplast membranes—the site of chlorophyll biosynthesis. Similar results are reported for ChlH, although they are not explored to the same depth as GUN4. These findings are consistent with GUN4 stimulating chlorophyll biosynthesis not only by activating Mg-chelatase but also by promoting interactions between ChlH and chloroplast membranes. (3) I developed stably transformed *Arabidopsis* plants that express new *gun4* alleles that were engineered using site-directed mutagenesis and encode single amino acid substitutions. These single amino acid substitutions lower the affinity of GUN4 for PPIX and Mg-PPIX. I use these site-directed mutants to show that the porphyrin-binding activity of GUN4 that was previously only demonstrated in vitro is also important in vivo. Specifically, I show that this porphyrin-binding activity of GUN4 contributes to the binding of GUN4 to chloroplast membranes and photooxidative stress tolerance. Using *chlH* mutants I show that ChlH activity also helps GUN4 to associate with chloroplast membranes and to attenuate the production of ROS. My data indicate that GUN4 helps

protect plants from photooxidative stress that can be generated when plants are exposed to high fluence rates of light and that GUN4 attenuates photooxidative stress by binding porphyrins and ChlH on chloroplast membranes.

## CHAPTER 2

### PORPHYRINS PROMOTE THE ASSOCIATION OF GENOMES UNCOUPLED 4 AND A MG-CHELATASE SUBUNIT WITH CHLOROPLAST MEMBRANES

This research was originally published in the *Journal of Biological Chemistry*.  
**Adhikari N, Orlor R, Chory J, Froehlich J, Larkin R.** Porphyrins Promote the  
Association of GENOMES UNCOUPLED 4 and a Mg-chelatase Subunit with  
Chloroplast Membranes. *Journal of Biological Chemistry*. 2009; Vol. 284: pp.  
24783-24796. © The American Society for Biochemistry and Molecular Biology.

THE  
7  
201



## PORPHYRINS PROMOTE THE ASSOCIATION OF GENOMES UNCOUPLED 4 AND A MG-CHELATASE SUBUNIT WITH CHLOROPLAST MEMBRANES

### **Abstract**

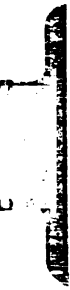
In plants, chlorophylls and other tetrapyrroles are synthesized from a branched pathway that is located within chloroplasts. GENOMES UNCOUPLED 4 (GUN4) stimulates chlorophyll biosynthesis by activating Mg-chelatase, the enzyme that commits porphyrins to the chlorophyll branch. GUN4 stimulates Mg-chelatase by a mechanism that involves binding the ChlH subunit of Mg-chelatase, as well as a substrate (protoporphyrin IX) and product (Mg-protoporphyrin IX) of Mg-chelatase. We chose to test whether GUN4 might also affect interactions between Mg-chelatase and chloroplast membranes—the site of chlorophyll biosynthesis. To test this idea, we induced chlorophyll precursor levels in purified pea chloroplasts by feeding these chloroplasts with 5-aminolevulinic acid, determined the relative levels of GUN4 and Mg-chelatase subunits in soluble and membrane-containing fractions derived from these chloroplasts, and quantitated Mg-chelatase activity in membranes isolated from these chloroplasts. We also monitored GUN4 levels in the soluble and membrane-containing fractions derived from chloroplasts fed with various porphyrins. Our results indicate that 5-aminolevulinic acid feeding stimulates Mg-chelatase activity in chloroplast membranes and that the porphyrin-bound forms of GUN4 and possibly ChlH associate most stably with chloroplast membranes. These findings are consistent with GUN4 stimulating chlorophyll biosynthesis not only by activating Mg-chelatase but also by promoting interactions between ChlH and chloroplast membranes.

## INTRODUCTION

Chlorophylls are produced from a branched pathway located within plastids that also produces heme, siroheme, and phytochromobilin. In photosynthetic organisms, the universal tetrapyrrole precursor 5-aminolevulinic acid (ALA) is derived from glutamyl-tRNA and subsequently converted into protoporphyrinogen IX in the chloroplast stroma. Protoporphyrinogen IX is converted to protoporphyrin IX (PPIX), then ultimately to chlorophylls on plastid membranes. Almost all the genes encoding chlorophyll biosynthetic enzymes have been identified. Transcriptional control provides coarse regulation of this pathway and the regulation of enzyme activities provides fine regulation (Tanaka and Tanaka, 2007; Stephenson and Terry, 2008).

*Arabidopsis* GUN4 (hereafter referred to as GUN4) was identified from a screen for plastid-to-nucleus signaling mutants (Susek et al., 1993; Mochizuki et al., 2001; Larkin et al., 2003). GUN4 is a major positive regulator of chlorophyll biosynthesis, but is not absolutely required for the accumulation of chlorophyll in *Arabidopsis* (Larkin et al., 2003). In *Synechocystis*, one of the GUN4 relatives, *sl10558* (hereafter referred to as SynGUN4), was subsequently shown also to be required for the accumulation of chlorophyll (Wilde et al., 2004; Sobotka et al., 2008). The 140-kDa subunit of Mg-chelatase copurifies with the 22-kDa GUN4 from solubilized *Arabidopsis* thylakoid membranes (Larkin et al., 2003); similar results were subsequently reported using *Synechocystis* (Sobotka et al., 2008). Mg-chelatase catalyzes the insertion of Mg<sup>2+</sup> into PPIX, yielding Mg-protoporphyrin IX (Mg-PPIX). This reaction diverts PPIX from heme biosynthesis and commits this porphyrin to chlorophyll biosynthesis. Mg-chelatase requires three subunits *in vitro* and *in vivo*.

THE  
7  
70!



These three subunits are conserved from prokaryotes to plants and are commonly referred to as BchH or ChlH, BchD or ChlD, and BchI or ChlI. In *Arabidopsis*, these subunits are 140, 79, and 40 kDa, respectively. ChlH is the porphyrin-binding subunit and is likely the  $Mg^{2+}$ -binding subunit of Mg-chelatase. ChlI and ChlD are related to AAA-type ATPases and form two associating hexameric rings that interact with ChlH and drive the ATP-dependent metalation of PPIX (Elmlund et al., 2008; Masuda, 2008). SynGUN4 stimulates *Synechocystis* Mg-chelatase (Larkin et al., 2003; Davison et al., 2005; Verdecia et al., 2005). Cyanobacterial relatives of GUN4 bind deuteroporphyrin IX (DPIX) and Mg-deuteroporphyrin IX (Mg-DPIX) (Larkin et al., 2003; Davison et al., 2005; Verdecia et al., 2005), which are more water-soluble derivatives of PPIX and Mg-PPIX. Crystal structures of SynGUN4 and *Thermosynechococcus elongatus* GUN4 indicate a novel fold that resembles a "cupped hand" that binds DPIX and Mg-DPIX (Davison et al., 2005; Verdecia et al., 2005). Preincubation experiments indicate that a SynGUN4-DPIX complex stimulates Mg-chelatase more potently than SynGUN4 (Larkin et al., 2003). SynGUN4 was found to lower the  $K_m^{DPIX}$  of *Synechocystis* Mg-chelatase (Verdecia et al., 2005) and to cause a striking increase in the apparent first-order rate constant for DPIX-Mg-chelatase interactions, an effect that is particularly striking at low  $Mg^{2+}$  concentrations (Davison et al., 2005). The Mg-DPIX-binding activity of SynGUN4 was also found to be essential for stimulating Mg-chelatase (Verdecia et al., 2005).

GUN4 and Mg-chelatase subunits have been found in both soluble and membrane-containing fractions of purified chloroplasts (Gibson et al., 1996; Guo et al., 1998; Nakayama et al., 1998; Luo et al., 1999; Larkin et al., 2003). In contrast,

H

protoporphyrinogen IX oxidase (PO) and Mg-PPIX methyl transferase (Mg-PPIX MT), which function immediately upstream and downstream of Mg-chelatase in the chlorophyll biosynthetic pathway, are found only in the membrane-containing fractions and not in stromal fractions when purified chloroplasts are lysed and fractionated (Lermontova et al., 1997; Che et al., 2000; Watanabe et al., 2001; Block et al., 2002; van Lis et al., 2005). PPIX and Mg-PPIX accumulate in chloroplast membranes rather than soluble fractions, which provides more evidence that these chlorophyll precursors are synthesized on chloroplast membranes (Mohapatra and Tripathy, 2007). If GUN4 promotes chlorophyll biosynthesis by not only stimulating Mg-chelatase activity but also promoting the formation of enzyme complexes that channel porphyrins into chlorophyll biosynthesis, GUN4 would be expected to more stably associate with chloroplast membranes by interacting with chloroplast membrane lipids or chlorophyll biosynthetic enzymes after binding porphyrins. In the following, we provide experimental evidence supporting this model.

## **MATERIALS AND METHODS**

*Construction of plasmids and strains-* For in vitro transcription/translation experiments, the entire GUN4 open reading frame (ORF) was amplified from bacterial artificial chromosome clone T1G3 (Arabidopsis Biological Resource Center, Ohio State University, Columbus OH) using CGGGATCCTATCTTCCCCTGACGTGAC, AACTGCAGAAAGACATCAGAAGCTGTAATTTG, and *PfuTurbo*® DNA polymerase (Stratagene, La Jolla CA). The resulting PCR product was ligated into pCMX-PL1 (Umesono et al., 1991) between *Bam*H I and *Pst* I. In vitro transcription



and translation of the control protein translocon at the inner envelope 40 (Tic40), the small subunit of Rubisco (SS), and a light-harvesting chlorophyll *a/b*-binding protein (LHCP) were as previously described (Olsen and Keegstra, 1992; Tripp et al., 2007). A glutathione *S*-transferase (GST)-tagged GUN4 deletion mutant that lacks the predicted 69-residue transit peptide (GST-GUN4  $\Delta$ 1-69) was used for the expression and purification of GUN4 from *E. coli*, as previously described (Larkin et al., 2003). Site-directed mutagenesis was performed on each of these plasmids using the QuickChange® XL Site-Directed Mutagenesis Kit (Stratagene) and oligonucleotides that were designed according to the manufacturer's recommendations (Table 2-1). All mutations were confirmed by sequencing at the Research Technology Support Facility (RTSF) (Michigan State University, East Lansing MI).

*Isolation of pea chloroplasts*- Intact chloroplasts were isolated from 6- to 8-day-old pea seedlings and purified over a Percoll gradient as previously described (Bruce et al., 1994). Intact pea chloroplasts were reisolated and resuspended in import buffer (330 mM sorbitol, 50 mM HEPES-KOH, pH 8.0) at a chlorophyll concentration of 1 mg/ml. Protein import was performed as previously described (Bruce et al., 1994).

*In vitro translation of precursor protein*- All precursor proteins used in this study were either radiolabeled with [<sup>35</sup>S]-methionine or [<sup>3</sup>H]-leucine and translated with the TNT® Coupled Reticulocyte Lysate System (Promega, Madison WI) according to the manufacturer's recommendations.

*Import Assays*- Large-scale import assays contained 50 mM HEPES-KOH, pH 8.0, 330 mM Sorbitol, 4 mM Mg-ATP, 100  $\mu$ l chloroplasts with a chlorophyll concentration of 1 mg/ml, and labeled precursor protein at a final volume of 300  $\mu$ l.



**Table 2-1. Oligonucleotides used for site-directed mutagenesis**

Substitution	Primers used for site-directed mutagenesis
L88F	TCGACGTTCTGGAGAACCATTTTGTCAATCAAAACTTCAGACAAG/ CTTGTCTGAAGTTTGTATTGACAAAATGGTTCTCCAGAACGTCGA
L103A	AGCCGACGAGGAGACACGGAGATTAGCTATTCAGATATCCGGAGAA GCCG/ CGGCTTCTCCGGATATCTGAATAGCTAATCTCCGTGTCTCCTCGTCGG CT
F120W	AAACGTGGCTACGTTTTCTGGTCCGAGGTGAAAACAATCTCCCC/ GGGAGATTGTTTTCACCTCGGACCAGAAAACGTAGCCACGTTT
V123A	TGGCTACGTTTTCTTCTCCGAGGCTAAAACAATCTCCCCGAAGATC/ GATCTTCGGGGGAGATTGTTTTAGCCTCGGAGAAGAAAACGTAGCCA
L131A	AAAACAATCTCCCCGAAGATGCTCAAGCTATCGACAATCTATGG/ CCATAGATTGTCGATAGCTTGAGCATCTTCGGGGGAGATTGTTTT
I134A	TCCCCGAAGATCTTCAAGCTGCTGACAATCTATGGATTAACAC/ GTGTTAATCCATAGATTGTCAGCAGCTTGAAGATCTTCGGGGGA
F191A	TACAGAGCGTTTCTGACGAAGCTAAGTGGGAGCTTAACGATG/ CATCGTTAAGCTCCCACTTAGCTTCGTCAGGAAACGCTCTGTA
E194A	TTTCTGACGAATTCAAGTGGGCTCTTAACGATGAAACGCCTTTAG/ CTAAAGGCGTTTCATCGTTAAGAGCCCACTTGAATTCGTCAGGAAA
R211A	TTACCGCTCACAAACGCCTTGGCTGGAACGCAGCTTCTGAAATGC/ GCATTCAGAAGCTGCGTTCAGCCAAGGCGTTTGTGAGCGGTAA
Q214A	ACAAACGCCTTGAGAGGAACGGCTCTTCTGAAATGCGTTTTAAGC/ GCTTAAAACGCATTTTCAGAAGAGCCGTTCTCTCAAGGCGTTTGT
Q214E	ACAAACGCCTTGAGAGGAACGGAACCTTCTGAAATGCGTTTTAAGC/ GCTTAAAACGCATTTTCAGAAGTTCCGTTCTCTCAAGGCGTTTGT
L216G	ACGCCTTGAGAGGAACGCAGCTTGGAAAATGCGTTTTAAGCCATCCT GC/ GCAGGATGGCTTAAAACGCATTTTCCAAGCTGCGTTCCTCTCAAGGCG T

THE  
7  
201



After a 30-min incubation at room temperature under white light provided by broad-spectrum fluorescent tube lamps at  $75 \mu\text{mol m}^{-2} \text{s}^{-1}$ , the import assay was divided into two 150- $\mu\text{l}$  aliquots. One aliquot was not further treated. For this aliquot, intact chloroplasts were directly recovered by centrifugation through a 40% Percoll cushion. The remaining aliquot was incubated with trypsin for 30 min on ice as previously described (Jackson et al., 1998). After stopping the protease treatment with trypsin inhibitor as previously described (Jackson et al., 1998), we again recovered chloroplasts by centrifugation through a 40% Percoll cushion. Recovered intact chloroplasts were resuspended in 200  $\mu\text{l}$  of lysis buffer (25 mM HEPES-KOH, pH 8.0, 4 mM  $\text{MgCl}_2$ ), incubated on ice for 20 min, and then fractionated into a soluble and membrane-containing pellet fraction by centrifugation at  $16,000 \times g$  for 5 min. The pellet fraction contains the outer envelope, inner envelope, and thylakoid membranes. All fractions were analyzed using SDS-PAGE and subjected to fluorography. Fluorograms were exposed to X-ray film (Eastman Kodak, Rochester NY) for 1 to 7 days. Import assays were quantitated by scanning developed films with the VersaDoc 4000 MP Imaging System and Quantity One software, as recommended by the manufacturer (Bio-Rad, Hercules CA).

*ALA and porphyrin feeding-* Prior to import, intact chloroplasts were incubated in import buffer (330 mM sorbitol, 50 mM HEPES-KOH, pH 8.0) that contained or lacked 10 mM ALA (Sigma-Aldrich, St. Louis MO) for 15 min at  $26^\circ\text{C}$  in the dark, unless indicated otherwise. PPIX, Mg-PPIX, uroporphyrin III, coproporphyrin III, hemin, and pheophorbide *a* were all purchased from Frontier Scientific (Logan UT). These porphyrins were first dissolved in DMSO and their concentrations were

determined spectrophotometrically as previously described (Rimington, 1960; Brown and Lantzke, 1969, 1969; Eichwurz et al., 2000; Rebeiz, 2002). These stock solutions were diluted with import buffer, giving final porphyrin concentrations of 20  $\mu$ M and final DMSO concentrations of 1-2%. Intact chloroplasts were incubated in these solutions exactly as described for ALA.

*Fractionation of chloroplasts into stroma, thylakoid, and envelope fractions-*  
Fractionation of chloroplasts was performed as previously described (Keegstra and Yousif, 1986), with modifications. First, large-scale import assays were performed with (+) or without (-) an ALA pretreatment as described above. After import, intact chloroplasts were recovered by centrifugation through a 40% Percoll cushion. The intact chloroplasts were then resuspended in 0.6 M sucrose containing 25 mM HEPES-KOH, pH 8.0, 2 mM  $MgCl_2$ , 8 mM EDTA. The suspension was placed on ice for 20 min and then placed at  $-20^{\circ}C$  overnight. Subsequently, the suspension was thawed at room temperature, gently mixed, and then diluted with 2 volumes of dilution buffer (25 mM HEPES-KOH, pH 8.0, 2 mM  $MgCl_2$ , 8 mM EDTA). This suspension was then centrifuged at  $1,500 \times g$  for 5 min. The resulting pellet predominantly contained the thylakoid fraction and was diluted twofold with 2X SDS-PAGE loading buffer (Sambrook and Russell, 2001). The remaining supernatant was then centrifuged at  $100,000 \times g$  for 1 hr. The resulting pellet fraction predominantly contained envelopes and was diluted twofold in 2X SDS-PAGE loading buffer. Cold acetone was added to the supernatant fraction to a final concentration of 80% and incubated on ice for 30 min, then centrifuged at  $15,000 \times g$  for 5 min. The precipitated soluble protein fraction was

H

resuspended in 2X SDS-PAGE loading buffer. All fractions were analyzed by SDS-PAGE.

*Analysis of porphyrins in purified chloroplasts-* PPIX and Mg-PPIX levels in purified chloroplasts were quantitated following ALA feeding and mock protein import. 0.1-ml aliquots of chloroplasts were collected by centrifugation at  $1,900 \times g$  for 5 min at 4°C through a 40% Percoll cushion. Recovered chloroplasts were lysed by resuspension in 700  $\mu$ l of acetone: 0.1 M  $\text{NH}_4\text{OH}$  (9:1, vol/vol). These lysates were clarified by centrifugation at  $16,000 \times g$  for 10 min at 4°C. Chlorophyll was removed from the resulting supernatants by hexane extraction as previously described (Rebeiz, 2002). We quantitated the amount of PPIX and Mg-PPIX in these hexane-extracted supernatants using fluorescence spectroscopy with a QuantaMaster™ spectrofluorometer (Photon Technology International, Inc., London Ontario) as previously described (Rebeiz, 2002). PPIX and Mg-PPIX, purchased from Frontier Scientific, were used to construct standard curves.

*Quantitative analysis of porphyrin binding-* GUN4  $\Delta$ 1-69 and versions of GUN4  $\Delta$ 1-69 that contain amino acid substitutions were expressed and purified from *E. coli* as previously described (Larkin et al., 2003). Binding constants were measured by quantitating the quenching of tryptophan fluorescence in GUN4  $\Delta$ 1-69 by bound porphyrins essentially as described for the cyanobacterial relatives of GUN4 (Larkin et al., 2003; Davison et al., 2005; Verdecia et al., 2005). Binding reactions were in 20 mM MOPS-KOH, pH 7.9, 1 mM DTT, 300 mM glycerol and contained 200 nM GUN4  $\Delta$ 1-69 or GUN4  $\Delta$ 1-69 with the indicated single amino acid changes and variable concentrations of DPIX and Mg-DPIX (Frontier Scientific). We determined binding

constants for PPIX, Mg-PPIX, and Mg-PPIX ME, uroporphyrin III, coproporphyrin III, hemin, and pheophorbide *a* using the same conditions except that binding reactions also contained 1% DMSO. Stock solutions of DPIX and Mg-DPIX were prepared as previously described (Karger et al., 2001). Stock solutions of all other porphyrins were prepared as described in *ALA and porphyrin feeding*. We calculated binding constants using DYNAFIT (Kuzmic, 1996) as previously described (Karger et al., 2001). The data fit best with a model that predicts a single binding site.

*Mg-chelatase assays*- Chloroplasts were purified from pea and subjected to hypotonic lysis as described above, except that lysis buffer also contained 1 mM DTT and 2 mM Pefabloc (Roche, Indianapolis IN). Supernatants were flash frozen in liquid nitrogen and stored at -80°C. We assayed pellet fractions for Mg-chelatase activity immediately by resuspending them in a Mg-chelatase assay buffer (50 mM Tricine-KOH, pH 7.8, 1 mM EDTA, 9 mM MgCl<sub>2</sub>, 4 mM MgATP, 1 mM DTT, 0.25% BSA, 5% glycerol, 60 mM phosphocreatine, 4 U/ml creatine phosphokinase) and incubating the resuspended pellets for 30 min at 30°C as previously recommended (Walker and Weinstein, 1991; Guo et al., 1998). PPIX dissolved in DMSO was added to particular reactions as indicated in the text. The final concentrations of PPIX and DMSO were 1.5 μM and 2%, respectively, as previously recommended (Walker and Weinstein, 1991). Aliquots of 8 μl were removed at 5-min intervals during a 30-min incubation and diluted into 200 μl of 90% acetone: 0.1 M NH<sub>4</sub>OH (9:1) and vortexed to terminate the reaction. The terminated reactions were centrifuged for 10 min at 16,000 × *g* at 4°C. Mg-PPIX in the resulting supernatants was quantitated as described in *Quantitative analysis of porphyrin binding*, above. We subtracted the amount of Mg-PPIX in the

membranes before the reactions were initiated from the amount of Mg-PPIX at the end of each time point. Three replicates were analyzed for each time point. Mg-PPIX accumulated linearly for the entire 30-min assay. To assay supernatants for Mg-chelatase activity, supernatants were rapidly thawed, clarified at  $16,000 \times g$  at  $4^{\circ}\text{C}$  for 10 min, and then concentrated nearly 5-fold using an Amicon Ultra Centrifugal Filter Device with a nominal molecular weight limit of 10,000 (Millipore, Billerica MA). The concentrated supernatants were diluted into a concentrated Mg-chelatase assay buffer yielding the same assay conditions described for pellets. Reactions were initiated by adding  $1.5 \mu\text{M}$  PPIX.

*Polyclonal anti-ChlH, anti-ChlI, and anti-ChlD antibody development-* Poly(A)<sup>+</sup> mRNA was isolated from *Arabidopsis thaliana* (Columbia-0 ecotype) using the Absolutely mRNA Kit (Stratagene). We prepared first-strand cDNA using Superscript II (Invitrogen, Carlsbad CA). A cDNA encoding a 62-kDa fragment of ChlH that lacks the first 823 amino acid residues (ChlH  $\Delta 1-823$ ) was amplified from this first-strand cDNA as described for GUN4  $\Delta 1-69$ , except that CCGGAATTCGCTGTGGCCACACTGGTCAAC and TCGCGTCGACTTATCGATCGATCCCTTCGATCTTGTC were used. To express ChlH  $\Delta 1-823$  as a His-tagged protein in *E. coli*, this PCR product was ligated into pHIS8-3 (Jez et al., 2000) between EcoR I and Sal I. The resulting plasmid was sequenced at the RTSF to confirm that no mutations were introduced during PCR. The His-tagged ChlH  $\Delta 1-823$  protein was expressed from the resulting plasmid in the *E. coli* strain BL21-CodonPlus® (DE3)-RIL (Stratagene) at  $18^{\circ}\text{C}$  in terrific broth (Sambrook and Russell, 2001). We induced expression by adding 1 mM isopropyl  $\beta$ -D-1-

thiogalactopyranoside (Sigma-Aldrich) when the OD<sub>600</sub> was 0.8. All subsequent steps were performed at 4°C, unless indicated otherwise. Cells were harvested by centrifugation at 6,000 × g for 10 min and resuspended in 20 ml buffer A (50 mM Tris-acetate, pH 7.9, 500 mM potassium acetate, 20 mM imidazole, 20 mM β-mercaptoethanol, 20% glycerol, 1% Triton X-100) per gram of bacterial pellet. Cells were lysed by sonication. The resulting lysate was clarified by centrifugation at 10,000 × g for 20 min. The supernatant was batch bound to Ni-NTA agarose (Qiagen, Valencia CA) equilibrated in buffer A. Bound proteins were batch washed twice with buffer A and twice with buffer A lacking Triton X-100. Ni-NTA agarose was poured into an Econo-Pac column (Bio-Rad, Hercules CA) and proteins were step eluted using buffer B (20 mM Tris-acetate, pH 7.9, 500 mM potassium acetate, 250 mM imidazole, 20 mM β-mercaptoethanol, 20% glycerol). Eluted proteins were dialyzed against buffer C (20 mM Tris-acetate, pH 7.9, 150 mM potassium acetate, 2.5 mM CaCl<sub>2</sub>, 20 mM β-mercaptoethanol, 20% glycerol), digested with thrombin (Sigma-Aldrich) at room temperature and applied to the aforementioned Ni-NTA agarose column equilibrated in buffer A. Proteins in the flow-through fraction were dialyzed against buffer D (20 mM Tris-acetate, pH 7.9, 100 mM potassium acetate, 1 mM EDTA, 1 mM DTT, 20 % glycerol), applied to a HiPrep™ 16/10 Q FF column (GE Healthcare, Piscataway NJ) that was equilibrated in buffer D at a flow rate of 1.0 ml/min, and eluted with a 200-ml linear gradient to buffer E (20 mM Tris acetate, pH 7.9, 1000 mM potassium acetate, 1 mM EDTA, 1 mM DTT, 20% glycerol) also at a flow rate of 1.0 ml/min. Fractions of 2.5 ml containing ChlH Δ1-823 were pooled, concentrated using an Amicon Ultra-15 centrifugal filter unit with a nominal molecular weight limit of 30,000 (Millipore),

dialyzed against storage buffer (50 mM Tricine-KOH, pH 7.9, 1 mM DTT, 50% glycerol), flash frozen with liquid N<sub>2</sub>, and stored in small aliquots at -80°C. For polyclonal antibody development, purified ChlH Δ1-823 was dialyzed extensively against phosphate-buffered saline, pH 7.4 (Sambrook and Russell, 2001) and used to develop anti-ChlH Δ1-823 polyclonal antisera in New Zealand white rabbits at Strategic Diagnostics, Inc. (Newark DE). IgGs were purified from these antisera using Affi-Gel protein A (Bio-Rad) as recommended by Harlow and Lane (Harlow and Lane, 1999). Anti-ChlH Δ1-823 antibodies were affinity-purified from total IgGs on ChlH Δ1-823 columns that were constructed by linking purified ChlH Δ1-823 to Affi-Gel 15 (Bio-Rad) at approximately 15 mg/ml. Antibodies were eluted from the ChlH Δ1-823 columns in buffer F (100 mM glycine-HCl, pH 2.5, 50% ethylene glycol) and immediately mixed with 1/10 volume 1M Tris-HCl, pH 8.0, as recommended by Harlow and Lane (Harlow and Lane, 1999). Protein-containing fractions were pooled, dialyzed against PBS, concentrated using Amicon Ultra-15 centrifugal filter units as described above, flash frozen with liquid N<sub>2</sub>, and stored at -80°C in small aliquots.

For anti-ChlI antibody development, ChlI was expressed and purified as described for ChlH Δ1-823, except that a cDNA encoding a ChlI ORF that lacks the predicted transit peptide (ChlI Δ1-60) was amplified using CCGGAATTCGCTGTGGCCCACTGGTCAAC and TCGCGTCGACTTATCGATCGATCCCTTCGATCTTGTC. ChlI Δ1-60 antibody development and affinity purification were as described for ChlH Δ1-823, except that ChlI Δ1-60, rather than ChlH Δ1-823, was linked to Affi-Gel 15.

THE  
7  
70

A

For anti-ChlD antibody development, ChlD was expressed and purified as described for ChlH  $\Delta$ 1-823, except that a cDNA encoding a ChlD ORF that lacks the first 516 residues (ChlD  $\Delta$ 1-516) was amplified using GCGGGATCCACCCTTAGAGCAGCTGCACCATAC and TCGCGTCTCGACTCAAGAATTCTTCAGATCAGATAGTGCATCC and ligated into pHis8-3 using BamHI and SalI. Another difference was that after elution from Ni-NTA agarose and thrombin digestion, ChlD  $\Delta$ 1-516 was further purified by fractionating on a HiLoad™ 26/60 Superdex™ 200 prep-grade column equilibrated in buffer G (Tris-HCl, pH 7.9, 500 mM NaCl, 1 mM EDTA, 1 mM DTT, 10% glycerol) at 2 ml/min and at 4°C. Anti-ChlD  $\Delta$ 1-516 antibodies were developed and purified as for anti-ChlH  $\Delta$ 1-823 and anti-ChlI  $\Delta$ 1-60 except that affinity purification was performed using ChlD  $\Delta$ 1-516 linked to Affi-Gel 10 rather than Affi-Gel 15.

All immunoblotting was done as previously described (Larkin et al., 2003) using SuperSignal® West Dura Extended Duration Substrate (Pierce, Rockford IL). We quantified immunoreactive bands with the VersaDoc 4000 MP and Quantity One software (Bio-Rad).

## RESULTS

*In vitro import of GUN4 into pea chloroplasts.* To test whether the porphyrin-binding activity of GUN4 affects interactions between GUN4 and chloroplast membranes, we imported GUN4 into purified pea chloroplasts *in vitro*. Because chlorophyll biosynthesis is well conserved among plant species (Eckhardt et al., 2004; Tanaka and Tanaka, 2007), we expected that GUN4 would interact similarly with



proteins associated with chloroplast membranes such as ChlH from pea and Arabidopsis. The full-length GUN4 precursor containing the transit peptide was produced by in vitro translation. During SDS-PAGE, this translation product migrated like a 30-kDa protein (Figure 2-1A), which was expected, based on the mass calculated from the derived amino acid sequence of GUN4 containing the predicted transit peptide (Larkin et al., 2003). We tested whether GUN4 could be imported into pea chloroplasts as judged by (i) a mobility shift that is consistent with the removal of the predicted 69-residue transit peptide (Larkin et al., 2003), and (ii) resistance to a trypsin protease treatment, which cannot digest proteins that are transported across the inner envelope of pea chloroplasts (Jackson et al., 1998).

After import into the pea chloroplast, GUN4 migrates as a doublet in SDS gels, with the predominant band migrating like a 22-kDa protein, consistent with the removal of the predicted transit peptide (Figure 2-1A). A similar doublet was previously observed when whole cell and various chloroplast extracts from Arabidopsis were analyzed by immunoblotting with affinity-purified anti-GUN4 antibodies (Larkin et al., 2003).

After GUN4 was imported, chloroplasts were digested with trypsin. Intact chloroplasts were then recovered using Percoll gradients, subjected to hypotonic lysis, and the soluble and membrane-containing fractions of the chloroplast were separated by centrifugation. GUN4 was observed in both the soluble and the membrane-containing pellet fractions (Figure 2-1), which indicates that GUN4 was imported into these chloroplasts and not digested by trypsin. Two control proteins, Tic40 and SS, accumulated in membrane and soluble fractions, respectively (Figure 2-1B and C), as has been previously demonstrated (Tripp et al., 2007).

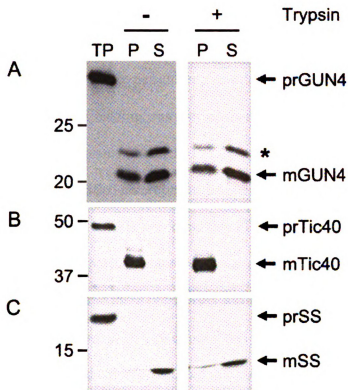


Figure 2-1. Distribution of GUN4, Tic40, and SS in fractionated chloroplasts. *A.* Distribution of GUN4 in fractionated pea chloroplasts. [ $^3\text{H}$ ]-labeled GUN4 leucine was imported into intact pea chloroplasts. Following the import reaction, chloroplasts were treated with (+) or without (-) trypsin. Intact chloroplasts were recovered by centrifugation through a 40% Percoll cushion, lysed, and fractionated into soluble (S) and membrane-containing pellet (P) fractions. All fractions were then analyzed by SDS-PAGE and fluorography. TP represents approximately 10% of the precursor added to an import assay. The position of the GUN4 precursor containing the transit peptide (prGUN4) and the major form of mature GUN4 generated by proteolytic removal of the transit peptide during import into the chloroplast (mGUN4) and a minor form of mature GUN4 (\*) are indicated. *B.* Distribution of Tic40 in fractionated pea chloroplasts. Chloroplast import and analysis were as described in *A* except that [ $^{35}\text{S}$ ]-labeled Tic40 was used rather than [ $^3\text{H}$ ]-labeled GUN4. *C.* Distribution of SS in fractionated pea chloroplasts. Chloroplast import and analysis were as described in *A* except that [ $^{35}\text{S}$ ]-labeled SS was used rather than [ $^3\text{H}$ ]-labeled GUN4. Masses of protein standards are indicated at the left in kDa.

*Subchloroplastic distribution of GUN4 in ALA-fed chloroplasts.* To test whether porphyrin binding might affect the interactions between GUN4 and chloroplast membranes, we imported GUN4 into pea chloroplasts that were fed with ALA prior to initiating protein import. ALA feeding was previously reported to induce the levels of PPIX and Mg-PPIX in whole plants (Granick, 1961; Gough, 1972) and to increase the levels of heme efflux from purified chloroplasts (Thomas and Weinstein, 1990). Consistent with these previous reports, we found that PPIX and Mg-PPIX levels increased 20- to 30-fold when purified chloroplasts were fed ALA under these conditions (Figure 2-2A) and that these porphyrins accumulated in the membrane-containing pellet fraction (Figure 2-2B). We found that half of GUN4 associated with the membrane fraction in unfed chloroplasts, and that the amount of GUN4 in the membrane fraction increased by 50% in ALA-fed chloroplasts (Figure 2-2C and D). In contrast, the distribution of Tic40 and SS did not change after ALA feeding (Figure 2-1A and B). Additionally, ALA feeding did not appear to change the total protein profile of the soluble and pellet fractions (Figure 2-3C). ALA feeding did not affect the nature of GUN4-chloroplast membrane interactions as judged by extracting chloroplast membranes with either Na<sub>2</sub>CO<sub>3</sub>, pH 11, or NP40 (Figure 2-4A and B). These data are consistent with (i) elevated porphyrin levels causing GUN4 to accumulate in the membrane-containing pellet fraction after GUN4 has been imported into the chloroplast, but also with (ii) the distinct targeting of GUN4 to the stroma and to the chloroplast membranes and ALA feeding inhibiting stromal targeting. To distinguish between these possibilities, we fed ALA to chloroplasts following the import of GUN4. We found that ALA feeding subsequent to the import of GUN4 leads to increased levels

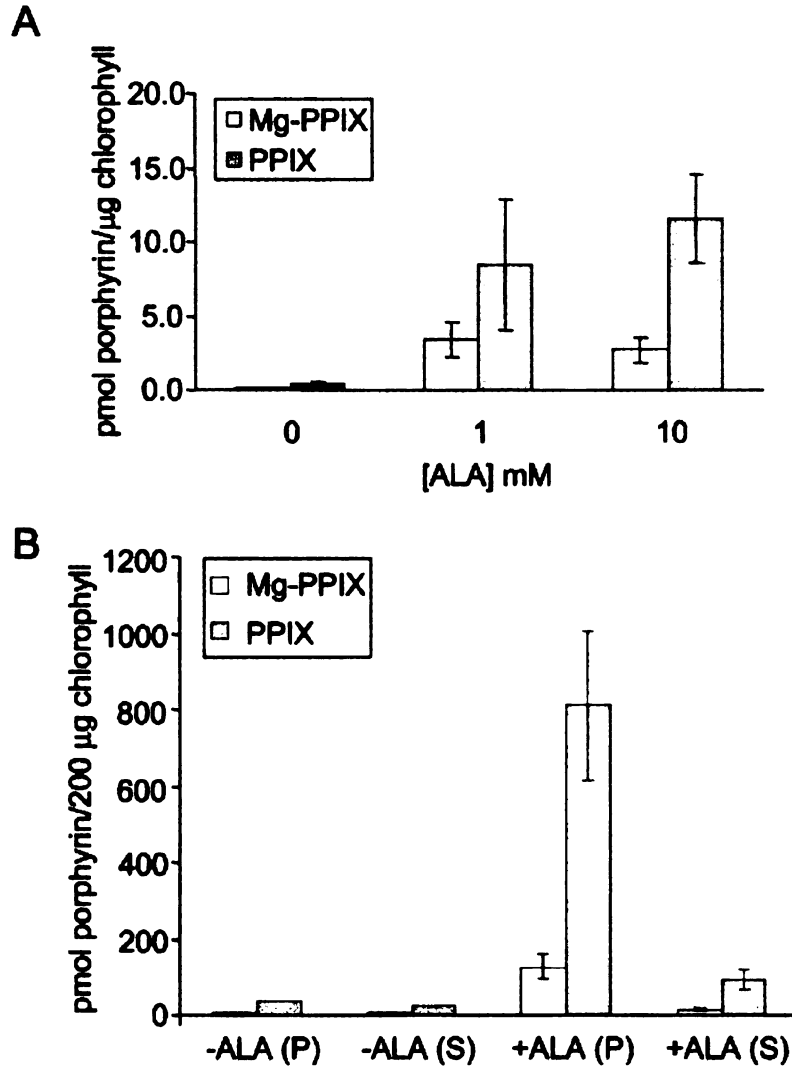


Figure 2-2. Subchloroplastic distribution of PPIX, Mg-PPIX, and GUN4 after ALA feeding. *A*. Quantitation of PPIX and Mg-PPIX levels in ALA-fed chloroplasts. PPIX and Mg-PPIX levels were quantitated in intact chloroplasts that had been treated with 0 mM, 1.0 mM, or 10 mM ALA. *N*=3. Error bars represent standard error. *B*.

Distribution of PPIX and Mg-PPIX in fractionated ALA-fed chloroplasts. Chloroplasts were fed with 10 mM ALA as in *A*. After ALA feeding, chloroplasts were lysed and separated in soluble (S) and membrane-containing pellet (P) fractions. PPIX and Mg-PPIX levels were determined in each fraction. *N*=3. *C*. Distribution of GUN4 in fractionated chloroplasts after ALA feeding. Chloroplasts were fed with ALA as described in *A*. Import and post-import analysis of GUN4 was performed as described in Figure 2-1A. Masses of protein standards are indicated at the left in kDa. *D*.

Quantitation of GUN4 in soluble and membrane fractions after ALA feeding. The amounts of radiolabeled GUN4 in soluble (S) and membrane-containing pellet (P) fractions were quantitated in independent experiments that were performed as in *C*, using different preparations of chloroplasts. The amount of [ $^3$ H]-GUN4 found either in the soluble (S) or pellet (P) fraction is presented as a percentage of total imported [ $^3$ H]-GUN4. Column numbers correspond to lane numbers in *B*. *N*=3. Error bars are as in *A*.

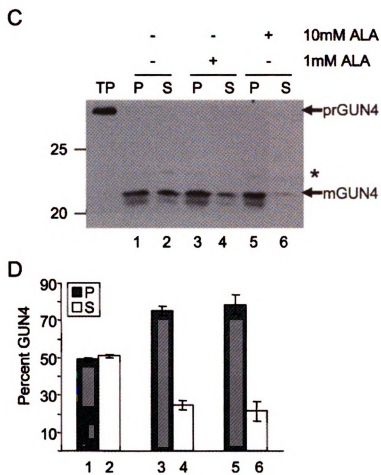


Figure 2-2 (continued). Subchloroplasmic distribution of PPIX, Mg-PPIX, and GUN4 after ALA feeding.

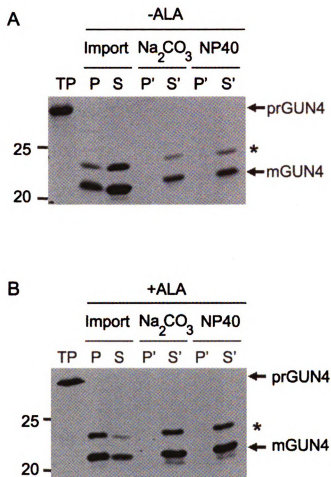


Figure 2-3. Subchloroplast distribution of Tic40, SS, and total protein after ALA feeding. *A.* Subchloroplast distribution of Tic40 after ALA feeding. ALA feeding was as described in Figure 2-2A. Import, chloroplast fractionation, and analysis of Tic40 were as described in Figure 2-1B. *B.* Subchloroplast distribution of SS after ALA feeding. ALA feeding was as described in Figure 2-2A. Import and analysis of SS were as described in Figure 2-1B. *C.* Subchloroplast distribution of total chloroplast protein after ALA feeding. ALA feeding was as described in Figure 2-2A. After ALA feeding, a mock import was performed as described in Figure 2-1A, without radiolabeled precursor proteins. All fractions were analyzed by SDS-PAGE and Coomassie blue staining. Masses of protein standards are indicated at the left in kDa.

THE

7

20

H

C

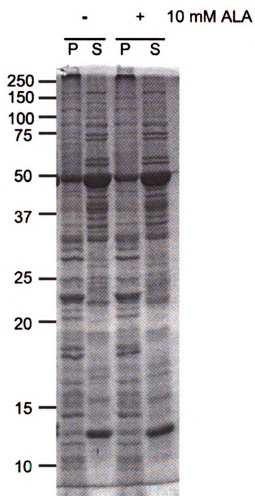


Figure 2-3 (continued). Subchloroplast distribution of Tic40, SS, and total protein after ALA feeding.

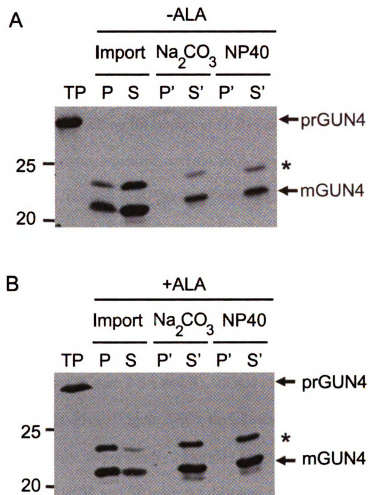


Figure 2-4. Analysis of GUN4-chloroplast membrane interactions in chloroplasts that were fed or not fed ALA. *A*. Analysis of interactions between GUN4 and chloroplast membranes in chloroplasts that were not fed ALA. [<sup>3</sup>H]-GUN4 was imported into pea chloroplasts. After import and chloroplast fractionation, a portion of the pellet fraction (P) was extracted with either Na<sub>2</sub>CO<sub>3</sub> or NP40 for 30 min on ice and centrifuged. A pellet fraction (P') containing integral membrane proteins and a soluble fraction (S') containing extracted proteins were obtained. All fractions were then analyzed by SDS-PAGE and fluorography. TP represents approximately 10% of precursor added to an import assay. *B*. Analysis of GUN4-chloroplast membrane interactions in ALA-fed chloroplasts. [<sup>3</sup>H]-GUN4 was imported into chloroplasts that had been pretreated with ALA. Analysis of the ALA-fed chloroplasts was as described in *A*. Masses of protein standards are indicated at the left in kDa.

of PPIX and Mg-PPIX and causes GUN4 to redistribute to the membrane-containing pellet fraction (Figure 2-5A, B, and C). Based on these data, we conclude that inducing a rise in PPIX and Mg-PPIX levels by ALA feeding causes GUN4 to accumulate in the pellet fraction rather than blocking the import of GUN4 into the stroma. GUN4 was previously detected in stroma, envelope, and thylakoid fractions derived from purified *Arabidopsis* chloroplasts (Larkin et al., 2003). To test whether ALA feeding preferentially causes the accumulation of GUN4 in the chloroplast envelope or thylakoid membranes, we imported GUN4 into chloroplasts that were either fed or not fed ALA and then compared the levels of GUN4 in the stromal, envelope, and thylakoid fractions. We found that ALA feeding caused GUN4 levels to increase in the envelope and thylakoid membranes (Figure 2-6A and B). In this experiment, Tic40, LHCP, and SS accumulated in the envelope (Figure 2-6C), thylakoids (Figure 2-6D), and stroma (Figure 2-6E), respectively, as previously reported (Tripp et al., 2007). The levels and distributions of Tic40, LHCP, and SS were not different from those previously reported after ALA feeding (Figure 2-6C, D, and E). To test whether the tendency of ALA to cause accumulation of GUN4 in the membrane-containing fractions was unique to the newly imported radiolabeled GUN4 or whether a similar affect might be observed with the endogenous pea GUN4, we monitored the distribution of pea GUN4 in the soluble and membrane fractions of purified pea chloroplasts after ALA feeding. We detected an immunoreactive band with essentially the same mobility as GUN4 during SDS-PAGE and found a 22% increase in the membrane-containing fraction and the same fold decrease in the soluble fraction after ALA feeding that caused PPIX and Mg-PPIX levels to increase (Figure 2-7A, B, C).

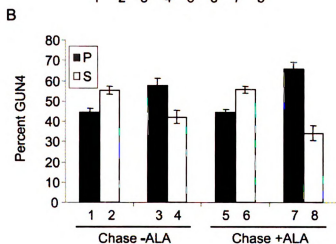
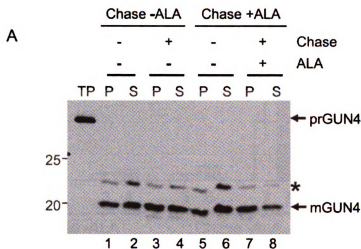


Figure 2-5. Subchloroplastic distribution of GUN4 following post-import ALA feeding.

**A.** Representative fluorogram showing the subchloroplastic distribution of GUN4 following post-import ALA feeding. [ $^3\text{H}$ ]-GUN4 was imported for 15 min into pea chloroplasts. Intact chloroplasts were recovered by centrifugation through a 40% Percoll cushion. A portion of the recovered chloroplasts was directly lysed and fractionated into either total soluble (S) or total membrane (P) fractions (Lanes 1-2 and 5-6). The remaining portion of chloroplasts was resuspended in import buffer containing ALA (Lanes 7-8) or lacking ALA (Lanes 3-4) and incubated for an additional 15 min at 26°C (Chase). The 'Chase' reactions were terminated by centrifuging the chloroplasts through a 40% Percoll cushion. Chloroplasts were then lysed and fractionated. Membrane-containing pellet fractions (P) or soluble (S) fractions were analyzed by SDS-PAGE and fluorography. TP represents approximately 10% of precursor added to an import assay. **B.** Quantitation of the subchloroplastic distribution of GUN4 following post-import ALA feeding. GUN4 found in the soluble (S) or pellet (P) fraction is presented as a percentage of the total amount of imported protein. Column numbers 1-8 correspond to lane numbers 1-8 in **A**. Error bars represent standard error.  $N=3$ . **C.** Quantitation of PPIX and Mg-PPIX in intact chloroplasts represented in **A**. Column numbers 1-8 correspond to lane numbers 1-8 in **A**. Error bars are as in **B**.

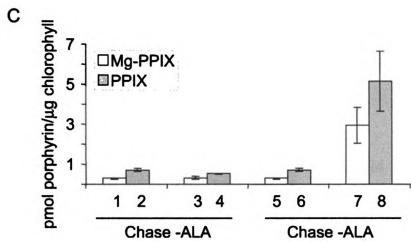


Figure 2-5 (continued). Subchloroplasmic distribution of GUN4 following post-import ALA feeding.

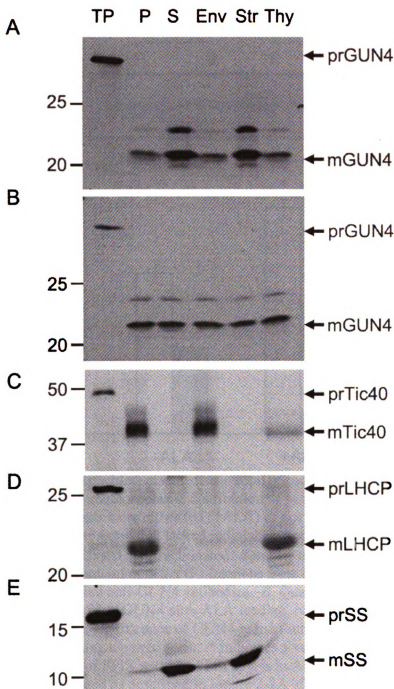


Figure 2-6. Distribution of GUN4 in the chloroplast envelope, thylakoid, and stroma fractions after ALA feeding. *A*, Chloroplasts were either pretreated without, or *B*, with ALA prior to the import of [ $^3$ H]GUN4. Control import assays with ALA-fed chloroplasts were likewise performed with *C*, [ $^{35}$ S]-prTic40; *D*, [ $^3$ H]prLHCP; and *E*, [ $^{35}$ S]-prSS. After import, chloroplasts were lysed and fractionated into soluble (S) and membrane-containing pellet fractions (P), or chloroplasts were separated into envelope (Env), stromal (Str) and thylakoid (Thy) fractions. All fractions were analyzed by SDS-PAGE as an equal load, using fluorography.

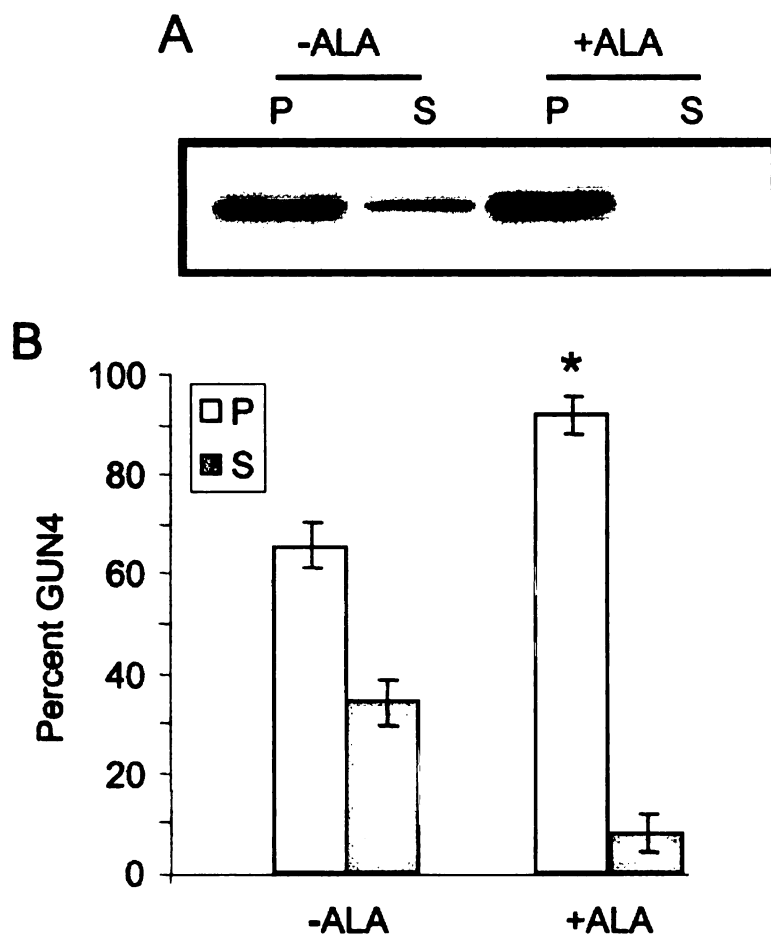


Figure 2-7. Subchloroplastic distribution of pea GUN4 and porphyrin levels after ALA feeding. *A*. Subchloroplastic distribution of pea GUN4 following ALA feeding. Intact pea chloroplasts were either fed (+ALA) or not fed (-ALA) ALA and then subjected to a mock import assay that lacked radiolabeled proteins. These chloroplasts were subsequently lysed and fractionated. Samples of 7  $\mu$ g of protein from soluble (S) and membrane-containing pellet (P) fractions were analyzed by immunoblotting with affinity-purified anti-GUN4 antibodies. *B*. Quantitation of the subchloroplastic distribution of pea GUN4 after ALA feeding. N=5. Error bars represent standard error. The statistical significance of GUN4 redistributing to the pellet during ALA feeding was tested using a paired t-test. \* indicates a very significant difference (P=0.008). *C*. Quantitation of PPIX and Mg-PPIX levels in ALA-fed chloroplasts. Porphyrin levels were quantitated as described in Figure 2-2A after ALA feeding as described in Figure 2-6A and B. N=5. Error bars are as in *B*.

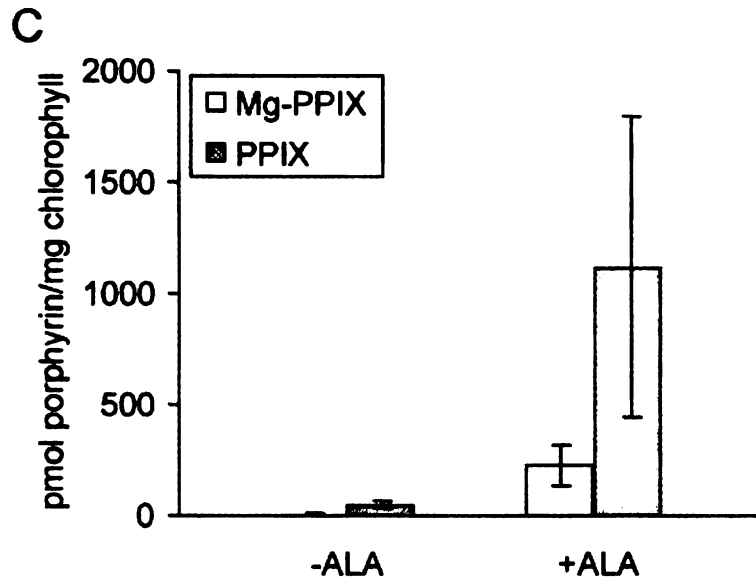


Figure 2-7 (continued). Subchloroplastic distribution of pea GUN4 and porphyrin levels after ALA feeding.

1  
2

H

*Quantitation of porphyrin binding by GUN4.* The above findings are consistent with either porphyrin binding causing GUN4 to accumulate in the membrane-containing pellet fraction or ALA feeding somehow promoting interactions between GUN4 and chloroplast membranes by some other mechanism. To distinguish between these possibilities, we took advantage of a previous structure-function analysis of SynGUN4 (Verdecia et al., 2005). Based on this previous work, we made 11 single amino acid changes in GUN4 using site-directed mutagenesis (Table 2-2). Homologous amino acid substitutions in SynGUN4 cause general defects in porphyrin binding or specific defects in binding either DPIX or Mg-DPIX (Verdecia et al., 2005). We also introduced the L88F substitution from the *gun4-1* missense allele. This amino acid substitution causes the GUN4 protein to accumulate at much lower levels in vivo compared to the wild type. An F substitution at the homologous L residue in *Thermosynechococcus elongatus* GUN4 and SynGUN4 causes a 6- to 15-fold increase in the affinities for DPIX and Mg-DPIX without affecting folding in the case of *T. elongatus* GUN4 (Davison et al., 2005). We expressed these site-directed mutants as GST-fusion proteins without the predicted 69-residue transit peptide, as previously described (Larkin et al., 2003). Six of these amino acid substitutions, including the L88F, caused GST-GUN4  $\Delta$ 1-69 to accumulate in the insoluble fraction (Table 2-2) and were not analyzed further. The remaining seven amino acid substitutions did not affect the solubility of GST-GUN4  $\Delta$ 1-69 in *E. coli* (Table 2-2) and were purified.

We determined the  $K_d^{\text{DPIX}}$  and  $K_d^{\text{Mg-DPIX}}$  for GUN4 (Table 2-3; Figure 2-8). During the course of these studies, we observed that including 1% DMSO in binding assays does not significantly affect the  $K_d^{\text{DPIX}}$  or the  $K_d^{\text{Mg-DPIX}}$  and that including 1%

7  
2



**Table 2-2.** Solubilities of GST-GUN4 $\Delta$ 1-69 containing the indicated amino acid substitutions when expressed in *E. coli*.

Amino acid substitutions in SynGUN4 that affect porphyrin binding	Homologous amino acid substitutions in GUN4	Solubilities of GST-GUN4 $\Delta$ 1-69 with the indicated amino acid substitutions
Wild type	Wild type	soluble
L100F	L88F	insoluble
L116A	L103A	insoluble
F132W	F120W	soluble
V135A	V123A	soluble
L143A	L131A	insoluble
I146A	I134A	insoluble
F196A	F191A	soluble
D199A	E194A	insoluble
R214A	R211A	soluble
R217A	Q214A	soluble
R217E	Q214E	soluble
A219G	L216G	insoluble

All amino acid substitutions in SynGUN4 that affect either or both  $K_d^{\text{DPIX}}$  and  $K_d^{\text{Mg-DPIX}}$  were reported by (Verdecia et al., 2005). L88F is the amino acid substitution caused by the *gun4-1* missense allele (Larkin et al., 2003). GST-GUN4  $\Delta$ 1-69 accumulated in either the soluble or the insoluble fraction when expressed in *E. coli*.

DMSO in binding assays solubilizes PPIX and Mg-PPIX sufficiently for us to perform binding assays with these natural ligands, which has not been reported for GUN4 from any species. We determined that the  $K_d^{\text{PPIX}}$  was almost twofold higher than  $K_d^{\text{DPIX}}$  and that the  $K_d^{\text{Mg-PPIX}}$  was 1.5-fold lower than  $K_d^{\text{Mg-DPIX}}$  (Table 2-3; Figure 2-9).

Based on previously published biochemical and genetic data, we suggest that the major function of GUN4 in vivo is to stimulate Mg-PPIX biosynthesis (Larkin et al., 2003; Davison et al., 2005; Verdecia et al., 2005). Nonetheless, we cannot rule out that GUN4 might participate in other reactions. To begin exploring this possibility, we tested whether GUN4 might bind other porphyrins. We performed binding assays with Mg-PPIX ME, which is the next chlorophyll precursor downstream of Mg-PPIX in the chlorophyll biosynthetic pathway. In this preparation of Mg-PPIX ME, either carboxyl group is methylated in a roughly 1:1 ratio. In contrast, only the carboxyl group associated with ring C is methylated in nature (Tanaka and Tanaka, 2007). We found that the  $K_d^{\text{Mg-PPIX ME}}$  was more than twofold higher than  $K_d^{\text{Mg-PPIX}}$  (Table 2-3; Figure 2-9). We found that GUN4 also binds uroporphyrin III, coproporphyrin III, hemin, and pheophorbide *a* (Table 2-3; Figure 2-10) and that the affinities of GUN4 for these porphyrins is intermediate between Mg-PPIX ME and PPIX.

The amino acid substitutions F120W, E194A, and Q214E in GUN4 did not affect  $K_d^{\text{DPIX}}$  and  $K_d^{\text{Mg-DPIX}}$  (N.D.A., unpublished data). The homologous substitutions (i.e., F132W, D199A, and R217E) significantly reduced the affinity of SynGUN4 for porphyrins (Verdecia et al., 2005). Amino acid substitutions V123A, F191A, and R211A caused both  $K_d^{\text{DPIX}}$  or  $K_d^{\text{Mg-DPIX}}$  to increase in GUN4 (Table 2-4; Figure 2-11A, B, and C), although the degrees of the porphyrin-binding defects were not exactly as

7  
7  
7



Table 2-3. Quantitation of porphyrin binding by GUN4

Porphyrin	1% DMSO	$K_d$ ( $\mu$ M)
DPIX	-	$6.4 \pm 0.21$
DPIX	+	$6.0 \pm 0.39$
Mg-DPIX	-	$2.7 \pm 0.29$
Mg-DPIX	+	$2.2 \pm 0.30$
PPIX	+	$11 \pm 0.50$
Mg-PPIX	+	$1.6 \pm 0.17$
Mg-PPIX ME	+	$4.0 \pm 0.20$
Hemin	+	$8.1 \pm 0.75$
Uroporphyrin III	+	$10 \pm 0.57$
Coproporphyrin III	+	$15 \pm 0.82$
Pheophorbide <i>a</i>	+	$3.8 \pm 0.33$

Binding reactions were performed with (+) or without (-) 1% DMSO.

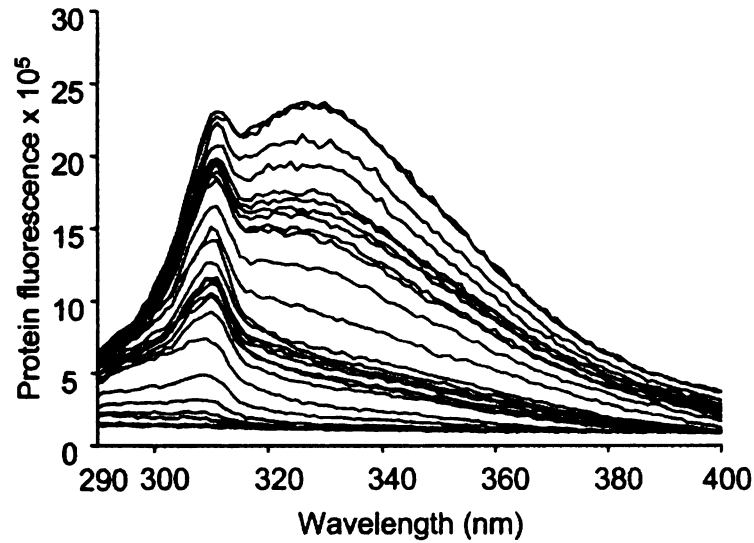
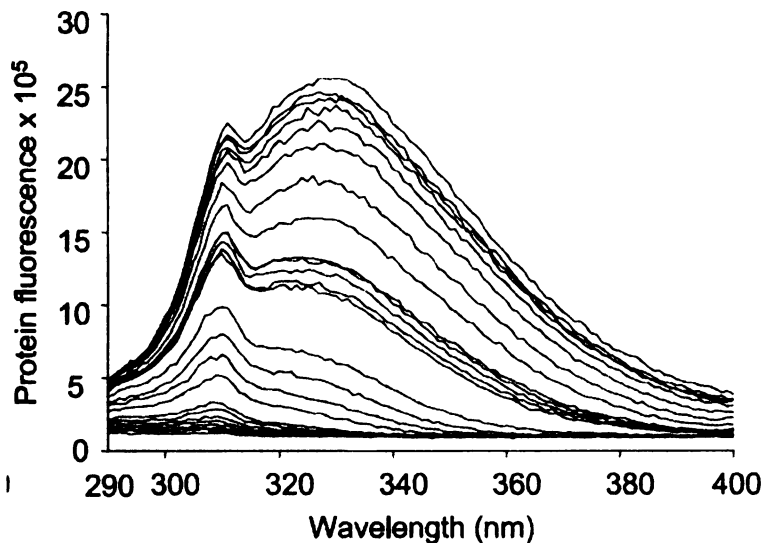
**A****B**

Figure 2-8. Quantitative analysis of GUN4-binding DPIX and Mg-DPIX. *A*. Emission spectra of GUN4 with various amounts of Mg-DPIX. Emission spectra were recorded at 25°C using an excitation wavelength of 280 nm. A series of spectra that show the quenching of GUN4 protein fluorescence by increasing concentrations of Mg-DPIX is presented. *B*. Emission spectra of GUN4 with various amounts of DPIX. Emission spectra were recorded and are presented as in *A*, except that DPIX, rather than Mg-DPIX, was used to quench GUN4 protein fluorescence. *C*. GUN4 fluorescence quenching by Mg-DPIX. GUN4 protein fluorescence was measured in the presence of increasing concentrations of Mg-DPIX. The inset shows 20  $\mu\text{g}$  of purified GUN4 analyzed by SDS-PAGE and Coomassie staining. *D*. GUN4 fluorescence quenching by DPIX. GUN4 protein fluorescence was measured as in *C*, except that protein fluorescence was quenched by increasing concentrations of DPIX.

7  
2



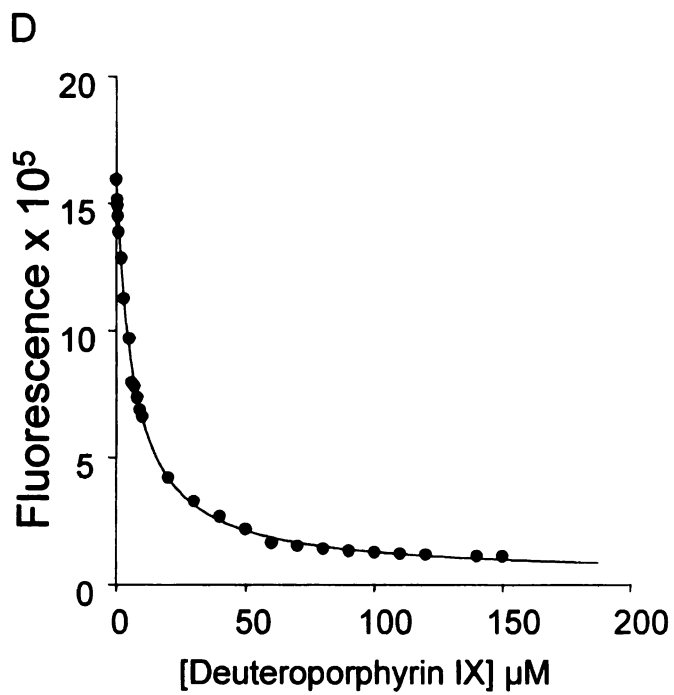
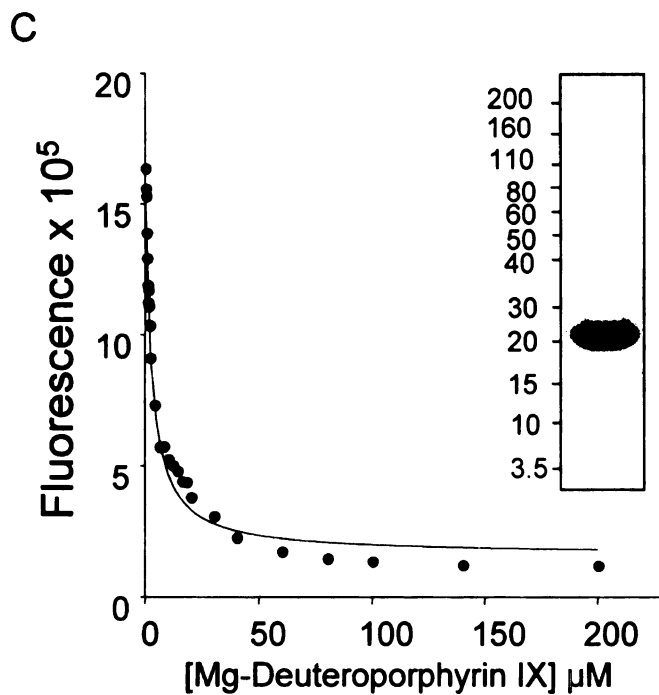
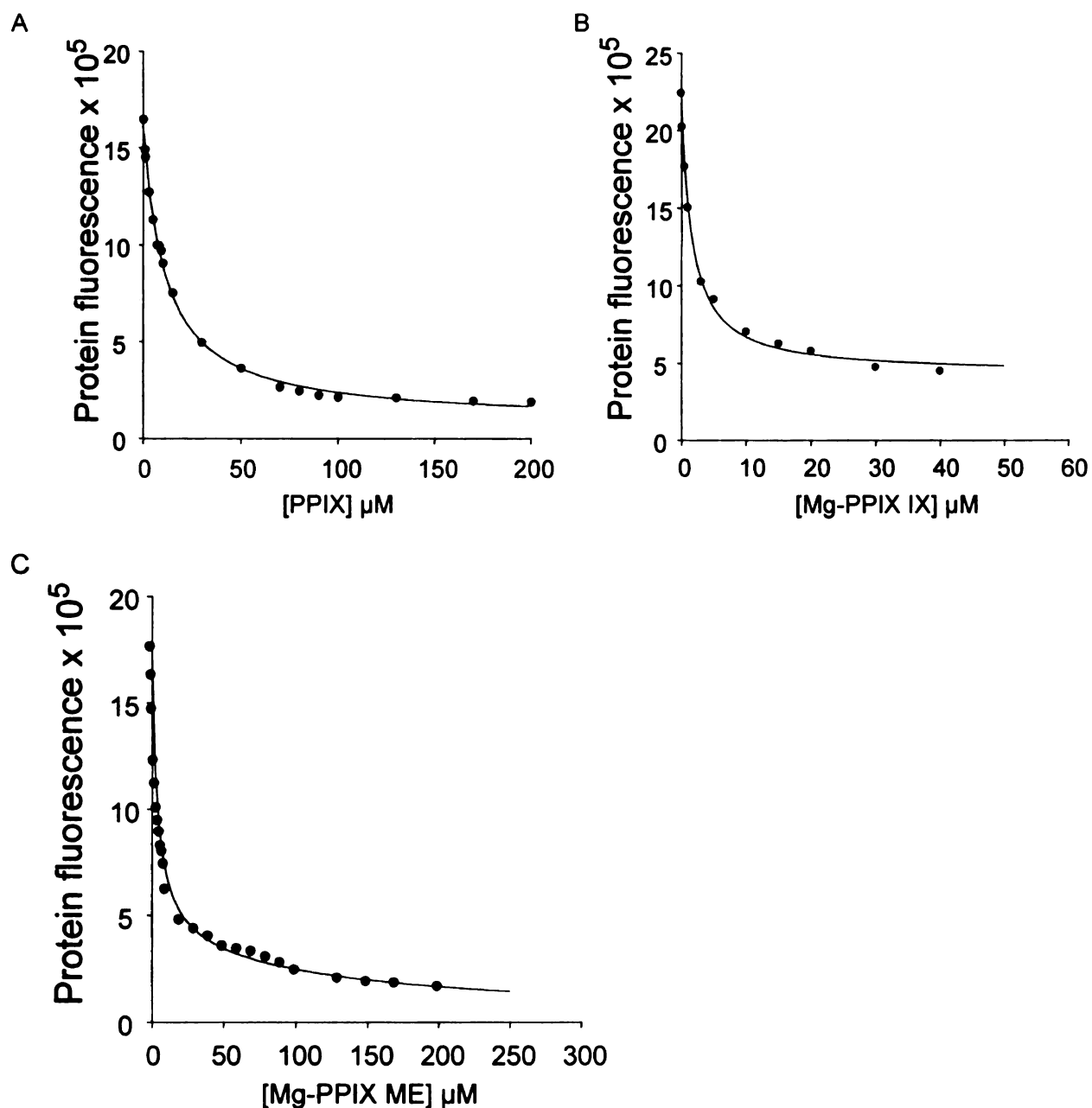


Figure 2-8 (continued). Quantitative analysis of GUN4-binding DPIX and Mg-DPIX.  
 A. Emission spectra of GUN4 with various amounts of Mg-DPIX.

7  
7

7



**Figure 2-9.** Quantitative analysis of GUN4 binding PPIX, Mg-PPIX, and Mg-PPIX ME. *A.* GUN4 fluorescence quenching by PPIX. GUN4 protein fluorescence was measured in the presence of increasing concentrations of PPIX. *B.* GUN4 fluorescence quenching by Mg-PPIX. GUN4 protein fluorescence was measured in the presence increasing concentrations of Mg-PPIX. *C.* GUN4 fluorescence quenching by Mg-PPIX ME. GUN4 protein fluorescence was measured in the presence of increasing concentrations of Mg-PPIX ME.



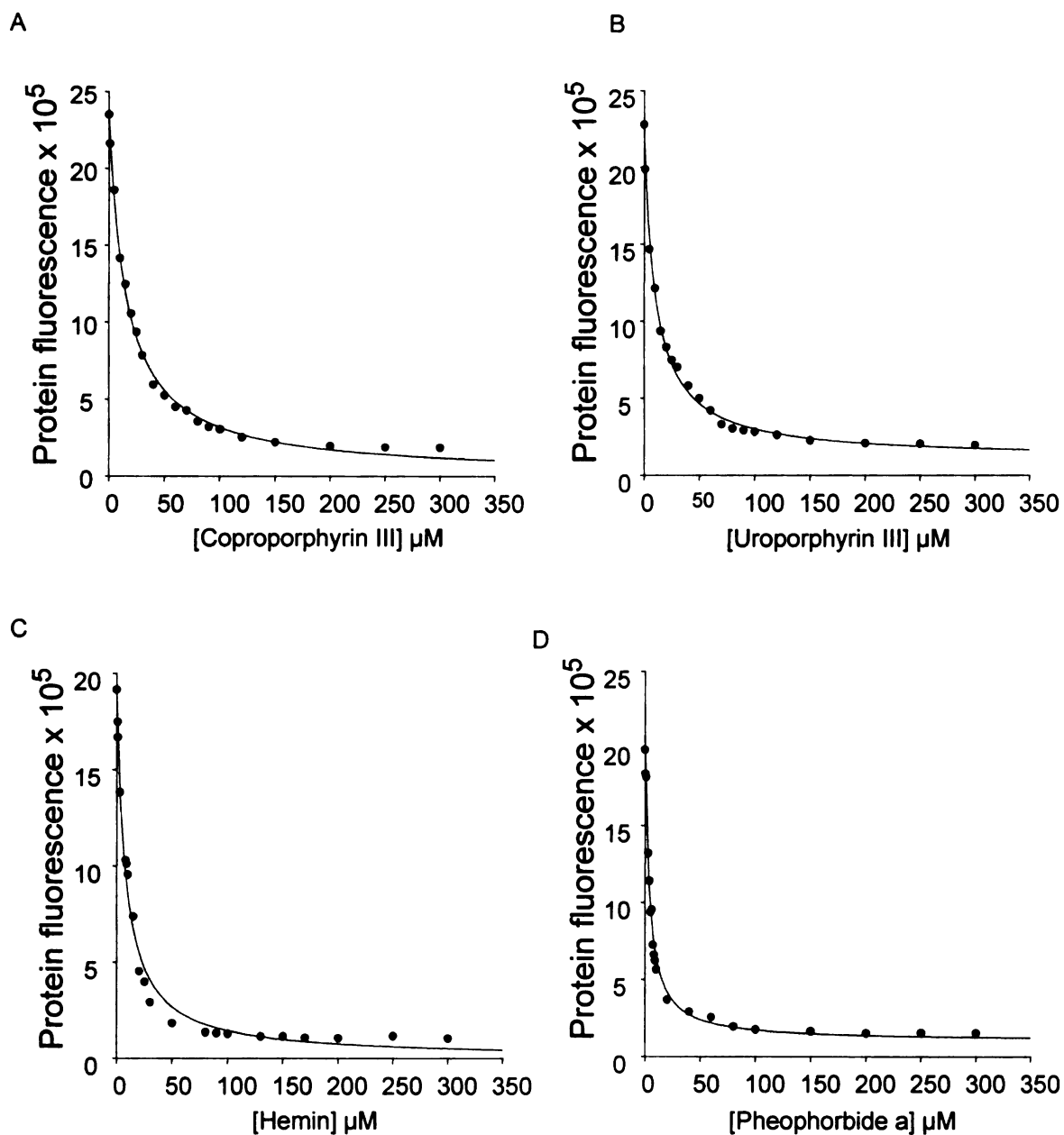
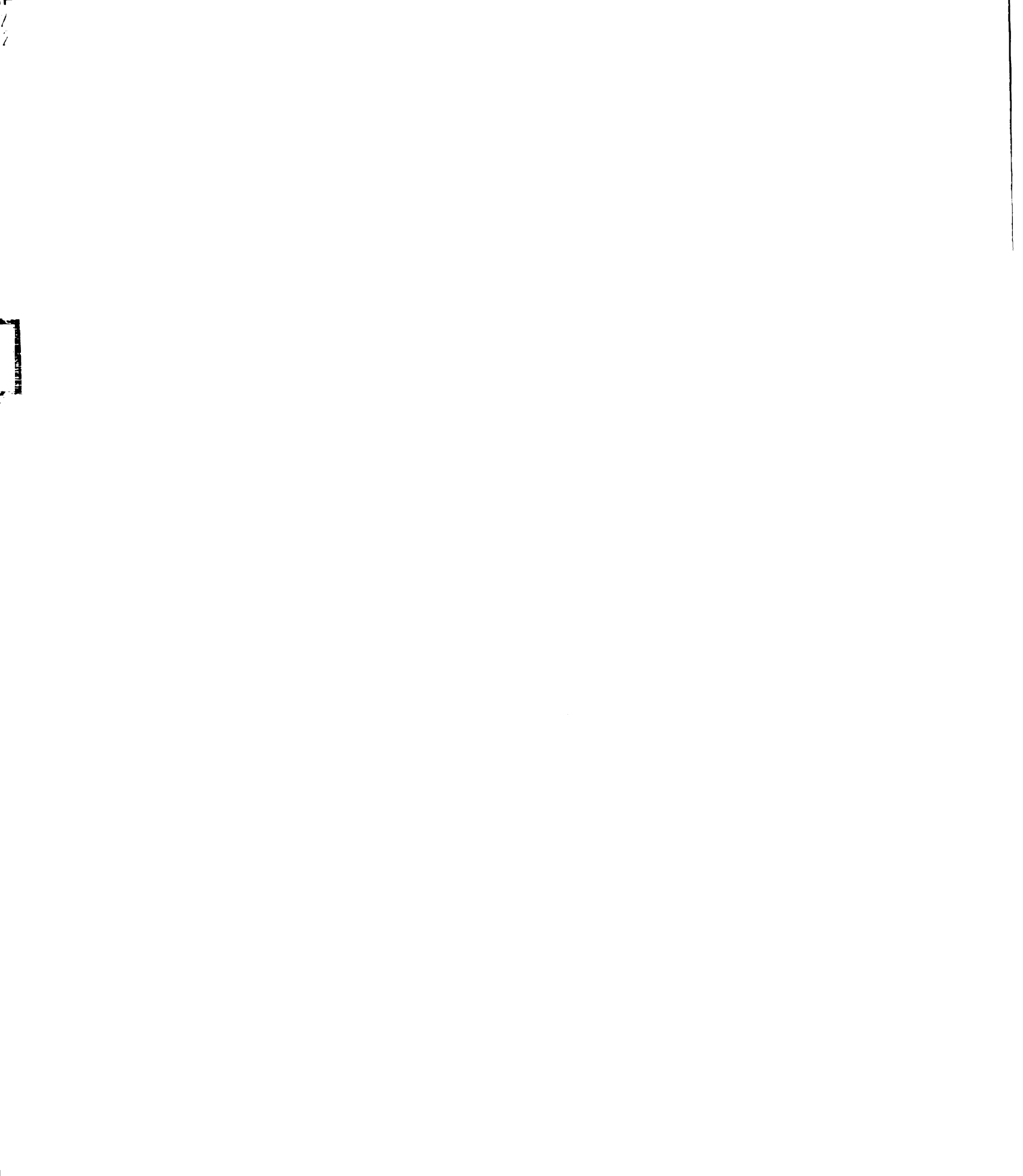


Figure 2-10. Quantitative analysis of GUN4 binding uroporphyrin III, coproporphyrin III, hemin, and pheophorbide *a*. *A*. GUN4 fluorescence quenching by uroporphyrin III. GUN4 protein fluorescence was measured in the presence of increasing concentrations of uroporphyrin III. *B*. GUN4 fluorescence quenching by coproporphyrin III. GUN4 protein fluorescence was measured in the presence of increasing concentrations of coproporphyrin III. *C*. GUN4 fluorescence quenching by hemin. GUN4 protein fluorescence was measured in the presence of increasing concentrations of hemin. *D*. GUN4 fluorescence quenching by pheophorbide *a*. GUN4 protein fluorescence was measured in the presence of increasing concentrations of pheophorbide *a*.



observed for the homologous residues (i.e., V135A, F196A, and R214A) in SynGUN4 (Verdecia et al., 2005). The solubilities of PPIX and Mg-PPIX were not sufficient for us to quantitate the affinities of F191A, V123A, and R211A for these natural ligands (N.D.A., unpublished data).

*Subchloroplastic distribution of GUN4 proteins with porphyrin-binding defects.*

To test whether porphyrin-binding defects might affect interactions between GUN4 and chloroplast membranes, we imported F191A, V123A, and R211A into ALA-fed chloroplasts and fractionated these chloroplasts into soluble and membrane-containing pellet fractions. A smaller percentage of V123A associated with the membrane-containing pellet fraction compared to the wild-type GUN4, and barely detectable levels of F191A and R211A were found in the pellet fraction (Figure 2-12). Additionally, and in contrast to wild-type GUN4, ALA feeding did not affect the subchloroplastic distribution of F191A, V123A, or R211A (Figure 2-12).

*Mg-chelatase activity in chloroplast membranes of ALA-fed chloroplasts.*

Because GUN4 binds ChlH and stimulates Mg-chelatase (Larkin et al., 2003; Davison et al., 2005; Verdecia et al., 2005), the finding that boosting PPIX and Mg-PPIX levels in purified chloroplasts by ALA feeding causes GUN4 to accumulate in the membrane-containing pellet fraction suggests that ALA feeding might affect the Mg-chelatase activity that was previously reported to associate with pea chloroplast membranes (Walker and Weinstein, 1991).

1  
2



Table 2-4. Quantitation of DPIX and Mg-DPIX binding by GUN4 containing the indicated amino acid substitutions

Substitution	$K_d^{\text{DPIX}}$ ( $\mu\text{M}$ )	$K_d^{\text{Mg-DPIX}}$ ( $\mu\text{M}$ )
V123A	$9.6 \pm 0.44$	$8.0 \pm 0.44$
F191A	$12 \pm 0.77$	$7.7 \pm 0.37$
R211A	$14 \pm 0.83$	$14 \pm 0.64$

7  
7

7

A

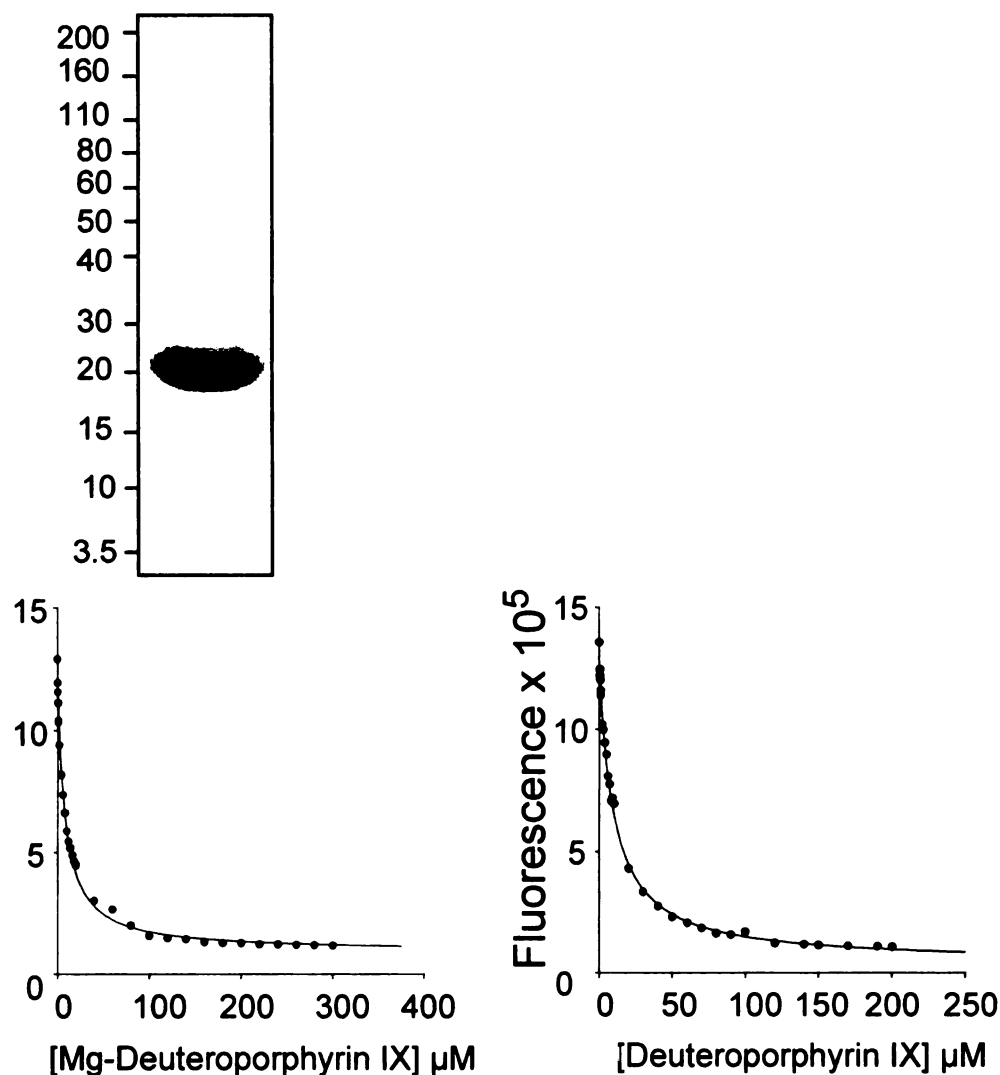


Figure 2-11. Quantitative analysis of V123A, F191A, and R211A binding DPIX and Mg-DPIX. *A.* Quantitative analysis of V123A binding Mg-DPIX and DPIX. Purified GUN4 (20  $\mu$ g) containing the V123A substitution was analyzed by SDS-PAGE and Coomassie staining (left). Fluorescence of GUN4 containing the V123A substitution was measured in the presence of increasing concentrations of Mg-DPIX (middle) or DPIX (right). *B.* Quantitative analysis of F191A binding Mg-DPIX and DPIX. Purified GUN4 (20  $\mu$ g) containing the F191A substitution was analyzed by SDS-PAGE and Coomassie staining (left). Fluorescence of GUN4 containing the F191A substitution was measured in the presence of increasing concentrations of Mg-DPIX (middle) or DPIX (right). *C.* Quantitative analysis of R211A binding Mg-DPIX and DPIX. Purified GUN4 (20  $\mu$ g) containing the R211A substitution was analyzed by SDS-PAGE and Coomassie staining (left). Fluorescence of GUN4 containing the R211A substitution was measured in the presence of increasing concentrations of Mg-DPIX (middle) or DPIX (right).

7  
7

7

**B**

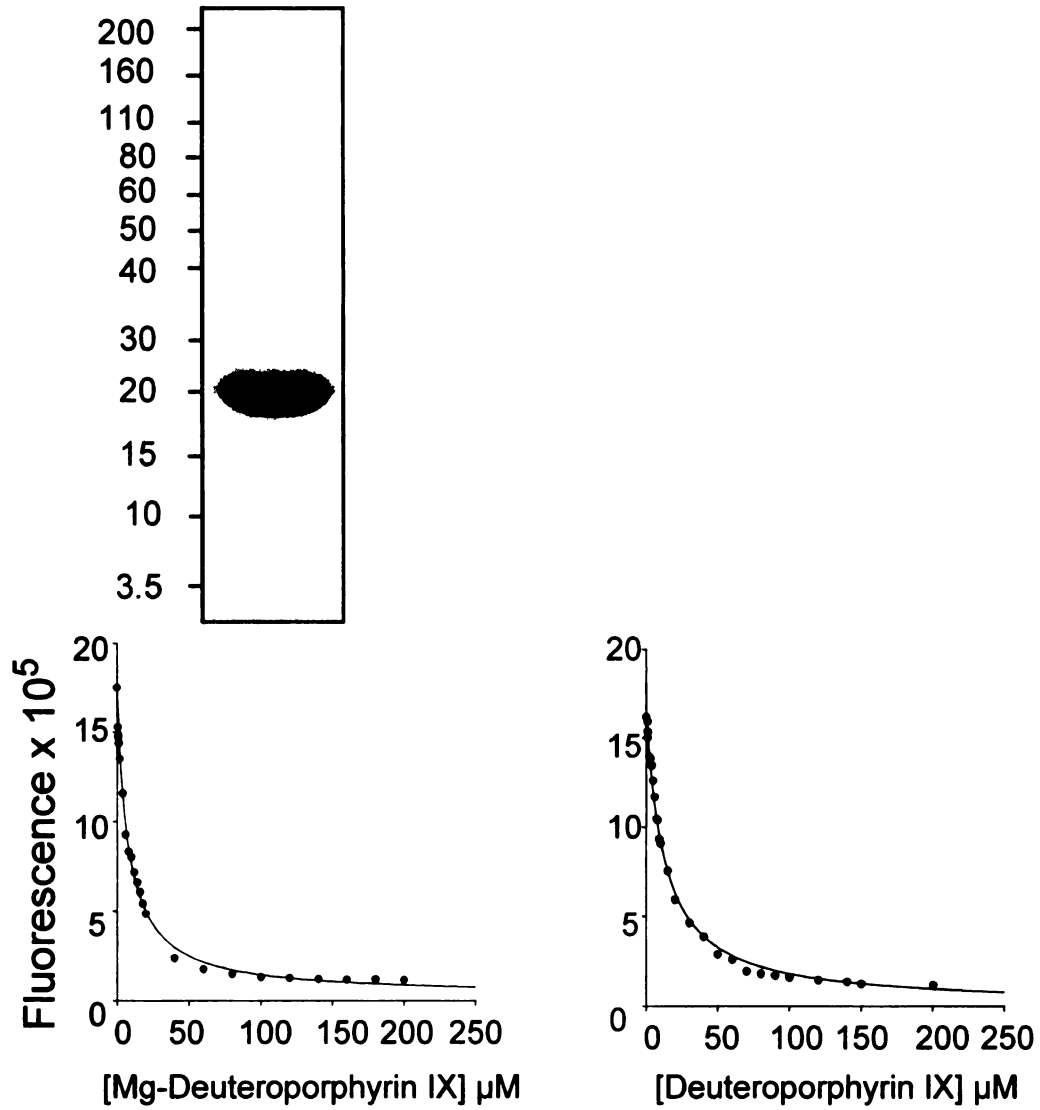


Figure 2-11 (continued). Quantitative analysis of V123A, F191A, and R211A binding DPIX and Mg-DPIX.

1  
2



C

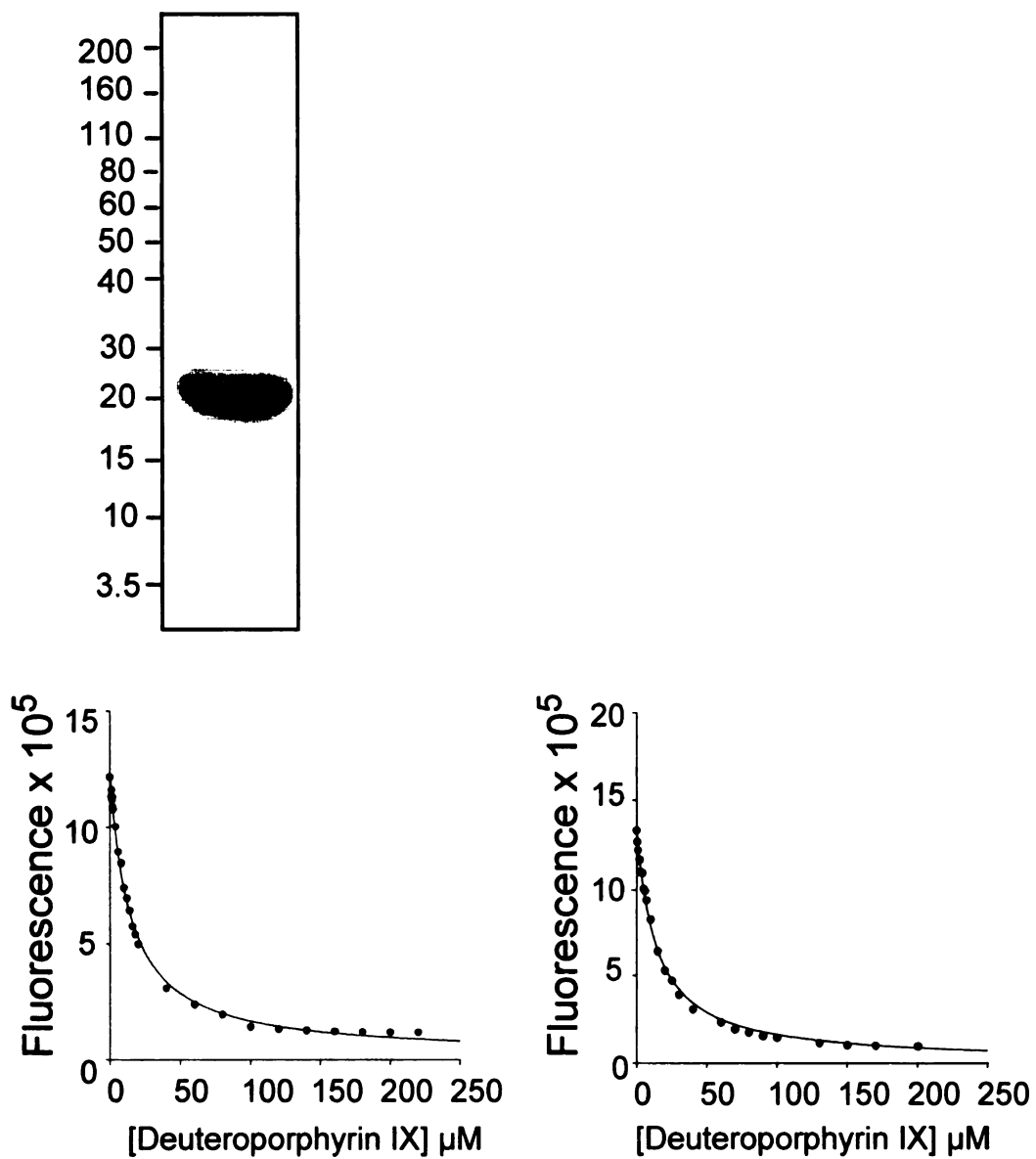


Figure 2-11 (continued). Quantitative analysis of V123A, F191A, and R211A binding DPIX and Mg-DPIX.

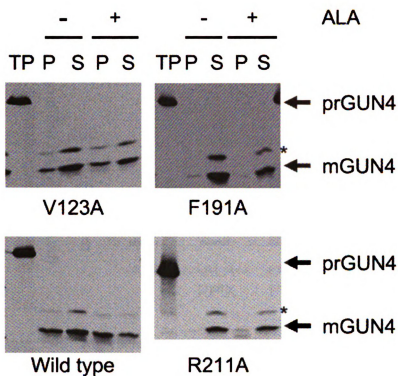
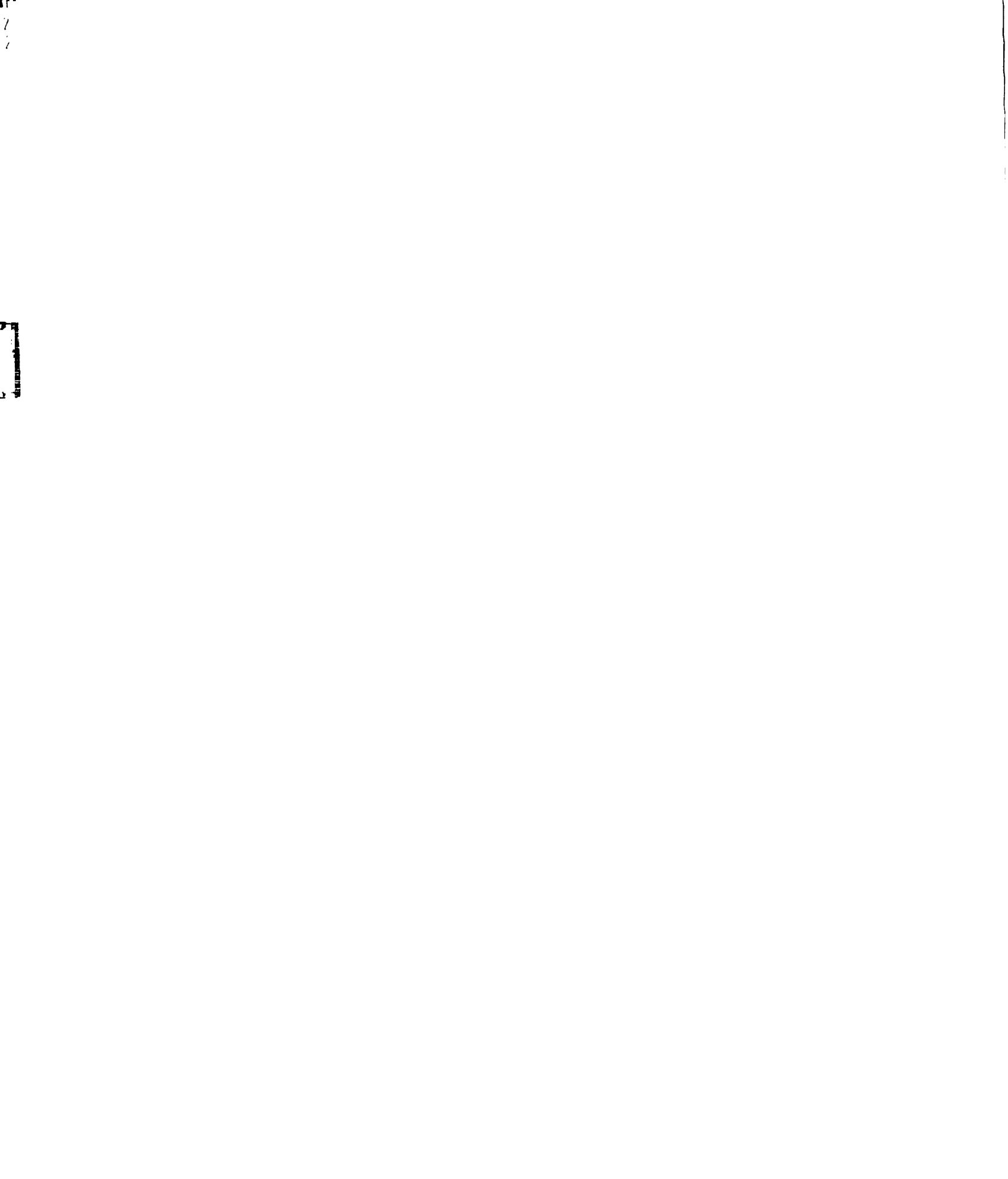


Figure 2-12. Subchloroplastic distribution of porphyrin-binding-deficient GUN4 after ALA feeding. GUN4 mutants with DPIX- and Mg-DPIX-binding defects were imported into chloroplasts that had been pretreated with or without ALA. After import, chloroplasts were lysed, fractionated, and analyzed as in Figure 2-1A. The position of the GUN4 precursor containing the transit peptide (prGUN4), the major form of mature GUN4 generated by proteolytic removal of the transit peptide during import into the chloroplast (mGUN4), and a minor form of mature GUN4 (\*) are indicated. Representative fluorograms from three independent experiments are shown for GUN4 containing the amino acid sequence found in wild type and for GUN4 containing the amino acid substitutions V123A, F191A and R211A.



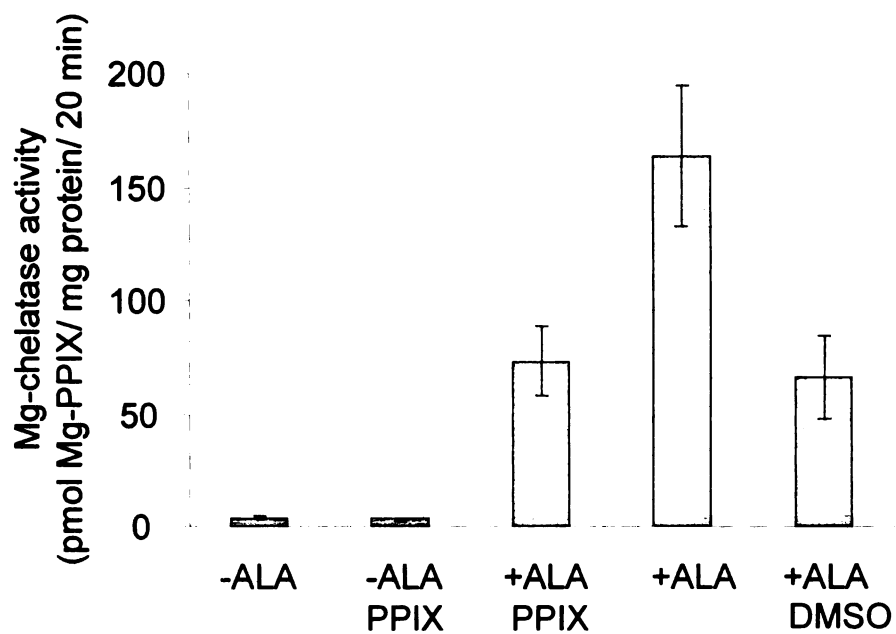


Figure 2-13. Mg-chelatase activity associated with chloroplast membranes after ALA feeding. Mg-chelatase assays were programmed with membranes that were isolated from chloroplasts that were either not fed (-ALA) or fed (+ALA) ALA. Mg-chelatase assays were not provided PPIX, or were supplied with exogenous PPIX dissolved in DMSO (PPIX) or DMSO without PPIX (DMSO). For each set of conditions,  $N \geq 3$ . Error bars represent standard error.



To test this idea, we assayed chloroplast membranes for Mg-chelatase after ALA feeding. Reactions were initiated by addition of PPIX dissolved in DMSO. When membranes derived from chloroplasts that were not fed ALA were provided or not provided PPIX, they could synthesize 4 or 3 pmol Mg-PPIX/20 min/mg protein, respectively (Figure 2-13), which is ten- to sixteen-fold less activity than previously reported for pea chloroplast membranes (Walker and Weinstein, 1991). These differences may be caused by the more dilute hypotonic lysis and the distinct hypotonic lysis buffer used here, compared to that of Walker and Weinstein (Walker and Weinstein, 1991). We observed up to a 43-fold increase in Mg-chelatase activity in membranes isolated from ALA-fed chloroplasts (Figure 2-13). The activity of membranes that were isolated from ALA-fed chloroplasts was reduced by more than twofold when exogenous PPIX was included in these assays (Figure 2-13). Additionally, we observed no significant difference in activity when membranes were assayed with (i) 2% DMSO containing 1.5  $\mu$ M PPIX or (ii) 2% DMSO not containing PPIX. These data indicate that Mg-chelatase does not utilize exogenous PPIX efficiently and that 2% DMSO has an inhibitory effect that is similar to PPIX dissolved in DMSO. Based on these data, we suggest that PO loads at least a fraction of the Mg-chelatase that associates with chloroplast membranes with PPIX during ALA feeding and that this preformed PPIX-Mg-chelatase complex turns over during the subsequent Mg-chelatase assay.

*Subchloroplastic distribution of Mg-chelatase subunits in ALA-fed chloroplasts.*

The elevated levels of Mg-chelatase activity in ALA-fed chloroplasts might not result solely from preloading Mg-chelatase with PPIX during ALA feeding. Porphyrins or a



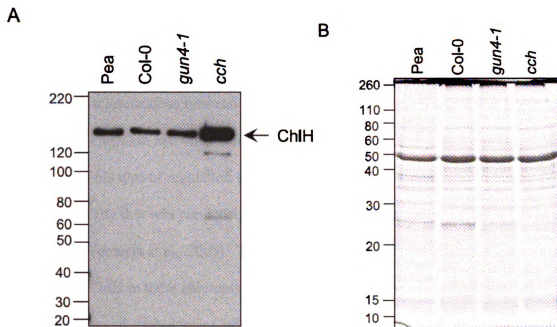


Figure 2-14. Characterization of affinity-purified anti-ChlH  $\Delta$ 1-823 antibodies. *A*. Immunoblotting of whole chloroplast extracts from pea, wild type Arabidopsis plants from the Columbia-0 ecotype (*Col-0*), *gun4-1*, and *cch* with affinity-purified anti-ChlH  $\Delta$ 1-823 antibodies. Chloroplasts were purified from pea or from wild-type Arabidopsis (*Col-0*), *gun4-1*, or *cch*. Total chloroplast protein was analyzed by SDS-PAGE using a 7% Laemmli gel and immunoblotting using affinity-purified anti-ChlH  $\Delta$ 1-823 antibodies. Each lane contains 2.5  $\mu$ g of total chloroplast protein from the indicated species or mutant. The band corresponding to ChlH is indicated. *B*. Coomassie-stained SDS gel of whole chloroplast extracts from pea, *Col-0*, *gun4-1*, and *cch*. Whole chloroplasts were solubilized in SDS-PAGE buffer, analyzed with a 12% Laemmli gel, and stained with Coomassie blue. Each lane contains 20  $\mu$ g of total chloroplast protein from the indicated species or mutant. The masses of standard proteins are indicated at the left in kDa.

GUN4-porphyrin complex might contribute to this elevated level of Mg-chelatase activity by promoting the redistribution of Mg-chelatase subunits from the soluble into the membrane-containing pellet fraction. For example, a GUN4-porphyrin complex might stabilize interactions between Mg-chelatase and chloroplast membrane lipids or between Mg-chelatase and other chlorophyll biosynthetic enzymes such as PO and Mg-PPIX MT. This type of regulation would be distinct from the stimulation of Mg-chelatase activity that was previously reported for GUN4 (Larkin et al., 2003; Davison et al., 2005; Verdecia et al., 2005). To begin exploring these possibilities, we monitored the levels of ChlH in these chloroplast fractions using polyclonal antibodies raised against a truncated Arabidopsis ChlH that lacks the first 823 residues and contains all of the remaining 558 carboxy-terminal residues (hereafter referred to as ChlH  $\Delta$ 1-823). We found that affinity-purified anti-ChlH  $\Delta$ 1-823 antibodies recognize a band that was extracted from chloroplasts purified from Arabidopsis and pea that migrates like a 150-kDa protein during SDS-PAGE (Figure 2-14A and B). The mass of Arabidopsis ChlH calculated from the derived amino acid sequence lacking the predicted transit peptide is 144 kDa. We also found that there is a striking increase in the level of this 150-kDa protein in the Arabidopsis mutant *cch* (Figure 2-14A and B), which is a strong loss-of-function allele of *ChlH* (Espineda et al., 1999; Mochizuki et al., 2001). We conclude that this band corresponds to ChlH. In four separate experiments, we observed that 40-70% of pea ChlH was in the soluble fraction of unfed chloroplasts and the remainder was in the pellet fraction. Although the distribution of ChlH in the soluble and pellet fractions was somewhat variable, we observed a statistically significant 15% increase of pea ChlH in pellet fractions after ALA feeding in each experiment (Figure 2-15).

1  
2  
2

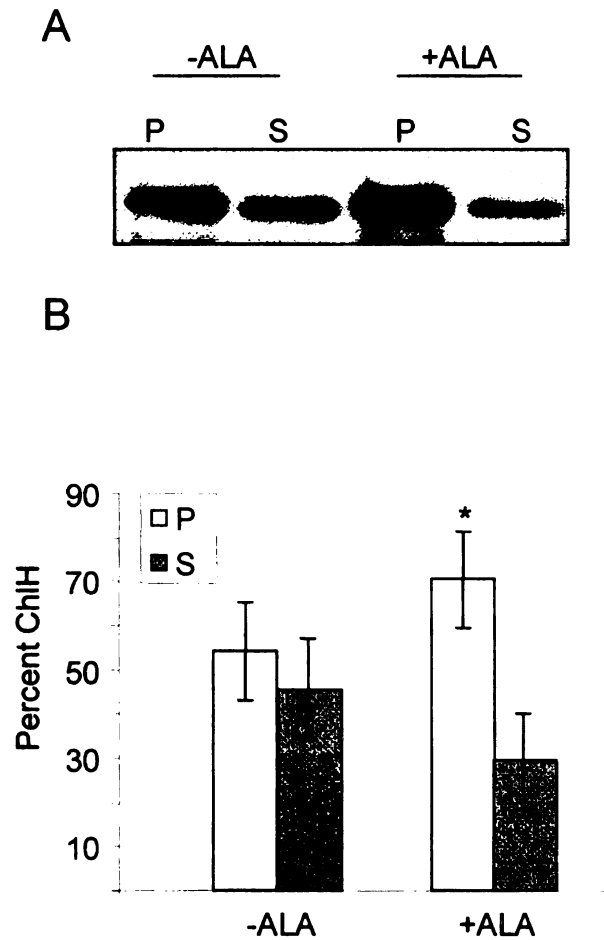
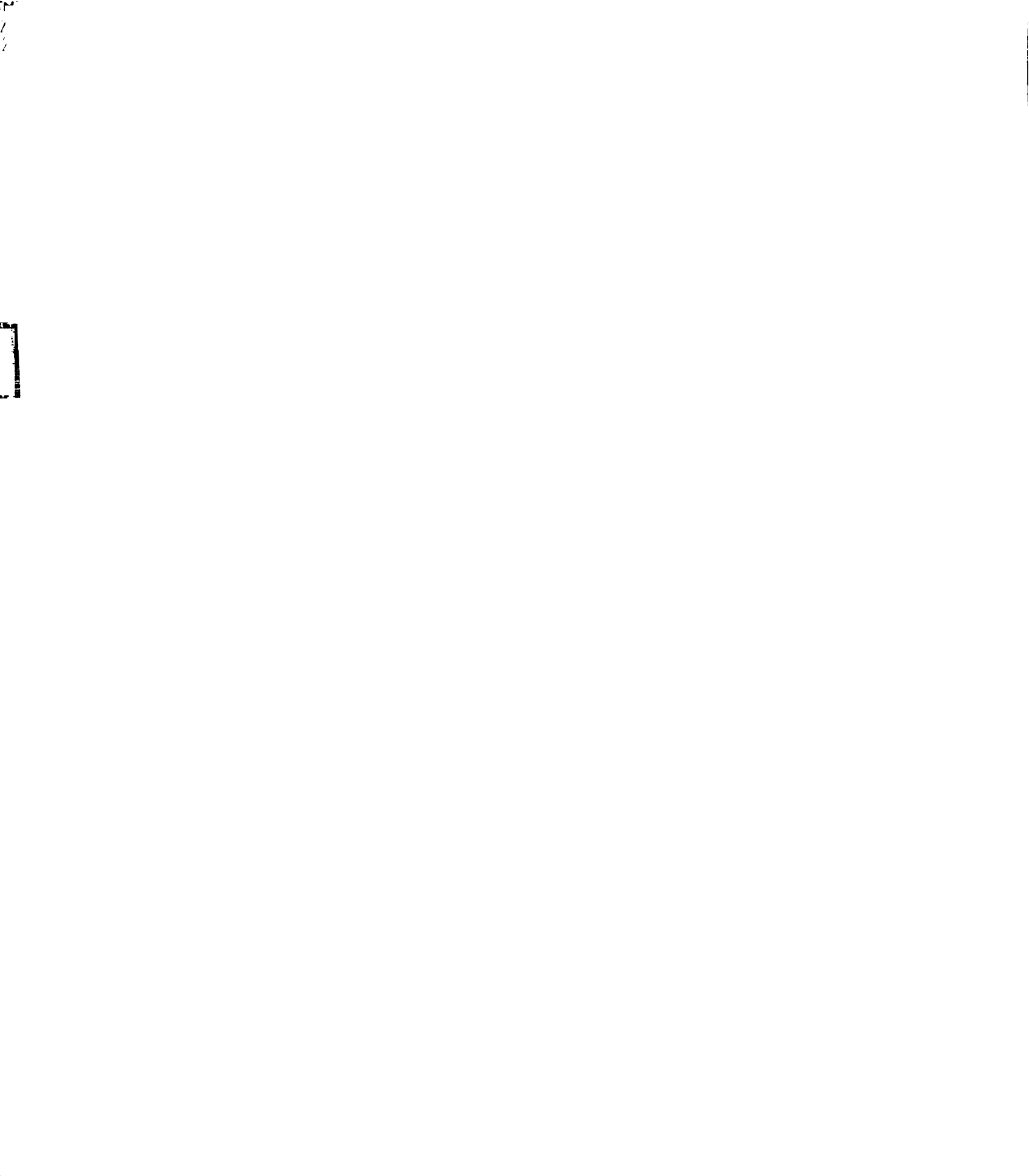


Figure 2-15. Subchloroplastic distribution of pea ChlH after ALA feeding. *A*. Representative immunoblot showing the subchloroplastic distribution of ChlH following ALA feeding. Intact pea chloroplasts were either fed (+ALA) or not fed (-ALA) ALA and then subjected to a mock import assay that lacked a radiolabeled precursor. These chloroplasts were subsequently lysed and fractionated. 2  $\mu$ g of protein from soluble (S) and membrane-containing pellet (P) fractions were analyzed by SDS-PAGE and immunoblotting with affinity-purified anti-ChlH  $\Delta$ 1-823 antibodies. *B*. Quantitation of the subchloroplastic distribution of pea ChlH following ALA feeding. N=4. Error bars represent standard error. The statistical significance of ChlH redistributing to the pellet during ALA feeding was tested using a paired t-test. \* indicates a significant difference (P=0.02).



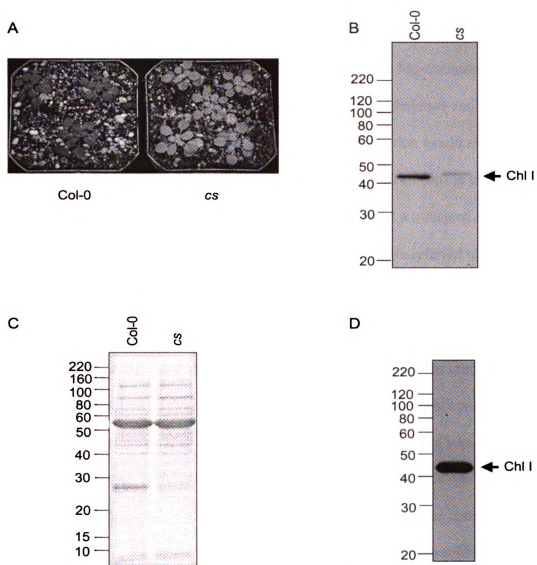


Figure 2-16. Characterization of affinity-purified anti-ChlI  $\Delta 1-60$  antibodies. *A*, Wild type and *cs* mutants. Wild type (Col-0) and *cs* mutants were grown in soil for 28 d. *B*, Analysis of whole plant extracts with affinity-purified anti-ChlI  $\Delta 1-60$  antibodies. Samples of 10  $\mu$ g of protein extracted from wild type (Col-0) and *cs* mutants shown in *A* were analyzed by immunoblotting with affinity-purified anti-ChlI  $\Delta 1-60$  antibodies. Masses of standard proteins are indicated at the left in kDa. The band corresponding to ChlI is indicated at the right. *C*, Total protein analysis of the immunoblot from *B*. Following immunoblotting with anti-ChlI antibodies as described in *B*, the PVDF membrane was stained with Coomassie blue. The mass of each standard protein is indicated at the left. *D*, Analysis of total pea chloroplasts with affinity-purified anti-ChlI  $\Delta 1-60$  antibodies. Whole pea chloroplasts containing a total of 5  $\mu$ g of chlorophyll were analyzed by immunoblotting with affinity-purified anti-ChlI  $\Delta 1-60$  antibodies. The mass of each standard is indicated at the left. The immunoreactive band that corresponds to pea ChlI is indicated at the right.

Pea ChII was previously reported to localize mostly within the soluble fraction when purified chloroplasts from pea were lysed and fractionated (Guo et al., 1998). If ALA feeding stabilizes not only the association of GUN4 with Mg-chelatase at the site of chlorophyll biosynthesis but also interactions between Mg-chelatase and chloroplast membranes, we would expect that ChII levels in the pellet fraction would also increase during ALA feeding. To test this idea, we monitored the levels of ChII in these chloroplast fractions using polyclonal antibodies raised against a truncated Arabidopsis ChII lacking the predicted sixty-residue transit peptide (hereafter referred to as ChII  $\Delta$ 1-60). We found that affinity-purified anti-ChII  $\Delta$ 1-60 antibodies recognize a 43-kDa protein in extracts prepared from wild-type Arabidopsis. The mass of Arabidopsis ChII calculated from the derived amino acid sequence lacking the predicted transit peptide is 40 kDa. We found that this immunoreactive band is present at a lower concentration in the Arabidopsis mutant *cs* (Figure 2-16A, B, and C), which contains a loss-of-function allele for *ChII* (Koncz et al., 1990), and that this immunoreactive band was less than 2 kDa larger in *cs* compared to wild type (Figure 2-16B). This decrease in mobility is consistent with the 0.8 kDa increase in the mass of the derived amino acid sequence reported for the *cs* allele (Koncz et al., 1990). We conclude that our affinity-purified anti-ChII antibodies specifically bind ChII. These antibodies specifically recognize a single 44-kDa band in pea chloroplasts (Figure 2-16D), which we conclude is pea ChII. Using these affinity-purified anti-ChII  $\Delta$ 1-60 antibodies, we tested the distribution of pea ChII in the same experiments in which we observed a 15% increase in pea ChII in the pellet fraction after ALA feeding. We found pea ChII predominantly in the

11-  
/



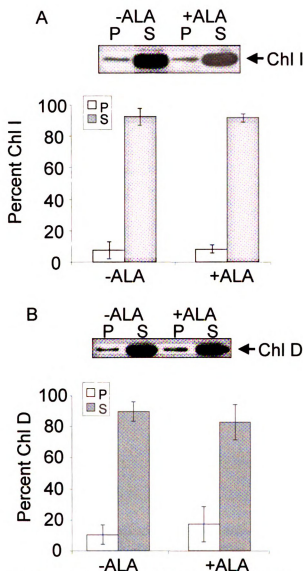


Figure 2-17. Subchloroplastic distribution of ChlI and ChlD after ALA feeding. *A*, Subchloroplastic distribution of ChlI after ALA feeding. Intact pea chloroplasts were either fed (+ALA) or not fed (-ALA) ALA and then subjected to a mock import assay that did not contain radiolabeled proteins. These chloroplasts were subsequently lysed and fractionated. Samples of 5  $\mu$ g of protein from soluble (S) and membrane-containing pellet (P) fractions were analyzed by SDS-PAGE and immunoblotting with affinity-purified anti-ChlI  $\Delta$ 1-60 antibodies. Immunoreactive bands from a representative experiment are shown (top). Immunoreactive bands were quantitated from four independent experiments prepared with different preparations of chloroplasts (bottom). Error bars represent standard error. *B*, Subchloroplastic distribution of ChlD after ALA feeding. Fractions were generated and analyzed as in *A* except that immunoblotting was performed with anti-ChlD  $\Delta$ 1-516 antibodies. Representative immunoreactive bands are shown (top). Immunoreactive bands were quantitated from four independent experiments prepared with different preparations of chloroplasts (bottom). Error bars represent standard error.

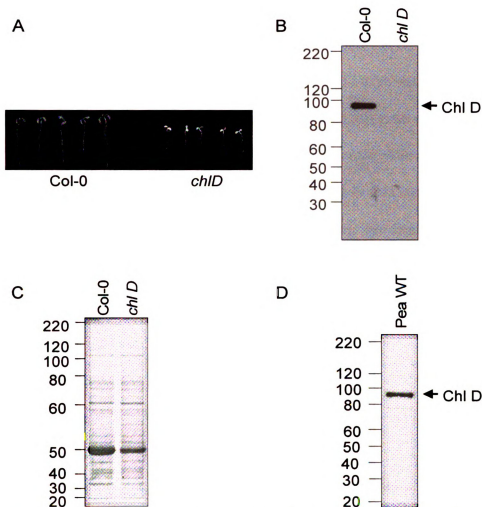


Figure 2-18. Characterization of affinity-purified anti-ChlD  $\Delta$ 1-516 antibodies. *A*, Wild-type and *chlD* mutants. Wild-type Arabidopsis (Col-0) and an Arabidopsis mutant containing the Salk\_150219 T-DNA insertion in an exon of *ChlD* (*chlD*) were grown on plates containing Linsmaier and Skoog media (Caisson Laboratories, North Logan UT), 1% sucrose, and 0.5% Phytoblend™ (Caisson Laboratories) for 7 d. The albino phenotype is linked to the T-DNA insertion (<1 cM; N.D.A., unpublished data). *B*, Analysis of whole plant extracts with affinity-purified anti-ChlD  $\Delta$ 1-516 antibodies. Samples of 1  $\mu$ g of protein extracted from 10-d-old wild type (Col-0) and *chlD* mutants shown in *A* were analyzed by immunoblotting with affinity-purified anti-ChlD  $\Delta$ 1-516 antibodies. Masses of the standard proteins are indicated at the left in kDa. The band corresponding to ChlD is indicated at the right. *C*, Total protein analysis of extracts from *B*. PVDF membranes containing 10  $\mu$ g of the extracts described in *B* were stained with Coomassie blue. The masses of the standard proteins are indicated at the left. *D*, Analysis of total pea chloroplasts with affinity-purified anti-ChlD  $\Delta$ 1-516 antibodies. Whole pea chloroplasts containing a total of 5  $\mu$ g of chlorophyll were analyzed by immunoblotting with affinity-purified anti-ChlD  $\Delta$ 1-516 antibodies. The masses of the standard proteins are indicated at the left. The immunoreactive band that corresponds to pea ChlD is indicated at the right.

supernatant, detectable pea ChII in the pellet, and no effect of ALA feeding on the distribution of ChII between soluble and pellet fractions (Figure 2-17A).

Pea ChID was previously reported to localize in light membranes (Luo et al., 1999) that we would not expect in pellet fractions prepared using our experimental conditions. We monitored the levels of pea ChID in these same chloroplast fractions using affinity-purified antibodies raised against a truncated Arabidopsis ChID lacking the first 516 residues (hereafter referred to as ChID  $\Delta$ 1-516). We found that affinity-purified anti-ChID  $\Delta$ 1-516 antibodies recognize an approximately 94-kDa protein in Arabidopsis whole-seedling extracts. The mass of Arabidopsis ChID calculated from the derived amino acid sequence lacking the predicted transit peptide is 79 kDa. This band is not detectable in an Arabidopsis mutant that contains a T-DNA insertion in an exon of *ChID* (Figure 2-18A, B, and C). We conclude that this band is Arabidopsis ChID. These antibodies also recognize a 93-kDa band extracted from pea chloroplasts (Figure 2-18D), which we conclude is pea ChID. Using these affinity-purified anti-ChID  $\Delta$ 1-516 antibodies, we tested the distribution of pea ChID in the same four independent experiments in which we observed a 22% increase in pea GUN4, a 15% increase in pea ChIH in the pellet fraction, and no change in the distribution of pea ChII after ALA feeding. Similar to our results with pea ChII, we found pea ChID predominantly in the supernatant fraction and only small quantities of ChID in the pellet fraction, regardless of whether chloroplasts were fed ALA (Figure 2-17B).

Our data are consistent with porphyrins affecting the distribution of only GUN4 and ChIH within pea chloroplasts. Next, we tested whether the redistribution of pea GUN4 and pea ChIH from the supernatant to the pellet fractions during ALA feeding

7  
7



might depend on chloroplast membranes or whether these proteins might accumulate in the pellet fraction for some other reason such as a fraction of a GUN4-ChlH complex denaturing and becoming insoluble during ALA feeding. To distinguish between these possibilities, we lysed pea chloroplasts, depleted the membranes from these lysates by centrifugation, and performed Mg-chelatase assays on the resulting supernatants. We found that supernatants prepared from three independent chloroplast preparations contained from 13-41 units of Mg-chelatase activity (Table 2-5), which is similar to the activity previously reported for such supernatants (Walker and Weinstein, 1991). After performing Mg-chelatase assays with these membrane-depleted supernatants, we centrifuged these reactions using the same conditions that caused pea GUN4 and pea ChlH from lysed chloroplasts to accumulate in the membrane-containing pellet fraction. We found that in contrast to the results that we obtained with lysed chloroplasts, pea GUN4 and pea ChlH remained entirely within the supernatant fraction when Mg-chelatase reactions were performed with membrane-depleted supernatants (Figure 2-19).

*Subchloroplastic distribution of GUN4 and Mg-chelatase subunits in chloroplasts fed with various porphyrins.* We expected that PPIX and Mg-PPIX would stabilize interactions between chloroplast membranes and the GUN4 and ChlH proteins because PPIX and Mg-PPIX are the only porphyrin substrate and product of Mg-chelatase and because ChlH and GUN4 are not known to catalyze other reactions. Nonetheless, our finding that GUN4 can bind a variety of porphyrins implies that GUN4 binding any of these ligands might cause a redistribution of GUN4 from the soluble to the membrane-containing pellet fraction. We expected that chloroplasts

12-  
1  
2



Table 2-5. Quantitation of Mg-chelatase activity in supernatants prepared from lysed chloroplasts

Preparation	Mg-chelatase activity (units)
1	16
2	13
3	41

A unit of Mg-chelatase activity produces one pmol Mg-PPIX/20 min/mg protein.

11-  
7  
2

1

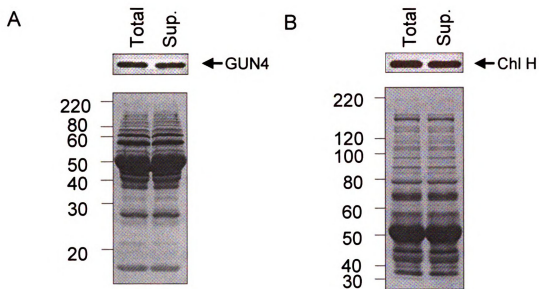


Figure 2-19. Solubility of pea GUN4 and pea ChlH in chloroplast-membrane-depleted Mg-chelatase assays. *A*, Solubility of pea GUN4 in chloroplast-membrane-depleted Mg-chelatase assays. Mg-chelatase assays that contained a total volume of 300  $\mu$ l were programmed with supernatants from lysed chloroplasts. After a 20-min Mg-chelatase reaction, 40  $\mu$ l of the reaction was removed (T). The reactions were then centrifuged at  $16,000 \times g$  for 10 min at 4°C, and 40  $\mu$ l of the supernatant (S) was removed. All fractions were analyzed by immunoblotting with affinity-purified anti-GUN4 antibodies (top). PVDF membranes were stained with Coomassie blue after immunoblotting (bottom). *B*, Solubility of pea ChlH in chloroplast-membrane-depleted Mg-chelatase assays. Fractions were prepared as in *A* and were analyzed by immunoblotting with affinity-purified anti-ChlH  $\Delta$ 1-823 antibodies (top). PVDF membranes were stained with Coomassie blue after immunoblotting (bottom).



would take up PPIX and other porphyrins in vitro and that GUN4 might bind these porphyrins after they are taken up because purified chloroplasts were previously reported to synthesize Mg-PPIX from exogenous PPIX (Fuesler et al., 1981; Fufslers et al., 1984; Walker and Weinstein, 1991). To test this idea, we fed pea chloroplasts with various porphyrins that GUN4 binds and monitored the distribution of GUN4 in soluble and membrane-containing fractions by immunoblotting. We found that similar to feeding chloroplasts ALA, feeding chloroplasts PPIX, Mg-PPIX, uroporphyrin III, coproporphyrin III, hemin, or pheophorbide *a* caused GUN4 to accumulate in the pellet fraction (Figure 2-20).

## **DISCUSSION**

GUN4 was previously localized to the thylakoid and envelope membranes but found mostly in the soluble fraction of chloroplasts that were purified from fully expanded rosette leaves of *Arabidopsis* (Larkin et al., 2003). Here, we report a roughly 50:50 distribution, or that GUN4 predominantly associates with the membrane-containing fraction depending on whether GUN4 was imported or pea GUN4 was monitored in 6- to 8-day-old pea leaves. Differences in the affinities of GUN4 and pea GUN4 for chloroplast membranes or differences in the chlorophyll biosynthetic capacities of fully expanded and young rapidly growing leaves may account for these differences. Consistent with the relatively higher rate of chlorophyll biosynthesis in young leaves stabilizing interactions between GUN4 and chloroplast membranes, we found that feeding ALA to purified chloroplasts causes a striking increase in the biosynthesis of PPIX and Mg-PPIX and also causes both GUN4 and ChlH to



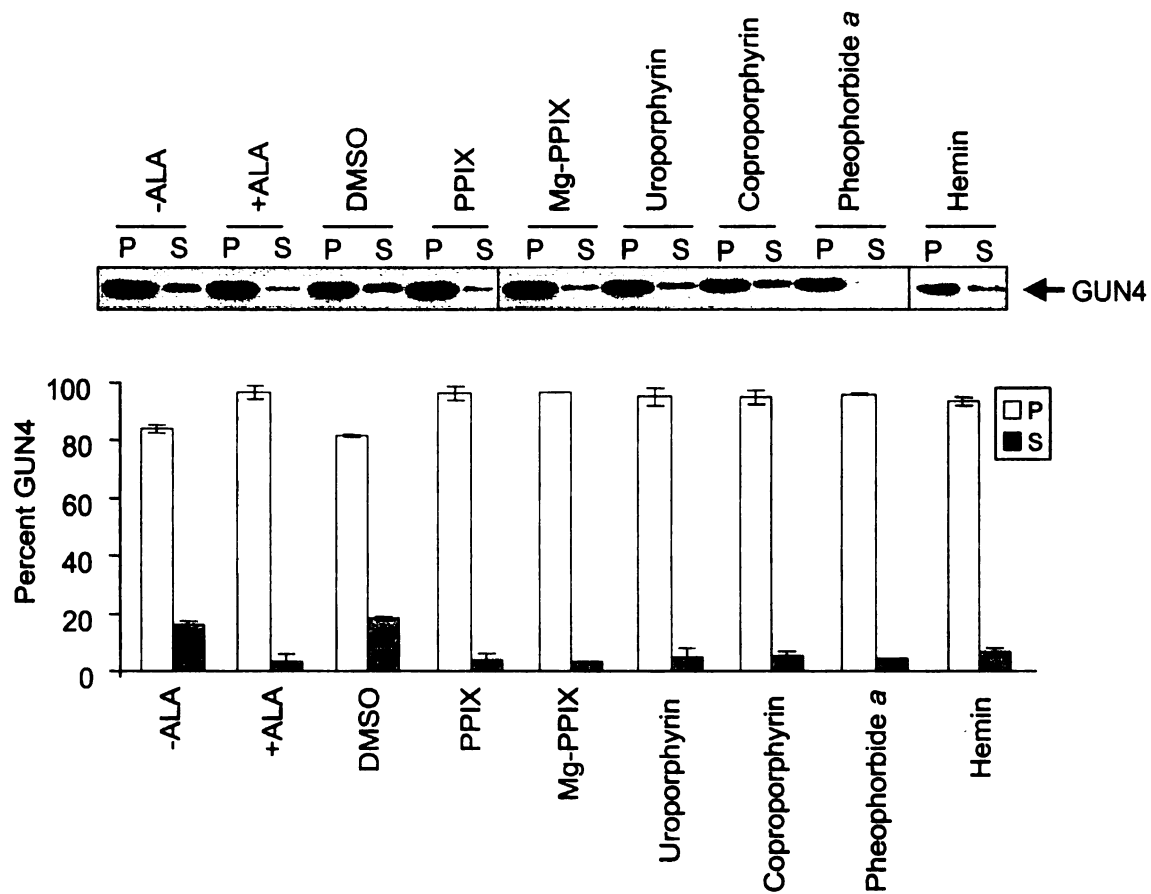


Figure 2-20. Subchloroplast distribution of GUN4 after feeding with ALA or various porphyrins. Pea chloroplasts were incubated in import buffer lacking ALA (-ALA), containing ALA (+ALA), containing 2% DMSO (DMSO), or 20  $\mu$ M of the indicated porphyrin and 1-2% DMSO. Next, the chloroplasts were subjected to a mock import assay that lacked a radiolabeled precursor. Chloroplasts were lysed and fractionated. Soluble (S) and membrane-containing pellet (P) fractions were analyzed by immunoblotting with affinity-purified anti-GUN4 antibodies. A representative immunoblot is shown (top). Immunoreactive bands were quantitated in fractions derived from at least two independent preparations of chloroplasts (bottom). Error bars represent standard error.

accumulate in the membrane-containing fraction at the expense of the soluble fraction. Although we cannot rule out possibilities such as porphyrin binding causing a rapid redistribution of GUN4, ChlH, or a GUN4-ChlH complex from the chloroplast stroma to the chloroplast membranes, this possibility seems unlikely because of the high viscosity of the chloroplast stroma (Köhler et al., 2000). The most parsimonious interpretation of our data is that (i) most of GUN4 and ChlH associate with chloroplast membranes; (ii) a fraction of GUN4, ChlH, or a GUN4-ChlH complex dissociates from chloroplast membranes and accumulates in the soluble fraction during chloroplast lysis and fractionation; and (iii) the porphyrin-bound conformations of GUN4 and ChlH have higher affinities for either chloroplast membrane lipids and/or chlorophyll biosynthetic enzymes that more stably associate with chloroplast membranes such as PO and Mg-PPIX MT.

Although GUN4-porphyrin complexes were previously reported to stimulate Mg-chelatase activity (Larkin et al., 2003; Davison et al., 2005; Verdecia et al., 2005), our findings suggest that GUN4 might regulate chlorophyll biosynthesis on another level. We propose that GUN4 or a GUN4-porphyrin complex helps to stabilize interactions between ChlH and chloroplast membranes (i.e., the site of chlorophyll biosynthesis), which was not previously reported for GUN4. Complexes of chlorophyll biosynthetic enzymes that include Mg-chelatase have been reported or suggested because Mg-chelatase and Mg-PPIX MT can convert PPIX to Mg-PPIX ME in vitro without appreciable accumulation of Mg-PPIX (Jensen et al., 1999) and because ChlH stimulates Mg-PPIX MT (Hinchigeri et al., 1997; Shepherd et al., 2005; Johnson and Schmidt-Dannert, 2008). However, all Mg-PPIX does not appear to be efficiently

channeled through a complex composed of Mg-chelatase and Mg-PPIX MT because Mg-PPIX accumulates in green *Arabidopsis* seedlings (Strand et al., 2003; Mochizuki et al., 2008). We propose that GUN4 binds at least a fraction of the Mg-PPIX that accumulates *in vivo* by itself or as part of a GUN4-ChlH complex. GUN4 may be necessary if Mg-chelatase-Mg-PPIX complexes are unstable or if a fraction of active ChlH does not associate with Mg-PPIX MT and might help prevent the photosensitizing chlorophyll precursors from causing photooxidative damage.

These findings may contribute to our understanding of the competition between Mg-chelatase and ferrochelatase for PPIX. By stabilizing complexes of enzymes that contain Mg-chelatase, GUN4 might help divert PPIX from heme biosynthesis and into chlorophyll biosynthesis. Both PO and ferrochelatase stably associate with chloroplast membranes (Lermontova et al., 1997; Che et al., 2000; Watanabe et al., 2001; Suzuki et al., 2002; van Lis et al., 2005) and have been predicted to form a complex based on their crystal structures (Koch et al., 2004). Porphyrin-bound GUN4 might help Mg-chelatase compete with ferrochelatase for interactions with PO, thereby helping to divert PPIX from heme to chlorophyll biosynthesis. Alternatively, if Mg-chelatase and ferrochelatase utilize separate pools of PPIX, as has been suggested (Cornah et al., 2003), we would expect that GUN4 would affect only chlorophyll biosynthesis.

Complexes of cooperating enzymes are expected to limit active site access of exogenously supplied substrates (Winkel, 2004; Jørgensen et al., 2005). Consistent with this idea, we found that exogenously supplied PPIX did not stimulate Mg-chelatase activity in our membrane-containing pellet fraction, but that PPIX derived from ALA feeding caused a striking increase in Mg-chelatase activity. Pea chloroplast membranes

were previously reported to contain low levels of Mg-chelatase activity when assayed with exogenous PPIX. Reactions lacking exogenous PPIX were not previously reported (Walker and Weinstein, 1991). The striking increase in Mg-chelatase activity caused by ALA feeding likely results from the 22% increase in GUN4 and the 15% increase in ChlH in the chloroplast membranes, along with the preloading of ChlH or a GUN4-ChlH complex with PPIX. Our finding that, in contrast to GUN4 and ChlH, ALA feeding does not stabilize interactions between chloroplast membranes and either ChlI or ChlD suggests that these Mg-chelatase subunits do not have a higher affinity for the porphyrin-bound form of ChlH or at least that such a difference cannot be detected with the chloroplast lysis and fractionation assay described here. The low levels of ChlI and ChlD that we observed in the pellet fraction likely explain the low Mg-chelatase activity that we and others (Walker and Weinstein, 1991) observed in membrane-containing pellet fractions relative to reactions programmed with both soluble and membrane-containing fractions (Walker and Weinstein, 1991).

$K_d^{\text{DPIX}}$  and  $K_d^{\text{Mg-DPIX}}$  have been reported for SynGUN4 and *T. elongatus* GUN4 (Larkin et al., 2003; Davison et al., 2005; Verdecia et al., 2005), but only qualitative porphyrin-binding experiments were previously reported for GUN4 (Larkin et al., 2003). We found similarities and differences in the porphyrin-binding constants of GUN4 and its cyanobacterial relatives. Like its cyanobacterial relatives (Larkin et al., 2003; Davison et al., 2005; Verdecia et al., 2005), GUN4 has a higher affinity for Mg-DPIX than DPIX, but GUN4 has a three- to ten-fold lower affinity for these porphyrins than its cyanobacterial relatives.  $K_d^{\text{PPIX}}$  and  $K_d^{\text{Mg-PPIX}}$  had not been reported previously for GUN4 or any cyanobacterial relatives of GUN4. We found that including 1%

DMSO in binding assays did not significantly affect  $K_d^{\text{DPIX}}$  and  $K_d^{\text{Mg-DPIX}}$ , but promoted the solubility of PPIX and Mg-PPIX, thereby allowing us to determine  $K_d^{\text{PPIX}}$  and  $K_d^{\text{Mg-PPIX}}$ , which resembled  $K_d^{\text{DPIX}}$  and  $K_d^{\text{Mg-DPIX}}$ , respectively. GUN4 has a slightly higher affinity for Mg-PPIX than for Mg-DPIX and has an almost twofold lower affinity for PPIX than for DPIX. The higher affinity of SynGUN4 for metalated porphyrins was previously attributed to these porphyrins assuming a planar conformation in contrast to unmetalated porphyrins, which assume a more puckered or ruffled conformation (Verdecia et al., 2005). Our findings indicate that this preference for metalated porphyrins is more striking for the natural ligands than for the deuteroporphyrins and we suggest that the vinyl groups that distinguish PPIX from DPIX contribute to this binding selectivity. This finding may at least partially explain why  $K_m^{\text{DPIX}}$  is lower than  $K_m^{\text{PPIX}}$  in lysed pea chloroplasts (Guo et al., 1998).

SynGUN4 was previously shown to bind a variety of porphyrins with  $K_d$  values that range from 0.26 to 11  $\mu\text{M}$  (Larkin et al., 2003; Davison et al., 2005; Verdecia et al., 2005). Here, we report that GUN4 can bind nine different porphyrins with  $K_d$  values ranging from 1.6 to 15  $\mu\text{M}$ . Most of the porphyrins that we analyzed are found in plants or are oxidized versions of porphyrins and porphyrinogens found in plants. Although the only difference in Mg-PPIX and hemin is a chelated magnesium or ferric ion, we found that GUN4 binds Mg-PPIX with a fivefold higher affinity than hemin. SynGUN4 was previously reported to bind cobalt (III) PPIX with an almost twofold higher affinity than hemin (Verdecia et al., 2005). Thus, like SynGUN4, GUN4 can distinguish between derivatives of PPIX that contain distinct metal ions. Modifications of the porphyrin ring were also reported to affect the affinities of SynGUN4 for porphyrins

(Verdecia et al., 2005). R214 of SynGUN4 is conserved as R211 in GUN4. In SynGUN4, R214 resides in the  $\alpha 6/\alpha 7$  loop that lies loosely across the “palm” region of the “cupped hand” domain and makes a major contribution to porphyrin binding, presumably by interacting with one of the carboxyl moieties of DPIX and Mg-DPIX (Verdecia et al., 2005). Methylation of a carboxyl moiety in Mg-PPIX ME could lower the affinities of both GUN4 and SynGUN4 for this porphyrin. Indeed, we observed that  $K_d^{\text{Mg-PPIX ME}}$  was 2.5-fold higher than  $K_d^{\text{Mg-PPIX}}$ . However, because either carboxyl moiety of the commercially available Mg-PPIX ME used here is methylated rather than the carboxyl moiety attached only to ring C, as observed in nature, these data do not unambiguously establish that GUN4 binds Mg-PPIX ME with a lower affinity than Mg-PPIX. GUN4 binding uroporphyrin III, coproporphyrin III, hemin, and pheophorbide *a*, indicates that GUN4 is similar to SynGUN4 in that GUN4 can bind a variety of porphyrins with diverse ring substituents (Verdecia et al., 2005). Moreover, we found that feeding uroporphyrin III, coproporphyrin III, hemin, or pheophorbide *a* to chloroplasts causes pea GUN4 to accumulate in the membrane-containing pellet fraction. These data lend further support to a model in which a porphyrin-bound conformation of GUN4 has an elevated affinity for chloroplast membranes. The finding that binding a variety of porphyrins promotes interactions between GUN4 and chloroplast membranes implies that GUN4 could be involved in other reactions besides the Mg-chelatase reaction. However, previous analyses of *gun4* mutants are consistent with GUN4 not having a major role in the metabolism of porphyrinogens and other porphyrins besides PPIX and Mg-PPIX. *Gun4* mutants are chlorophyll deficient (Vinti et al., 2000; Mochizuki et al., 2001; Larkin et al., 2003); *gun4* nulls are albino under

optimal growth conditions but viable when they are provided sucrose (Larkin et al., 2003). Although these phenotypes are expected for mutants that cannot synthesize chlorophyll, we expect that mutants with severe defects in plastid heme metabolism would exhibit more severe or lethal phenotypes regardless of whether sucrose is provided. Additionally, *gun4* mutants were not reported to exhibit lesions (Vinti et al., 2000; Mochizuki et al., 2001; Larkin et al., 2003) like those present in mutants with reduced levels of uroporphyrinogen III decarboxylase and coproporphyrinogen III oxidase (Mock and Grimm, 1997; Mock et al., 1999; Ishikawa et al., 2001). Moreover, although we found that GUN4 binds pheophorbide *a*, an early intermediate in chlorophyll catabolism, we observed that *gun4* mutants do not exhibit phenotypes like those with defects in the enzymes that degrade chlorophyll such as the stay-green phenotype (Pruzinská et al., 2005; Schelbert et al., 2009) (Figure 2-21). From these data we conclude that GUN4 does not appear to promote chlorophyll catabolism. In summary, although GUN4 can bind diverse porphyrins in vitro and binding any of these porphyrins causes GUN4 to more stably associate with chloroplast membranes, the simplest interpretation of these new data and previous analyses of *gun4* mutants is that the major function of GUN4 in vivo is to promote the biosynthesis of Mg-PPIX and to bind Mg-PPIX.

Several amino acid substitutions that do not affect the solubility of His-tagged SynGUN4 expressed in *E. coli* appear to cause GST-GUN4  $\Delta$ 1-69 to accumulate as inclusion bodies. Species-specific differences in stability, or technical explanations such as the use of different tags, may explain these apparent differences in solubility. Among the seven amino acid substitutions that did not cause GST-GUN4  $\Delta$ 1-69 to

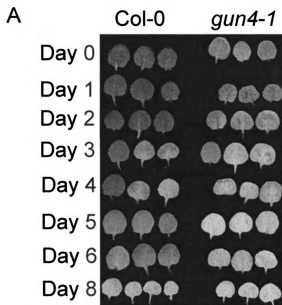


Figure 2-21. Analysis of leaf senescence in *gun4-1*. Wild type (Col-0) and *gun4-1* mutants were grown on soil for 21 d at 22°C in a diurnal light cycle of 50  $\mu\text{mol m}^{-2} \text{s}^{-1}$  white light followed by 8 h of darkness. Leaf senescence was assayed as previously described (Park et al., 2007). Briefly, leaves were removed and placed on parafilm that was floated on Milli-Q H<sub>2</sub>O in petri dishes that were kept in complete darkness in light-tight containers. These containers were opened under extremely dim green light and at least three leaves were removed and photographed at 1-d intervals.

accumulate in inclusion bodies, only V123A, F191A, and R211A reduced the affinity of GUN4 for porphyrins. The finding that four amino acid substitutions inhibit porphyrin binding in SynGUN4 but not GUN4 is consistent with species specificity in particular binding determinants or in indirect effects on binding. V123 in GUN4 is homologous to V135 in SynGUN4. In SynGUN4, V135 contributes to a concave and hydrophobic surface referred to as the “greasy palm” of the “cupped hand” domain (Verdecia et al., 2005). F191 in GUN4 is homologous to F196 in SynGUN4. Like R214 of SynGUN4, F196 resides on the  $\alpha 6/\alpha 7$  loop, which lies across the “greasy palm” (Verdecia et al., 2005). Because V123A, F191A, and R211A elevate  $K_d^{\text{DPIX}}$  and  $K_d^{\text{Mg-DPIX}}$ , we expected that these amino acid substitutions would also impair the porphyrin-mediated interactions between GUN4 and chloroplast membranes. Indeed, we found that much less V123A, F191A, and R211A associated with membranes. However, because we found that these amino acid substitutions impair rather than abolish binding, and because ALA feeding causes a striking increase in PPIX and Mg-PPIX, we expected that ALA feeding might stabilize interactions between these proteins and chloroplast membranes, thereby causing more V123A, F191A, and R211A to accumulate in the membrane-containing pellet fraction. However, we found that ALA feeding could not stabilize interactions between chloroplast membranes and V123A, F191A, or R211A. These data are consistent with pea GUN4 competing much more effectively with V123A, F191A, and R211A relative to wild-type GUN4. These data are also consistent with V123A, F191A, and R211A not only affecting porphyrin binding but also directly or indirectly affecting interactions between GUN4 and other molecules that might tether GUN4 to chloroplast membranes such as ChlH.

The L88F substitution derived from the *gun4-1* missense allele causes the GUN4 protein to accumulate at much lower levels than in wild-type Arabidopsis, as judged by immunoblotting (Larkin et al., 2003). The homologous amino acid substitution in *T. elongatus* GUN4 does not cause misfolding and causes a striking decrease in the  $K_d^{\text{DPIX}}$  and  $K_d^{\text{Mg-DPIX}}$  for *T. elongatus* GUN4 and SynGUN4. Together, these data provide evidence that GUN4 might be degraded more rapidly when bound to porphyrins. However, the observation that the L88F substitution promotes insolubility of GST-GUN4  $\Delta$ 1-69 expressed in *E. coli* reported here suggests that, in Arabidopsis, less GUN4 accumulates in *gun4-1* because of protein instability caused by misfolding, as previously suggested (Larkin et al., 2003), rather than from protein instability caused by a striking increase in the affinities for porphyrins.

In summary, our major finding is that porphyrin binding helps stabilize interactions between GUN4 and possibly ChlH with chloroplast membranes. Based on these data, we suggest that porphyrins and/or GUN4-porphyrin complexes might stabilize interactions between ChlH and chloroplast membranes, thereby facilitating the channeling of porphyrins into chlorophyll biosynthesis. These findings support a model in which GUN4-porphyrin complexes promote chlorophyll biosynthesis not only by stimulating Mg-chelatase activity but also by affecting interactions between ChlH and chloroplast membranes.

## CHAPTER 3

### GENOMES UNCOUPLED 4 CONTRIBUTES TO PORPHYRIN CHANNELING AND PHOTOOXIDATIVE STRESS TOLERANCE IN *ARABIDOPSIS THALIANA*

**Neil D. Adhikari, Stephanie M. Buck, John E. Froehlich, and Robert M. Larkin**  
(2010) GENOMES UNCOUPLED 4 contributes to porphyrin channeling and  
photooxidative stress tolerance in *Arabidopsis thaliana*. Submitted for publication.

## CHAPTER 3

### GENOMES UNCOUPLED 4 CONTRIBUTES TO PORPHYRIN CHANNELING AND PHOTOOXIDATIVE STRESS TOLERANCE IN *ARABIDOPSIS THALIANA*

#### **Abstract**

Tetrapyrroles such as chlorophylls are synthesized from a branched pathway that is located within chloroplasts. The GUN4 protein stimulates chlorophyll biosynthesis by binding chlorophyll precursors, by binding the ChlH subunit of Mg-chelatase, and by activating Mg-chelatase, the enzyme that commits porphyrins to the chlorophyll branch. GUN4 was proposed to help channel porphyrins into the chlorophyll branch and to help attenuate the production of reactive oxygen species (ROS) yielded by collisions between O<sub>2</sub> and light-exposed porphyrins by binding and shielding porphyrins from such collisions, binding ChlH, and promoting interactions between ChlH and chloroplast membranes—the site of chlorophyll biosynthesis. To test this idea, we engineered Arabidopsis plants that express only porphyrin-binding-deficient versions of GUN4. We found that porphyrin-binding deficiencies in GUN4 and loss-of-function alleles of *ChlH* cause both GUN4 and ChlH to less stably associate with chloroplast membranes, promote chlorophyll deficiencies, enhance sensitivity to high-intensity light, and elevate the expression of ROS-inducible genes. Based on these findings, we conclude that a GUN4-ChlH complex promotes chlorophyll biosynthesis and photooxidative stress tolerance by binding porphyrins on chloroplast membranes. Our findings provide insight into mechanisms that allow plants to accumulate readily detectable levels of photosensitizing chlorophyll precursors without suffering from photooxidative stress.

## INTRODUCTION

GENOMES UNCOUPLED 4 from *Arabidopsis thaliana* (hereafter referred to as GUN4) is a chloroplast-localized protein of 22 kDa that was identified in a screen for mutants with defects in plastid-to-nucleus signaling. GUN4 is encoded by a single-copy gene and is required for the accumulation of chlorophyll when plants are grown in optimal conditions (Larkin et al., 2003). GUN4 is conserved among organisms that perform oxygenic photosynthesis, but is absent in *Rhodobacter* species, which perform anoxygenic photosynthesis (Larkin et al., 2003). In *Synechocystis* sp. PCC 6803 (hereafter referred to as *Synechocystis*), *sll0558* is one of three GUN4 relatives (hereafter referred to as SynGUN4) that was also shown to be required for the accumulation of chlorophyll (Wilde et al., 2004; Sobotka et al., 2008).

GUN4 promotes the accumulation of chlorophyll at least in part by stimulating Mg-chelatase; Mg-chelatase commits porphyrins to chlorophyll biosynthesis by catalyzing the insertion of Mg<sup>2+</sup> into PPIX, yielding Mg-protoporphyrin IX (Mg-PPIX). Mg-chelatase requires three subunits in vitro and in vivo. These three subunits are conserved from prokaryotes to plants and are commonly referred to as BchH or ChlH, BchD or ChlD, and BchI or ChlI. In *Arabidopsis*, these subunits are 140, 79, and 40 kDa, respectively. ChlH is the porphyrin-binding subunit and is likely the Mg<sup>2+</sup>-binding subunit of Mg-chelatase. ChlI and ChlD are related to AAA-type ATPases and form an oligomer that interacts with ChlH and drives the ATP-dependent metalation of PPIX (Masuda, 2008). GUN4 and cyanobacterial relatives of GUN4 stimulate their respective

Mg-chelatases by a mechanism that involves binding the ChlH subunit of Mg-chelatase and binding the porphyrin substrate and product of Mg-chelatase (Larkin et al., 2003; Davison et al., 2005; Verdecia et al., 2005). The porphyrin-binding activity was first quantified only for cyanobacterial relatives of GUN4. These studies utilized deuteroporphyrin IX (DPIX) and Mg-deuteroporphyrin IX (Mg-DPIX); DPIX and Mg-DPIX lack two vinyl groups found in PPIX and Mg-PPIX and are therefore significantly more water soluble than PPIX and Mg-PPIX, respectively. Recently, a modification to a porphyrin-binding assay allowed for the quantification of GUN4 binding to PPIX, Mg-PPIX, and various other porphyrins found in nature. GUN4 was found to bind Mg-PPIX with significantly higher affinity than all other porphyrins tested (Adhikari et al., 2009). These findings are consistent with the Mg-PPIX-binding activity of GUN4 contributing significantly to the Mg-chelatase stimulatory activity of GUN4, as was suggested from previous analyses of the porphyrin-binding and Mg-chelatase-stimulatory activities of cyanobacterial GUN4 (Verdecia et al., 2005).

A proteinaceous cofactor that regulates an enzyme by binding the enzyme as well as a substrate and a product is unique. This novel enzymology was proposed to protect plants from reactive oxygen species (ROS) that can be produced from collisions between O<sub>2</sub> and porphyrins that are exposed to bright light. Larkin et al. (2003) proposed that a GUN4 or a GUN4-ChlH complex envelops and thereby shields PPIX and Mg-PPIX from collisions with O<sub>2</sub> that can lead to the production of reactive oxygen species (ROS) when porphyrins are exposed to bright light. Such ROS can trigger necrotic and apoptotic cell death (Kim et al., 2008) and inactivate Mg-chelatase

(Willows et al., 2003). This shielding activity is expected to be significant because PPIX and Mg-PPIX are not rapidly and completely utilized for chlorophyll biosynthesis, but accumulate to readily detectable levels in chloroplast membranes *in vivo*. This accumulated PPIX and Mg-PPIX is presumably used for chlorophyll biosynthesis (Pöpperl et al., 1998; Papenbrock et al., 1999; Mohapatra and Tripathy, 2007; Mochizuki et al., 2008; Moulin et al., 2008). PPIX and Mg-PPIX would cause lethal photooxidative stress if they could freely diffuse throughout chloroplast membranes prior to their conversion into chlorophyll.

GUN4 and ChlH are found in both soluble and membrane-containing fractions when purified chloroplasts are lysed and fractionated. Inducing a rise in chloroplastic PPIX and Mg-PPIX promotes interactions between pea chloroplast membranes and *in vitro* translated and imported GUN4, pea GUN4, and pea ChlH. Inducing a rise in PPIX and Mg-PPIX also increases the amount of Mg-chelatase activity associated with chloroplast membranes. These data are consistent with GUN4 and/or GUN4-ChlH complexes binding and shielding the PPIX and Mg-PPIX that accumulate in chloroplast membranes from collisions with O<sub>2</sub> that might yield ROS. These data are also consistent with GUN4 helping to channel accumulating porphyrins into chlorophyll biosynthesis by binding chlorophyll precursors and ChlH on chloroplast membranes, activating Mg-chelatase on chloroplast membranes, and by helping to form an enzyme complex on chloroplast membranes that channels PPIX into chlorophyll biosynthesis (Adhikari et al., 2009).

*gun4* alleles that encode porphyrin-binding deficient versions of GUN4 expressed in Arabidopsis are required to test this model. All previously available *gun4* mutants were either severe loss-of-function alleles that accumulate barely detectable levels of GUN4 protein or protein nulls (Larkin et al., 2003; Wilde et al., 2004; Sobotka et al., 2008). Additionally, analyses of the interactions between pea chloroplast membranes and porphyrin-binding-deficient versions of GUN4 imported into pea chloroplasts yielded some ambiguous results: the data from these experiments are consistent with (1) amino acid residue substitutions that inhibit the porphyrin-binding activity of GUN4 in vitro also inhibiting other functions besides the porphyrin-binding activity of GUN4 in vivo or (2) technical limitations of the pea system preventing a definitive test of this model (Adhikari et al., 2009). Thus, we prepared transgenic Arabidopsis plants in which the wild-type *GUN4* gene is knocked out and that express *gun4* alleles that encode porphyrin-binding-deficient versions of GUN4. Based on results from experiments that were performed with these transgenic lines, we conclude that amino acid residue substitutions that disrupt the porphyrin-binding activity of GUN4 in vitro also disrupt the porphyrin-binding activity of GUN4 in vivo and that the porphyrin-binding activity of GUN4 promotes interactions between GUN4 and chloroplast membranes in vivo. Additionally, we report results from experiments with these transgenic lines and with both *gun4* and *chlH* mutants that support a model in which GUN4 and ChlH form a PPIX- and Mg-PPIX-binding complex on chloroplast membranes that not only channels porphyrins into chlorophyll biosynthesis but also contributes to photooxidative stress tolerance.

## MATERIALS AND METHODS

Wild type and all mutants were *Arabidopsis thaliana* plants of the Columbia-0 (Col-0) ecotype. *gun5*, *cch*, and *gun4-2* were previously described (Mochizuki et al., 2001; Larkin et al., 2003). Salk\_039005 that contains a T-DNA insertion in *sgs3* was obtained from the Arabidopsis Biological Resource Center (Ohio State University, Columbus OH). *gun4-2* and *sgs3* were crossed and the F2 progeny that were homozygous for the *sgs3* and heterozygous for the *gun4-2* T-DNA insertion alleles were identified using PCR-based genotyping with strategies recommended by the Salk Institute Genomic Analysis Laboratory (La Jolla CA, <http://signal.salk.edu/>).

ACACAATCATTGCTTTCCTGTGACGGTTC and

ACACAGTGATGGTAGATTCGGATACAGC were used to score *gun4-2*.

ACTCTCAAGGTTCTCTCCCC and GAGCTGTTCCAAAGCCTCATC were used to score *sgs3*. The *sgs3 gun4-2* mutants were transformed with transgenes in which the native promoter drives expression of the wild-type GUN4 protein or GUN4 proteins in which the F191A and R211A amino acid substitutions were engineered by site-directed mutagenesis. GUN4 proteins containing these amino acid substitutions are hereafter referred to as F191A and R211A. Site-directed mutants were prepared using the QuickChange® XL Site-Directed Mutagenesis Kit (Stratagene, La Jolla CA), as previously described (Adhikari et al., 2009). All mutations were confirmed by sequencing at the Research Technology Support Facility (RTSF) (Michigan State University, East Lansing MI). These transgenes included a genomic fragment that contained the complete *GUN4* coding sequence as well as 845 bp upstream and 164 bp downstream of the complete *GUN4* coding sequence inserted into pPZP221, as

previously described (Larkin et al., 2003). Two lines each for F191A and R211A were judged to contain single transgenes by scoring for the gentamicin resistance gene that is linked to the *GUN4* genes during segregation analysis. Using PCR-based genotyping, we determined that these lines are homozygous for the *sgs3* and the *gun4-2* alleles. We propagated these primary transformants and obtained lines that are homozygous GUN4-, F191A-, and R211A-expressing transgenes, *gun4-2*, and *sgs3*.

We isolated *gun5-101* from a previously described *gun* mutant screen (Ruckle et al., 2007). This mutant allele was identified by positional cloning after *gun5-101* mutants were crossed to a Landsberg *erecta* line. F2 progeny that exhibited a pale phenotype were used to map *gun5-101* with SSLP markers (Konieczny and Ausubel, 1993; Bell and Ecker, 1994) using the Cereon Genomics Indel database (Jander et al., 2002) (Table 3-1) and previously described procedures (Weigel and Glazebrook, 2002). To sequence the *gun5-101* allele, the *GUN5* coding sequence was amplified by means of Platinum® Pfx DNA polymerase (Invitrogen, Carlsbad CA) using *GUN5*-specific oligonucleotides in at least 10 aliquots that were subsequently pooled, purified from agarose gels using the QIAquick Gel Extraction Kit (Qiagen, Valencia CA), and sequenced with gene-specific oligonucleotides by the Research Technology Support Facility (Michigan State University, East Lansing MI).

Seeds for all lines were surface sterilized by incubation first in 70% ethanol, 0.5% Triton X-100 solution for 10 min on a tube mixer, then in 95% ethanol for 10 min on a tube mixer, followed by air drying on filter paper soaked in 95% ethanol in a laminar

Table 3-1. SSLP and CAPS markers used for mapping *gun5-101*

1	2	3	4
T24H18	CAAACCCCAAATTCCCATACATAATG/ CTTCCTCTTCTGCTGCTTCACC	NA	263/207
T31B5	CTTGTTTTCCGATTTGAACCACATTCC/ GTCATGTCCAGACGTTGTAACCTGT	TaqI	232 + 80/ 312
T22N19	GAAGAGGAAGAAGATTTGGAGTCG/ CTATGAGCATCTATCGCCATCATG	ScrFI	230/ 107 + 123
T6I14	TGGATAAGTCACAATGAGGTAGCTG/ CCACCCATCTCTTGATAACAGCA	NA	197/187
MXE10	TTTGCGCTTAACAACGGTTTGTTGAC/ CCATTTGGGTGCCTGCACATTG	NA	204/192
MAC12	CCACTTGGACCCACTTAATACATACC/ CCCGTTCTCAGATTCACGATCATAACA	ClaI	117/ 114 + 60
MUA22	GTCTCAGCCCTCTTGCAGAAAG/ CATGAAGCTCTAGCGCATTGCTTG	NA	228/216

1. Marker name, 2. Primer sequences (forward primer/reverse primer), 3. Restriction endonucleases required for CAPS markers, 4. Lengths of PCR products (bp) derived from SSLP markers or digested CAPS markers (Columbia-0/Landsberg *erecta*).

flow hood. Seeds were plated on Linsmaier and Skoog media containing 1% sucrose and 0.5% phytoblend (Caisson Laboratories Inc., Logan UT). Seeds were stratified for 4 d at 4° C and grown for the indicated number of d at 21° C and under the indicated fluence rate of white light from broad-spectrum fluorescent tube lamps. For high-intensity-light (HL) experiments, a combination of high-pressure sodium and metal halide lamps was used. White light was filtered through neutral density filters (Roscolux #397; Rosco Laboratories, Stamford CT) to obtain particular fluence rates. Fluence rates were measured with an LI-250A photometer using a PAR sensor (LI-COR Biosciences, Lincoln Nebraska).

Chlorophyll was extracted and quantified as exactly as previously described (Porra et al., 1989) except that 50 mg of seedlings were homogenized in 1.5 ml microfuge tubes that contained a single 3 mm very high density zirconium oxide bead (Glen Mills Inc., Clifton NJ) using a Retsch TissueLyser (Qiagen).

Intact chloroplasts were purified from wild-type *Arabidopsis* plants and the indicated *Arabidopsis* mutants and transgenic lines after the indicated growth period under 125  $\mu\text{mol m}^{-2}\text{s}^{-1}$  white light from broad-spectrum fluorescent tube lamps with a diurnal cycle that contained 12 h of light and 12h of dark. Chloroplasts were purified from 40 g of 10-d-old *Arabidopsis* seedlings, as previously described (Kubis et al., 2008). Relative amounts of chloroplasts were determined by quantifying total protein rather than chlorophyll because a striking variation in chlorophyll levels was observed among the wild type and the various transgenic lines and mutants. We determined the levels of

GUN4 and Mg-chelatase subunits using affinity purified anti-GUN4, -ChlH, -ChII, and -ChlD antibodies and immunoblotting as previously described (Larkin et al., 2003; Adhikari et al., 2009). Quantitative analysis of immunoblots was performed by quantifying the chemiluminescence from immunoreactive bands using the Versadoc MP 4000 (BioRad, Hercules CA) as described by Adhikari et al. (2009).

For quantitative reverse transcription polymerase chain reaction (qRT-PCR) analyses, we extracted total RNA using the RNeasy Plant Mini Kit (Qiagen, Valencia CA). We synthesized cDNA using the Superscript III (Invitrogen, Carlsbad CA). The oligonucleotides used for amplifying cDNAs encoding WRKY40 (At1g80840), ZAT10 (At1g27730), and UBQ10 (At4g05320) were as previously reported (Czechowski et al., 2005; Walley et al., 2007; Giraud et al., 2008). We assayed transcript levels using the Fast SYBR® Green Master Mix and the ABI 7500 Fast Real-time PCR system (Applied Biosystems Inc., Foster City CA). *WRKY40* and *ZAT10* expression were normalized to *UBQ10* expression.

## **RESULTS**

### **Analysis of chlorophyll deficiencies in *gun4* and *chlH* mutants**

To test the in vivo significance of the porphyrin-binding activities that were previously quantified for GUN4 in vitro, we stably transformed Arabidopsis plants with transgenes in which the native *GUN4* promoter drives expression of wild-type *GUN4* (Larkin et al., 2003) and *gun4* alleles that encode R211A and F191A substitutions in the derived amino acid sequence, all of which lower the binding affinity of GUN4 for porphyrins.

The R211A and F191A substitutions cause a ca. 2-fold increase in  $K_d^{\text{DPIX}}$  and a 3- to 5-fold increase in  $K_d^{\text{Mg-DPIX}}$  (Adhikari et al., 2009). Homologous amino acid substitutions lower the affinity of SynGUN4 for DPIX and Mg-DPIX and reduce the Mg-chelatase stimulatory activity of SynGUN4 in vitro (Davison et al., 2005; Verdecia et al., 2005). We transformed lines that are heterozygous for *gun4-2*, a null allele (Larkin et al., 2003), and homozygous for a T-DNA insertion allele for *suppressor of gene silencing 3* (*sgs-3*; NDA unpublished data) that confers resistance to transgene-induced silencing (Butaye et al., 2004). *GUN4*-expressing transgenes induce robust cosuppression of *GUN4* in Arabidopsis (Larkin et al., 2003). These stably transformed Arabidopsis plants were determined to contain single *GUN4*-expressing transgenes by scoring antibiotic resistance in segregating populations (NDA, unpublished data). We isolated lines that were homozygous for the *GUN4*-expressing transgene, *gun4-2*, and *sgs-3* (Figure 3-1A). *gun4-1* and *gun4-2* are the only two previously described mutant alleles for *GUN4* in Arabidopsis. *gun4-1* encodes an L88F substitution and accumulates barely detectable levels of GUN4 protein (Larkin et al., 2003). *gun4-2* is a protein null (Larkin et al., 2003). In contrast, immunoblotting analysis of whole seedling extracts prepared from 7-d-old transgenic seedlings indicates that the transgenic lines GUN4-14, F191A-14, and R211A-2.2 express similar but slightly higher levels of GUN4, R211A, and F191A proteins, respectively, relative to the wild type (Figure 3-1B). We found that other transgenic lines prepared by the same procedures express much higher (F191A-1) or much lower (R211A-2.5) levels of either F191A or R211A than wild type (Figure 3-1B). We attribute these differences to the insertion of these transgenes into different positions within the genome.

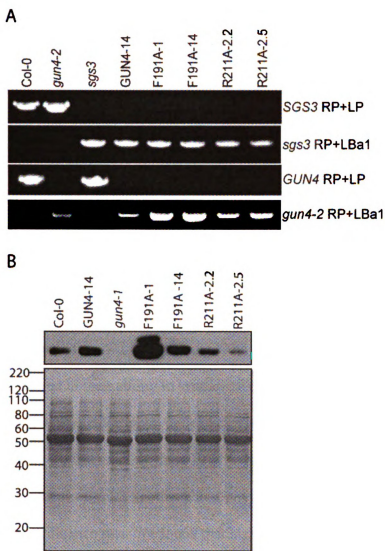


Figure 3-1. Analysis of stably transformed Arabidopsis plants containing *GUN4*-related transgenes. (A) Screening of stably transformed Arabidopsis plants containing *GUN4*-related transgenes for *sgs3* and *gun4-2* T-DNA insertion alleles. Genomic DNA was extracted from the indicated mutant or the indicated stably transformed line. Transgenic plants were from the T5 generation or a subsequent generation. Plants were screened for wild type and T-DNA insertion alleles by PCR-based genotyping with oligonucleotides that can amplify PCR products from *SGS3* (*SGS3* RP + LP), *GUN4* (*GUN4* RP + LP) or particular T-DNA insertion alleles (*sgs3* RP + LBa1 or *gun4-2* RP + LBa1). PCR products were identified by electrophoresis in agarose gels followed by staining with ethidium bromide. (B) Analysis of *GUN4* protein levels in stably transformed Arabidopsis plants containing *GUN4*-related transgenes. Protein was extracted from the indicated mutant or the indicated stably transformed line grown in  $100 \mu\text{mol m}^{-2} \text{s}^{-1}$  broad spectrum white light. Aliquots of these whole seedling extracts that contained  $10 \mu\text{g}$  of protein were analyzed by immunoblotting using anti-*GUN4* antibodies (upper panel). After immunoblotting each membrane was stained with Coomassie blue (lower panel). Mass standards are indicated at the left in kDa.

Based on previous analyses of GUN4 and SynGUN4 (Verdecia et al., 2005; Adhikari et al., 2009), we predicted that lines expressing F191A and R211A would contain reduced Mg-chelatase activity and therefore would exhibit chlorophyll deficiencies relative to wild type. Indeed, we found that, like the chlorophyll-deficient *gun4-1* (Vinti et al., 2000; Mochizuki et al., 2001), the F191A- and R211A-expressing lines accumulate 1.3- to 2.0-fold less chlorophyll per mg fresh weight than wild type when these seedlings were grown for 7 d in  $100 \mu\text{mol m}^{-2} \text{s}^{-1}$  white light (Figure 3-2; Figure 3-3A and B). Under these conditions, *gun4-1* accumulated 2.9-fold less chlorophyll per mg fresh weight than wild type (Figure 3-2; Figure 3-3), which is consistent with previous analyses of *gun4-1* (Vinti et al., 2000; Mochizuki et al., 2001). Mutants that are impaired in their ability to synthesize chlorophyll were previously reported to exhibit more severe chlorophyll deficiencies after fluence rates were increased (Falbel et al., 1996). To test whether these F191A- and R211A-expressing lines exhibit light-sensitive phenotypes similar to other chlorophyll-deficient mutants, we transferred them to a higher fluence rate. We found that high-intensity light enhances chlorophyll deficiencies in *gun4-1* and the F191A- and R211A-expressing lines. When 3-d-old seedlings were transferred from  $100 \mu\text{mol m}^{-2} \text{s}^{-1}$  to  $850 \mu\text{mol m}^{-2} \text{s}^{-1}$  and grown for an additional 4 d, the transgenic lines contained two- to 4-fold less chlorophyll than wild type and *gun4-1* contained 40-fold less chlorophyll than wild type (Figure 3-2; Figure 3-4A and B).

Next, we tested whether available Arabidopsis *chlH* mutants exhibited light-sensitive phenotypes similar to *gun4-1*, R211A, and F191A. For these experiments, we tested

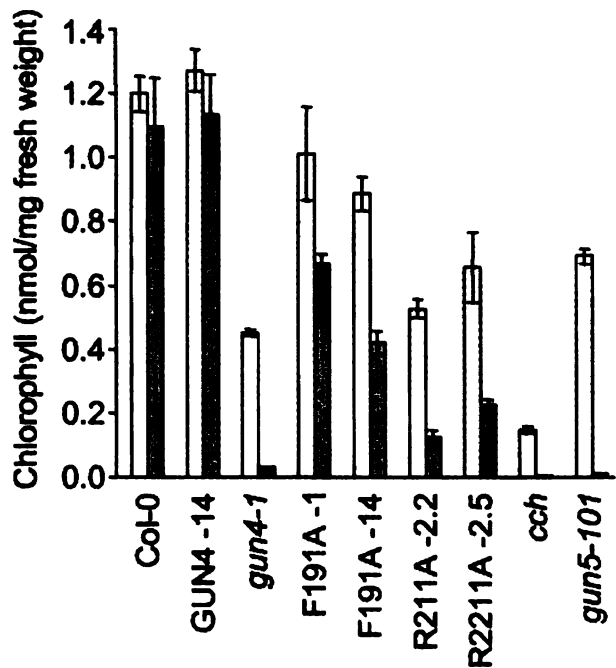


Figure 3-2. Analysis of chlorophyll levels in *gun4* and *chlH/gun5* mutants grown under different fluence rates. Seedlings were grown in continuous  $100 \mu\text{mol m}^{-2} \text{s}^{-1}$  white light for 7d (white bars) or seedlings were grown for 3d in continuous  $100 \mu\text{mol m}^{-2} \text{s}^{-1}$  white light then 4d in continuous  $850 \mu\text{mol m}^{-2} \text{s}^{-1}$  white light (gray bars). Chlorophyll was extracted from at least three biological replicates for each mutant or line in each condition. Error bars indicate 95% confidence intervals.

1

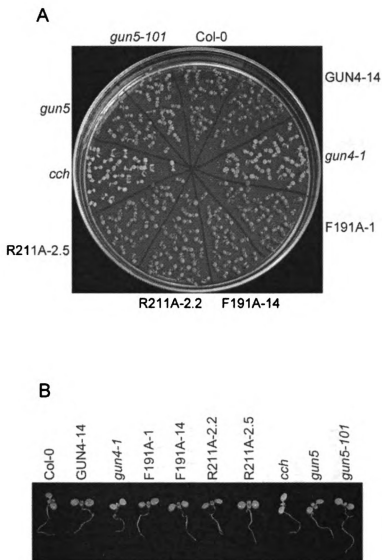


Figure 3-3. Images of seedlings grown in  $100 \mu\text{mol m}^{-2} \text{s}^{-1}$  white for 7d.  
 (A) Representative plate containing seedlings grown in  $100 \mu\text{mol m}^{-2} \text{s}^{-1}$  white light for 7d. Each sector contains >20 seedlings. Wild type (Col-0), mutants, and transgenic lines are indicated. (B) Representative individual seedlings grown in  $100 \mu\text{mol m}^{-2} \text{s}^{-1}$  white light for 7d. Wild type (Col-0), mutants, and transgenic lines are indicated.

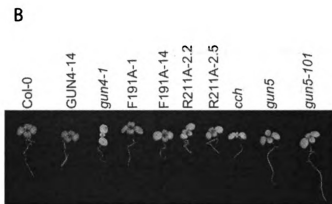
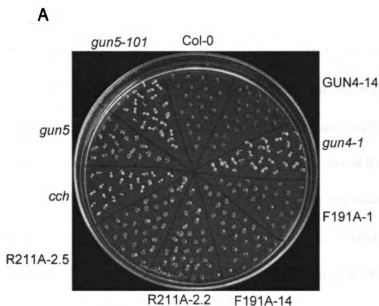


Figure 3-4. Images of seedlings grown in  $100 \mu\text{mol m}^{-2} \text{s}^{-1}$  white light for 4d and then shifted to  $850 \mu\text{mol m}^{-2} \text{s}^{-1}$  white light for 3d. (A) Representative plate containing seedlings grown in  $100 \mu\text{mol m}^{-2} \text{s}^{-1}$  white light for 4d then shifted to  $850 \mu\text{mol m}^{-2} \text{s}^{-1}$  white light for 3d. Each sector contains >20 seedlings. Wild type (Col-0), mutants, and transgenic lines are indicated. (B) Representative individual seedlings grown in  $100 \mu\text{mol m}^{-2} \text{s}^{-1}$  white light for 4d then shifted to  $850 \mu\text{mol m}^{-2} \text{s}^{-1}$  white light for 3d. Wild type (Col-0), mutants, and transgenic lines are indicated.

*gun5* and *cch* mutants, which are missense alleles of the *ChlH* gene in Arabidopsis (Mochizuki et al., 2001). We hereafter refer to this gene as *ChlH/GUN5* to avoid the confusion that can come from different nomenclature. We also tested the Arabidopsis *gun5-101* mutant, which we isolated from a new *gun* mutant screen (Ruckle et al., 2007). *gun5-101* was mapped (Figure 3-5A) and found to be a novel missense allele that causes a P450L substitution in the derived amino acid sequence of ChlH/GUN5 (Figure 3-5B). We also tested the *cs* mutant, which is strikingly deficient in chlorophyll because of a defect in the ChlI subunit of Mg-chelatase (Koncz et al., 1990; Mochizuki et al., 2001; Adhikari et al., 2009). *gun5*, *cch*, and *gun5-101* accumulate 2.0- to 6.7-fold less chlorophyll than wild type when seedlings are grown in  $100 \mu\text{mol m}^{-2} \text{s}^{-1}$  for 7 d (Figure 3-2; Figure 3-3A and B). *gun5* and *gun5-101* accumulate 10- and 120-fold less chlorophyll, respectively, than wild type when seedlings are grown in  $100 \mu\text{mol m}^{-2} \text{s}^{-1}$  for 3 d and then transferred to  $850 \mu\text{mol m}^{-2} \text{s}^{-1}$  for 4 d (Figure 3-2; Figure 3-4A and B). We could not extract detectable levels of chlorophyll when *cch* was grown under these conditions (Figure 3-2; Figure 3-4A and B). The *cs* mutant contains 2-fold less chlorophyll than wild type when seedlings are grown in  $100 \mu\text{mol m}^{-2} \text{s}^{-1}$  for 7 d and 8-fold less chlorophyll than wild type when 3-d-old seedlings are transferred from  $100 \mu\text{mol m}^{-2} \text{s}^{-1}$  to  $850 \mu\text{mol m}^{-2} \text{s}^{-1}$  and grown for an additional 4 d. Thus, all of the transgenic lines exhibit chlorophyll deficiencies compared to wild type, as previously observed for chlorophyll-deficient mutants. To explore the mechanism underlying these light-sensitive phenotypes, we next monitored the levels of GUN4 and Mg-chelatase subunit levels by immunoblotting. We observed a striking reduction in GUN4 protein levels in R211A, F191A, *gun4-1*, *cch*, and

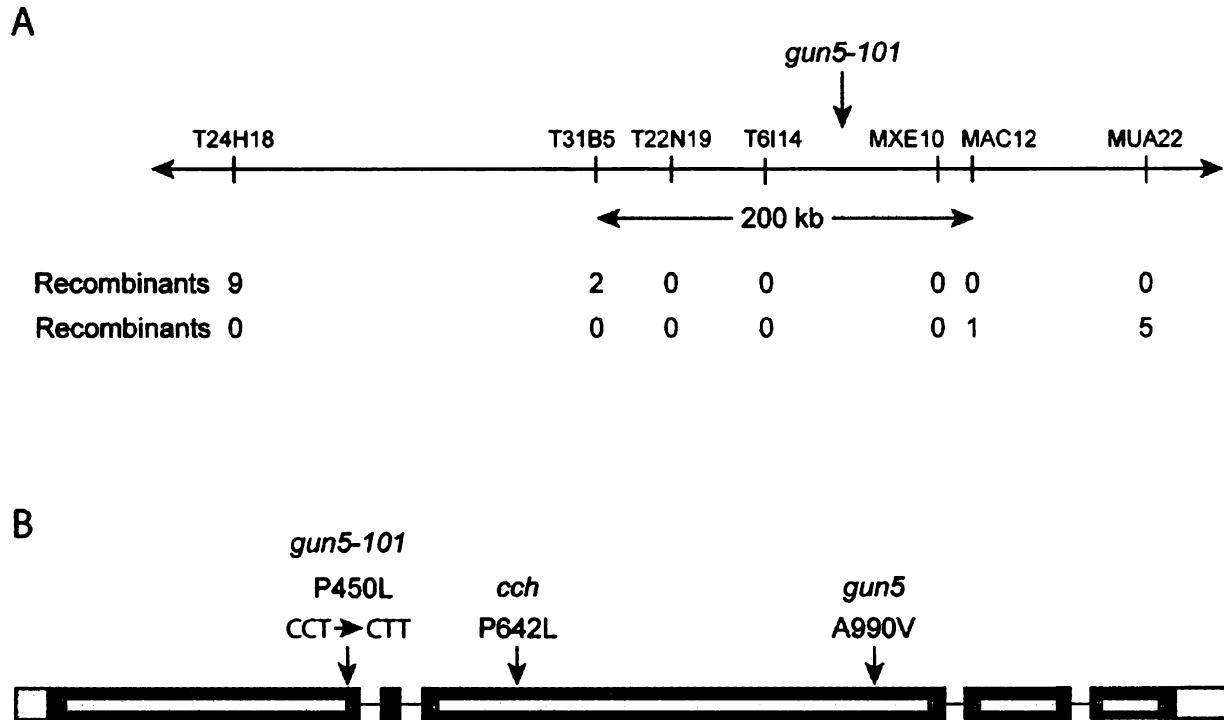


Figure 3-5. Positional cloning and sequence analysis of *gun5-101*. (A) Positional cloning of *gun5-101*. The chlorophyll-deficient phenotype was mapped based on an analysis of 2110 chromosomes from F2 progeny that resulted from a *gun5-101* × *Landsberg erecta* cross and exhibited a chlorophyll-deficient phenotype similar to *gun5-101*. Chromosomes were analyzed using SSLP and CAPS markers (12). The relative positions and names of bacterial artificial chromosome clones from which each marker was derived are indicated. The recombinants that are centromere distal (top) and centromere proximal (bottom) relative to *gun5-101* are indicated. The location of *gun5-101* within the 200 kb interval that is defined by the recombinants is indicated. (B) Nucleotide and derived amino acid sequences of *gun5-101*. Lines and boxes indicate introns and exons, respectively. Light gray boxes indicate untranslated exons. The altered codon and the substitution in the derived amino acid sequence found in *gun5-101* are indicated. The positions of the single nucleotide substitutions and the substitutions in the derived amino acid sequence found in *gun5* and *cch* are also indicated.

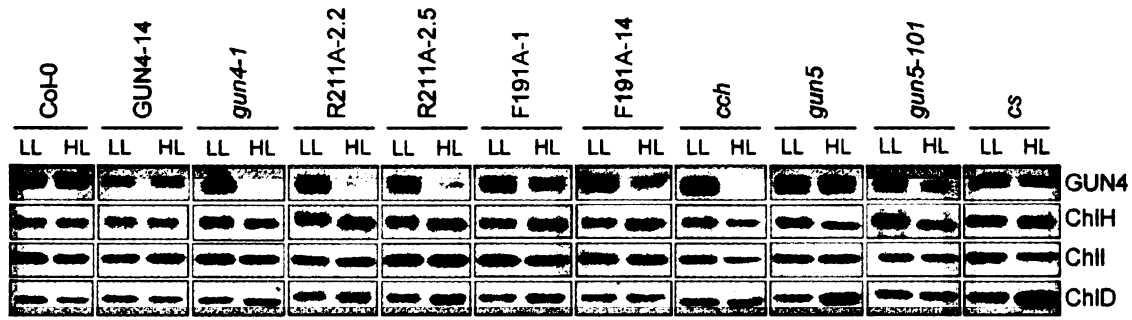


Figure 3-6. Analysis of GUN4 and Mg-chelatase subunit levels in  $100 \mu\text{mol m}^{-2} \text{s}^{-1}$  and  $850 \mu\text{mol m}^{-2} \text{s}^{-1}$  white light. Seedlings were grown in  $100 \mu\text{mol m}^{-2} \text{s}^{-1}$  for 7d (LL) and  $100 \mu\text{mol m}^{-2} \text{s}^{-1}$  for 3d and  $850 \mu\text{mol m}^{-2} \text{s}^{-1}$  white light for 4d (HL) as indicated in Figure 3-2. Protein was extracted from the indicated mutant or the indicated stably transformed line. Aliquots of these whole seedling extracts that contained  $10 \mu\text{g}$  of protein were analyzed by immunoblotting using anti-GUN4 antibodies, anti-ChlH antibodies, anti-ChlI antibodies, or anti-ChlD antibodies. Exposures were adjusted so that the faint bands in HL extracts are observable.

*gun5-101* relative to wild type after seedlings are transferred from 100  $\mu\text{mol m}^{-2} \text{s}^{-1}$  to 850  $\mu\text{mol m}^{-2} \text{s}^{-1}$  (Figure 3-6). In contrast, ChlH/GUN5, ChlI, and ChlD levels were either unaffected or only slightly reduced following these fluence-rate shifts (Figure 3-6). Transferring *cs* and *gun5* to higher fluence rates had no effect on the accumulation of the GUN4 protein (Figure 3-6). These data indicate that the striking reduction of GUN4 protein levels that occurs in bright light is dependent on particular amino acid substitutions in GUN4 and ChlH; weak loss-of-function alleles of *ChlH*, such as *gun5*, and strong loss-of-function alleles of *ChlI*, such as *cs*, have no effect (Figure 3-6).

#### **Analysis of interactions between GUN4, ChlH/GUN5, and chloroplast membranes**

Previous findings indicate that porphyrin binding promotes the association of GUN4 with chloroplast membranes (Adhikari et al., 2009). Based on these findings, we expected that F191A and R211A would not associate with chloroplast membranes as stably as GUN4. We also analyzed *gun4-1* (Larkin et al., 2003). A similar or greater percentage of GUN4 is expected in the membrane-containing pellet fractions derived from *gun4-1* and wild type because amino acid substitutions homologous to L88F increase the porphyrin-binding affinities of *Thermosynechococcus elongatus* GUN4 and *Synechocystis* GUN4 (Davison et al., 2005). Indeed, we found that when purified chloroplasts were lysed and fractionated, significantly less GUN4 was associated with the membrane-containing pellet fractions derived from R211A and F191A than with those derived from wild type and that the distribution of GUN4 in soluble and membrane-containing pellet fractions was similar in *gun4-1* and wild type (Figure 3-7A and B; Figure 3-8).

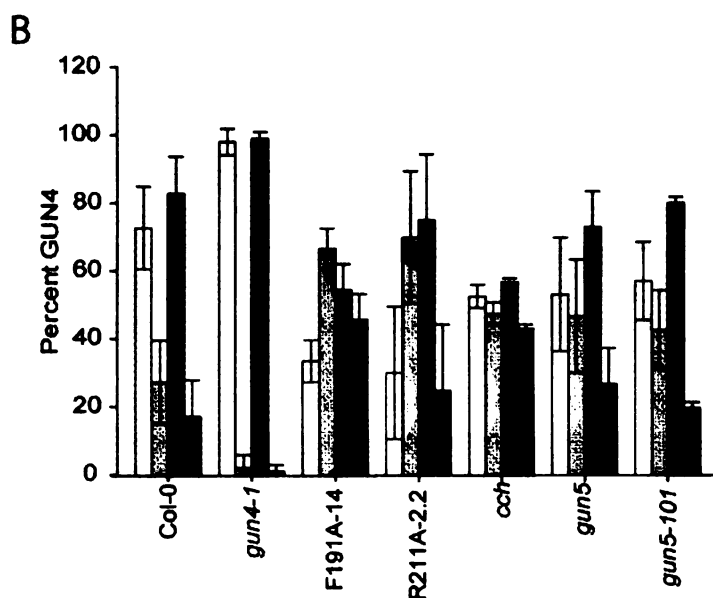
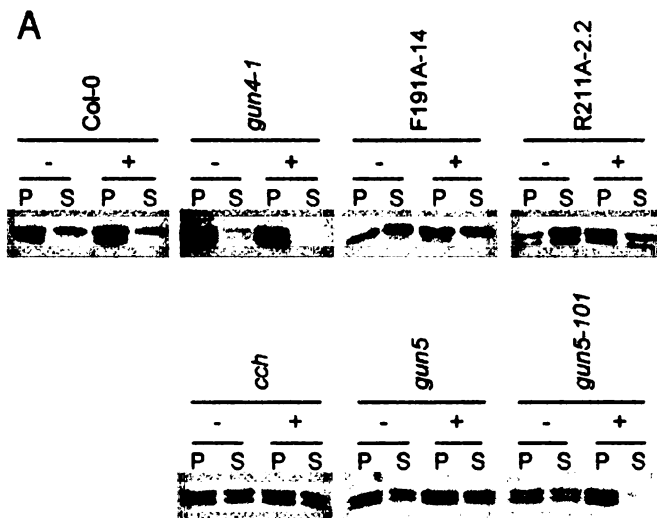


Figure 3-7. Distribution of GUN4 in lysed and fractionated chloroplasts that were purified from *gun4* and *chlH/gun5* mutants and were either fed or not fed with PPIX. (A) Representative immunoblots showing the distribution of GUN4 in lysed and fractionated chloroplasts that were purified from *gun4* and *chlH/gun5* mutants and fed or not fed with PPIX. Purified intact chloroplasts (200  $\mu$ g) were either fed (+) or not fed (-) with 20  $\mu$ M PPIX. These chloroplasts were then fractionated into soluble and membrane-containing pellet fractions of equal volume. Equal volumes were analyzed by SDS-PAGE and immunoblotting with anti-GUN4 antibodies. (B) Quantitative analysis of GUN4 immunoblots showing the distribution of GUN4 in fractionated chloroplasts that were purified from *gun4* and *chlH/gun5* mutants and fed or not fed with PPIX. The percent of GUN4 in the pellet (white bars) and supernatant (light-gray bars) fractions derived from chloroplasts that were not fed PPIX and the percent GUN4 in the pellet (medium-gray bars) and supernatant (dark-gray bars) fractions derived from chloroplasts that were fed PPIX are indicated for wild type (Col-0) and each mutant and transgenic line. Results from at least 2 independent experiments are shown. Error bars represent 95% confidence intervals.

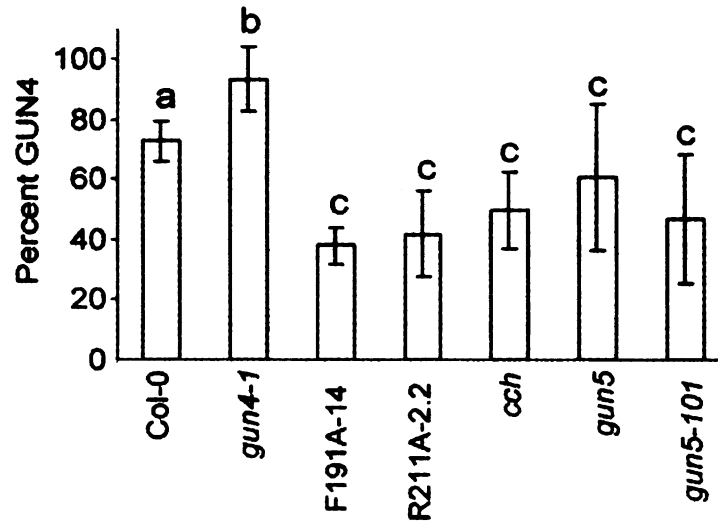


Figure 3-8. Statistical analysis of GUN4 in membrane-containing pellet fractions derived from purified and fractionated chloroplasts. Chloroplasts were purified from wild type (Col-0) or the indicated mutants or transgenic lines. These chloroplasts were fractionated and GUN4 protein levels determined in membrane-containing pellet fractions as described in Figure 4. Significance differences among genetic backgrounds were tested among replicates and independent experiments using the unpaired t-test. Data from at least three and as many as 11 independent experiments are shown. a, GUN4 protein levels in the membrane-containing pellet fractions derived from Col-0 chloroplasts were found to be very significantly different from those derived from *gun4-1*, F191A-14, R211A-2.2, *cch*, *gun5-101* ( $P < 0.005$ ) but not *gun5* ( $P = 0.2$ ). b, GUN4 protein levels in the membrane-containing pellet fractions derived from *gun4-1* were found to be significantly different from those derived from *gun5* ( $P = 0.05$ ) or very significantly different from those derived from *gun4-1*, F191A-14, R211A-2.2, *cch*, *gun5-101* ( $P < 0.009$ ). c, GUN4 protein levels in the membrane-containing pellet fractions derived from *gun4-1*, F191A-14, R211A-2.2, *cch*, *gun5*, and *gun5-101* were not significantly different from each other ( $P \geq 0.1$ ).

Although previous findings indicate that GUN4 associates with ChlH and that both proteins interact with chloroplast membranes, whether interaction between these two proteins is required for their association with chloroplast membranes is not clear (Larkin et al., 2003; Adhikari et al., 2009). To test whether the interactions between GUN4 and chloroplast membranes depend on ChlH/GUN5, we purified chloroplasts from *gun5*, *cch*, and *gun5-101*, then lysed and fractionated them into soluble and membrane-containing pellet fractions. We found that significantly less GUN4 associated with the membrane-containing pellet fractions derived from *cch* and *gun5-101* than with those derived from wild type (Figure 3-7A and B; Figure 3-8). The weakness of the *gun5* allele relative to *gun5-101* and *cch* (Vinti et al., 2000; Mochizuki et al., 2001) likely explains the lack of a significant effect in *gun5* relative to wild type (Figure 3-7; Figure 3-8). This effect on the membrane association of GUN4 appears specific to strong alleles of *gun4* and *gun5* because we did not find significantly less GUN4 protein in the membrane-containing pellet fractions derived from either *gun5* or *cs* relative to wild type (Figure 3-9). In these same experiments, more ChlH/GUN5 accumulated in the supernatant and less in the membrane-containing pellet fraction among these transgenic lines, mutants, and wild type (Figure 3-10; Table 3-2). The reduction in the association between ChlH/GUN5 and chloroplast membranes in these transgenic lines, mutants, and wild type is somewhat muted compared to our findings with GUN4.

The distribution of pea GUN4 and in vitro translated and imported GUN4 are similar in fractionated pea chloroplasts to those reported here for fractionated Arabidopsis

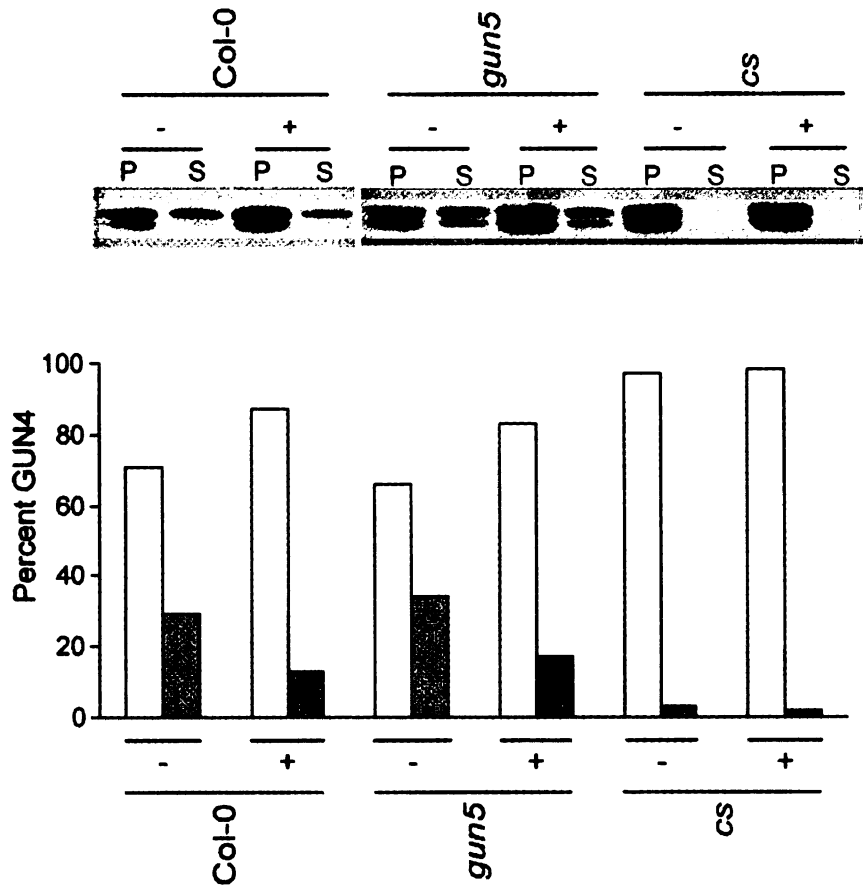


Figure 3-9. Distribution of GUN4 in soluble and membrane-containing pellet fractions derived from wild type, *gun5*, and *cs* chloroplasts. Intact chloroplasts were purified from wild type (Col-0), *gun5*, and *cs*. Purified chloroplasts were fed (+) or not fed (-) with PPIX, fractionated, and analyzed by immunoblotting with anti-GUN4 antibodies as described in Figure 3-7. The membrane-containing pellet (P or white bars) and supernatant fractions (S or gray bars) in the resulting immunoblot (above) were quantified by chemiluminescence from the immunoreactive bands (below).

Table 3-2. Percent decrease in the membrane association of ChlH in untreated samples compared to WT. Error is represented by standard error of 2 independent experiments.

Line	Decrease in membrane association of ChlH in untreated samples
<i>gun4-1</i>	13 ( $\pm 6$ ) %
F191A 14	9 ( $\pm 6$ ) %
R211A 2-2	14 ( $\pm 1$ ) %
<i>cch</i>	20 ( $\pm 1$ ) %
<i>gun5</i>	17 ( $\pm 5$ ) %
<i>gun5-101</i>	20 ( $\pm 2$ ) %

chloroplasts. Additionally, the interactions between pea chloroplast membranes and both pea GUN4 and the in vitro translated and imported GUN4 were previously reported to be enhanced by inducing an increase in the porphyrin levels of purified chloroplasts. In contrast, in vitro translated and imported R211A or F191A do not associate with pea chloroplast membranes, regardless of whether porphyrin levels are increased (Adhikari et al., 2009). The inability of elevated porphyrin levels to promote interactions between pea chloroplast membranes and either R211A or F191A is consistent with (1) R211A and F191A not only affecting porphyrin binding but also disrupting interactions between GUN4 and chloroplast membranes by inhibiting some other function of GUN4 besides porphyrin binding or (2) a technical limitation of the pea system such as the vast molar excess of pea GUN4 competing more effectively with in vitro translated and imported R211A and F191A than with in vitro translated and imported wild-type GUN4. To distinguish between these possibilities, we induced an increase in the porphyrin levels of chloroplasts that were purified from *gun4* and *gun5/chlH* mutants by feeding these chloroplasts with PPIX, as previously described by Adhikari et al. (2009). PPIX feeding did not have a major impact on the membrane association of GUN4 protein in wild type, *gun4-1*, or *cs* (Figure 3-7A and B; Figure 3-9). Further promotion by PPIX of interactions between GUN4 and chloroplast membranes may not be possible in wild type, *gun4-1*, and *cs* because the bulk of GUN4 already stably associates with the membrane-containing pellet fractions of unfed chloroplasts purified from wild type, *gun4-1*, and *cs* when chloroplasts are lysed and fractionated under these conditions (Figure 3-7A and B; Figure 3-9). In contrast, feeding PPIX to chloroplasts purified from the F191A- and R211A-expressing lines

caused a 20% and 45% increase in the amount of F191A and R211A, respectively, retained in the membrane-containing pellet fraction (Figure 3-7A and B; Table 3-3). Based on these findings, we conclude that R211A and F191A can disrupt porphyrin binding *in vivo*. We also conclude that *in vitro* translated and imported R211A or F191A probably do not associate with pea chloroplast membranes regardless of whether porphyrin levels are increased, because the vast molar excess of pea GUN4 competes more effectively with R211A and F191A than with wild type GUN4, as previously suggested by Adhikari et al. (2009). We also observed that PPIX feeding of chloroplasts purified from *gun5* and *gun5-101*—but not *cch*—caused at least a 20% increase in GUN4 protein levels in the membrane-containing pellet fractions (Figure 3-7; Table 3-3). Based on these findings, we conclude that interactions between GUN4 and chloroplast membranes are promoted by GUN4 binding both PPIX and ChlH/GUN5. By analyzing these same fractions by immunoblotting with anti-ChlH/GUN5 antibodies, we found that the interactions between GUN5/ChlH and chloroplast membranes are disrupted in all of these mutants relative to wild type. However, in contrast to GUN4, PPIX feeding did not affect the interactions between GUN5/ChlH and chloroplast membranes in any of these mutants (Figure 3-10).

#### **Analysis of ROS-inducible gene expression**

Because porphyrins are photosensitizers, misregulated chlorophyll biosynthesis driving elevated ROS-induced cellular damage was previously suggested to in part explain the light sensitivity of chlorophyll-biosynthesis mutants (Falbel et al., 1996). However, ROS is produced not only from collisions between chlorophyll precursors and O<sub>2</sub> in

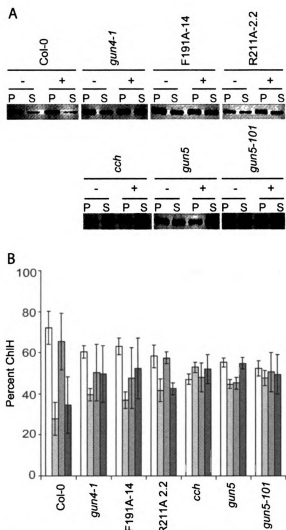


**Figure 3-10.** Distribution of ChlH/GUN5 in lysed and fractionated chloroplasts that were purified from *gun4* and *chlH/gun5* mutants and were either fed or not fed with PPIX. (A) Representative immunoblots showing the distribution of ChlH/GUN5 in lysed and fractionated chloroplasts that were purified from *gun4* and *chlH/gun5* mutants and fed (+) or not fed (-) with PPIX. The same fractions described in Figure 4 were analyzed by immunoblotting with anti-ChlH/GUN5 antibodies. As described for Figure 4, 200  $\mu$ g of purified intact chloroplasts were either fed (+) or not fed (-) with 20  $\mu$ M PPIX. These chloroplasts were then fractionated into soluble and membrane-containing pellet fractions of equal volume. Equal volumes were analyzed by SDS-PAGE and immunoblotting. (B) Quantitative analysis of ChlH/GUN5 immunoblots showing the distribution of GUN4 in chloroplasts that were purified from *gun4* and *chlH/gun5* mutants and fed or not fed with PPIX. The percent ChlH/GUN5 in the pellet (white bars) and supernatant (light-gray bars) fractions derived from chloroplasts that were not fed PPIX and the percent ChlH/GUN5 in the pellet (medium-gray bars) and supernatant (dark-gray bars) fractions derived from chloroplasts that were fed PPIX are indicated for wild type (Col-0) and each mutant and transgenic line. Results from at least two independent experiments are shown. Error bars represent 95% confidence intervals.

Table 3-3. Percent increase in GUN4 protein in the membrane -containing pellet fraction following PPIX feeding.

Line	Percent increase in GUN4 protein in the membrane-containing pellet fraction following PPIX feeding
Col-0	13±5%
<i>gun4-1</i>	1±2%
F191A	21±2%
R211A	45±0%
<i>cch</i>	4±2%
<i>gun5</i>	20±16%
<i>gun5-101</i>	23±10%

Error is represented by 95% confidence intervals. N≥2

bright light but can also be produced from photosystems and the photosynthetic electron transfer (Niyogi, 1999; Li et al., 2009). To distinguish between these possibilities, we grew the *gun4* and *chlH/gun5* mutants under  $10 \mu\text{mol m}^{-2} \text{s}^{-1}$  white light. The levels of chlorophyll, levels and compositions of the photosystems, and thylakoid ultrastructures were previously reported to be more similar in comparisons between particular chlorophyll-deficient mutants and wild type when plants are grown under low fluence rates (Allen et al., 1988; Falbel et al., 1996). We noted that in  $10 \mu\text{mol m}^{-2} \text{s}^{-1}$  white light, the chlorophyll levels of *gun4-1*, both F191A lines, both R211A lines, *gun5*, and *gun5-101* are essentially the same as in wild type (Figure 3-11A, B, and C). Chlorophyll levels in *cch* were slightly less than wild type (Figure 3-11A, B, and C). Therefore, in this  $10 \mu\text{mol m}^{-2} \text{s}^{-1}$  light and shortly after seedlings are transferred to  $850 \mu\text{mol m}^{-2} \text{s}^{-1}$  white light, we expect that differences in ROS levels among these mutants, transgenic lines, and wild type will largely result from misregulated chlorophyll metabolism and that different electron transport activities will be responsible for a smaller proportion of the ROS.

To test whether elevated ROS might contribute to the light sensitivities of these mutants and transgenic lines, we monitored the expression levels of ROS-inducible genes following fluence rate increases. We chose to monitor the expression of *WRKY40* and *ZAT10* because the expression of these genes is induced 10- to 250-fold in response to diverse ROS (Gadjev et al., 2006) and the expression levels of these genes range from the 60th to 88th percentile based on publicly available microarray data (NDA, unpublished observations). Therefore, monitoring the expression of these genes provides a sensitive

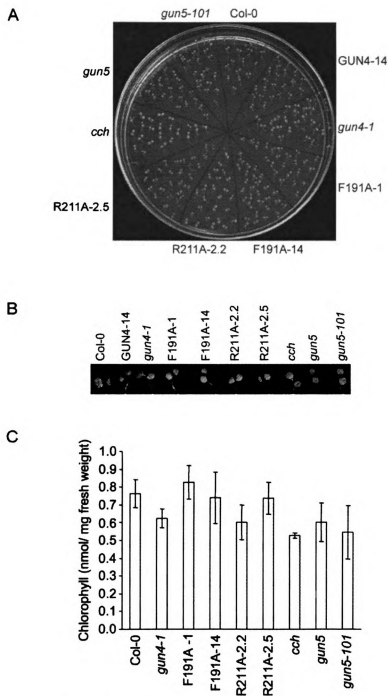


Figure 3-11. Analysis of chlorophyll levels in *gun4* and *chlH/gun5* mutants grown in  $10 \mu\text{mol m}^{-2} \text{s}^{-1}$  white light. (A) Representative plate containing seedlings grown in  $10 \mu\text{mol m}^{-2} \text{s}^{-1}$  white light. Seedlings were grown in  $10 \mu\text{mol m}^{-2} \text{s}^{-1}$  white light for 7d. (B) Representative cotyledons from seedlings described in A. (C) Quantitative analysis of chlorophyll levels in seedlings described in A. Seedlings were grown as described in A. Chlorophyll was extracted from at least three biological replicates for wild type (Col-0) and for each of the indicated mutants and transgenic lines. Error bars indicate 95% confidence intervals.

assay for the production of ROS. We grew the seedlings in  $10 \mu\text{mol m}^{-2} \text{s}^{-1}$  white light for 7 d and then transferred them to  $850 \mu\text{mol m}^{-2} \text{s}^{-1}$  white light. We extracted RNA from seedlings that were collected immediately before this fluence-rate shift (0 h) and at 0.5 h, 1 h, and 3 h after this shift. We then quantified the levels of mRNA transcribed from *WRKY40* and *ZAT10*. Consistent with this previous work (Gadjev et al., 2006), we found that *WRKY40* and *ZAT10*-derived transcripts accumulate in wild type after the fluence-rate shift (Figure 3-12). Additionally, we found that the mRNAs transcribed from *WRKY40* and *ZAT10* were present at elevated levels in R211A and F191A relative to wild type when seedlings were grown in  $10 \mu\text{mol m}^{-2} \text{s}^{-1}$  white light and at levels similar to wild type after this fluence-rate shift (Figure 3-12).

To further test whether the induced expression of *WRKY40* and *ZAT10* that was observed in  $10 \mu\text{mol m}^{-2} \text{s}^{-1}$  is triggered by porphyrin-derived ROS, we monitored their expression in continuous and diurnal light. There is a burst of PPIX and Mg-PPIX biosynthesis at dawn that causes PPIX and Mg-PPIX to accumulate to readily detectable levels (Pöpperl et al., 1998; Papenbrock et al., 1999); this buildup of porphyrins in diurnal relative to continuous light causes photooxidative stress in mutants with defects in porphyrin metabolism (Meskauskiene et al., 2001; Peter and Grimm, 2009). (1) To test whether GUN4 and/or ChlH/GUN5 perform porphyrin-binding functions that are distinct from their chlorophyll biosynthetic functions and (2) to further test whether these elevated levels of *WRKY40* and *ZAT10* expression are triggered by porphyrin-derived ROS, we quantified their expression levels in a diurnal cycle that contained 12 h of  $2 \mu\text{mol m}^{-2} \text{s}^{-1}$  white light followed by 12 h of darkness. If GUN4 or a GUN4-

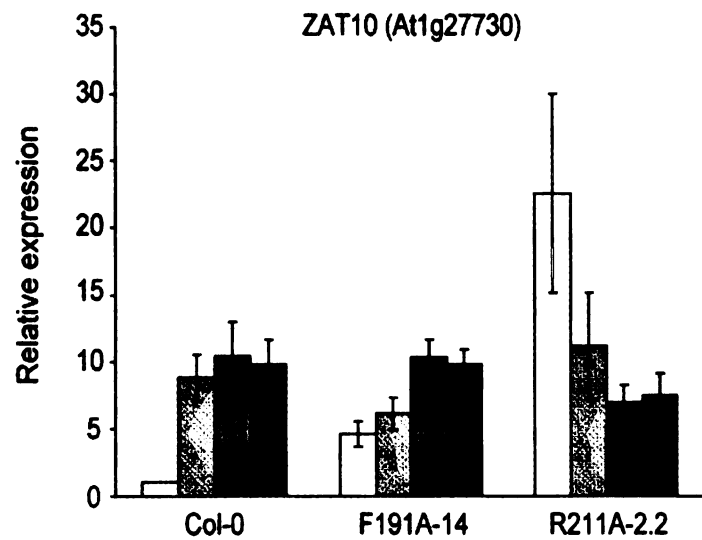
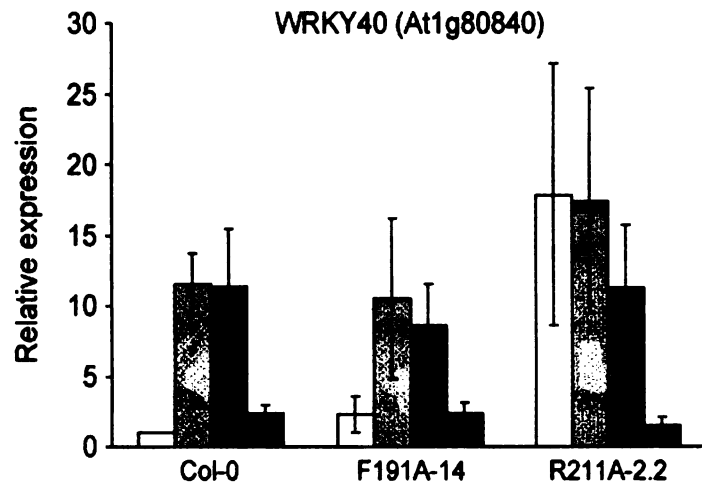


Figure 3-12. Induction of *WRKY40* and *ZAT10* expression during a fluence-rate shift. Wild type (Col-0), F191A-14, and R211A-2.2 were grown for 7d in  $10 \mu\text{mol m}^{-2} \text{s}^{-1}$  white light and then transferred to  $850 \mu\text{mol m}^{-2} \text{s}^{-1}$ . Transcripts from *WRKY40* (At1g80840; upper panel) and *ZAT10* (At1g27730; lower panel) were quantified by means of qRT-PCR at 0h (white bars), 0.5h (light-gray bars), 1h (medium-gray bars), and 3h (dark gray bars) after the fluence rate shift. Expression is reported relative to Col-0 at 0h, which was assigned a value of 1. Four biological replicates were analyzed at each time point. Error bars represent standard error.

ChlH/GUN5 complex binds these pools of porphyrins that accumulate during the diurnal cycle to shield them from collisions with O<sub>2</sub> and if these GUN4-porphyrin and GUN4-ChlH/GUN5-porphyrin complexes are a distinct pool relative to the GUN4-porphyrin and the GUN4-ChlH/GUN5-porphyrin complexes that are associated with the chlorophyll biosynthetic pathway, R211A and *cch* should accumulate more ROS than *cs* and the mRNAs transcribed from *WRKY40* and *ZAT10* should accumulate to higher levels in R211A and *cch* relative to *cs* in both continuous and diurnal light. Any ROS derived from only impaired Mg-chelatase activity is expected to be similar in R211A-2.2 and *cs* because these mutants have similar chlorophyll-deficient phenotypes (Figure 3-2). The expression of both *WRKY40* and *ZAT10* was significantly induced 6- to 17-fold in R211A-2.2, *cs*, and *cch* relative to wild type under these diurnal conditions (Figure 3-13). Neither R211A nor *cch* accumulated significantly more ROS than *cs*. Based on the gene expression assay used here, we conclude that transgenic lines that express only porphyrin-binding-deficient versions of GUN4 and mutants with defects in either ChlH/GUN5 or ChlI exhibit similar ROS phenotypes.

## **DISCUSSION**

Mg-chelatase is an unusual enzyme in that in most species, it requires a regulatory protein that binds one of its subunits, one of its substrates, and one of its products for robust activity. This proteinaceous cofactor, GUN4, was proposed to have evolved in part to attenuate the production of ROS by shielding PPIX and Mg-PPIX from collisions with O<sub>2</sub> (Larkin et al., 2003; Verdecia et al., 2005) and to channel PPIX and Mg-PPIX into chlorophyll biosynthesis by binding PPIX, Mg-PPIX, and ChlH/GUN5

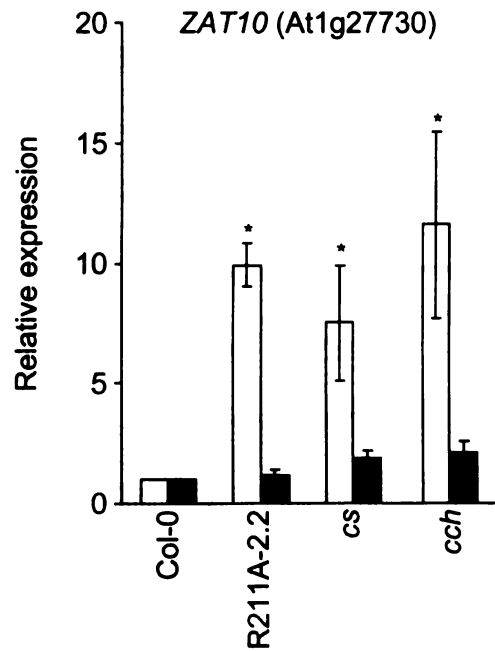
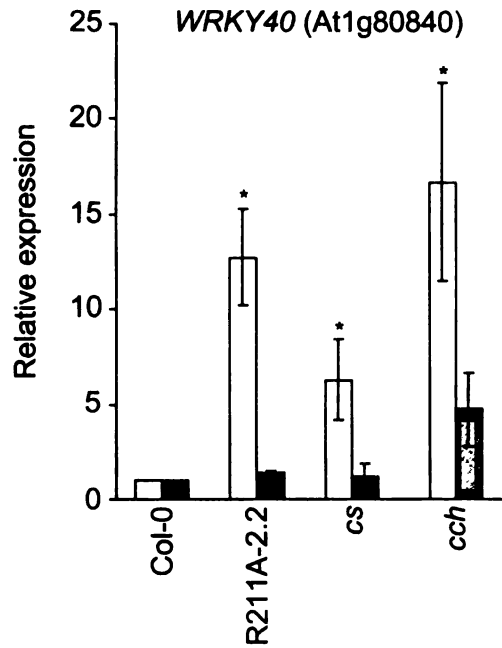


Figure 3-13. Analysis of *WRKY40* and *ZAT10* expression in diurnal and continuous light. Seedlings were grown for 7d in  $2 \mu\text{mol m}^{-2} \text{s}^{-1}$  white light that was a diurnal cycle containing 12h of light and 12 h of dark (white bars) or was continuous light (gray bars). All seedlings were harvested 1h after dawn. Transcripts from *WRKY40* (At1g80840; upper panel) and *ZAT10* (At1g27730; lower panel) were quantified by means of qRT-PCR. Expression is reported relative to Col-0 in continuous light, which was assigned a value of 1. Four biological replicates were analyzed at each time point. Error bars represent standard error. \*, indicates a significant difference ( $P < 0.05$ ) relative to wild type according to the unpaired t-test.

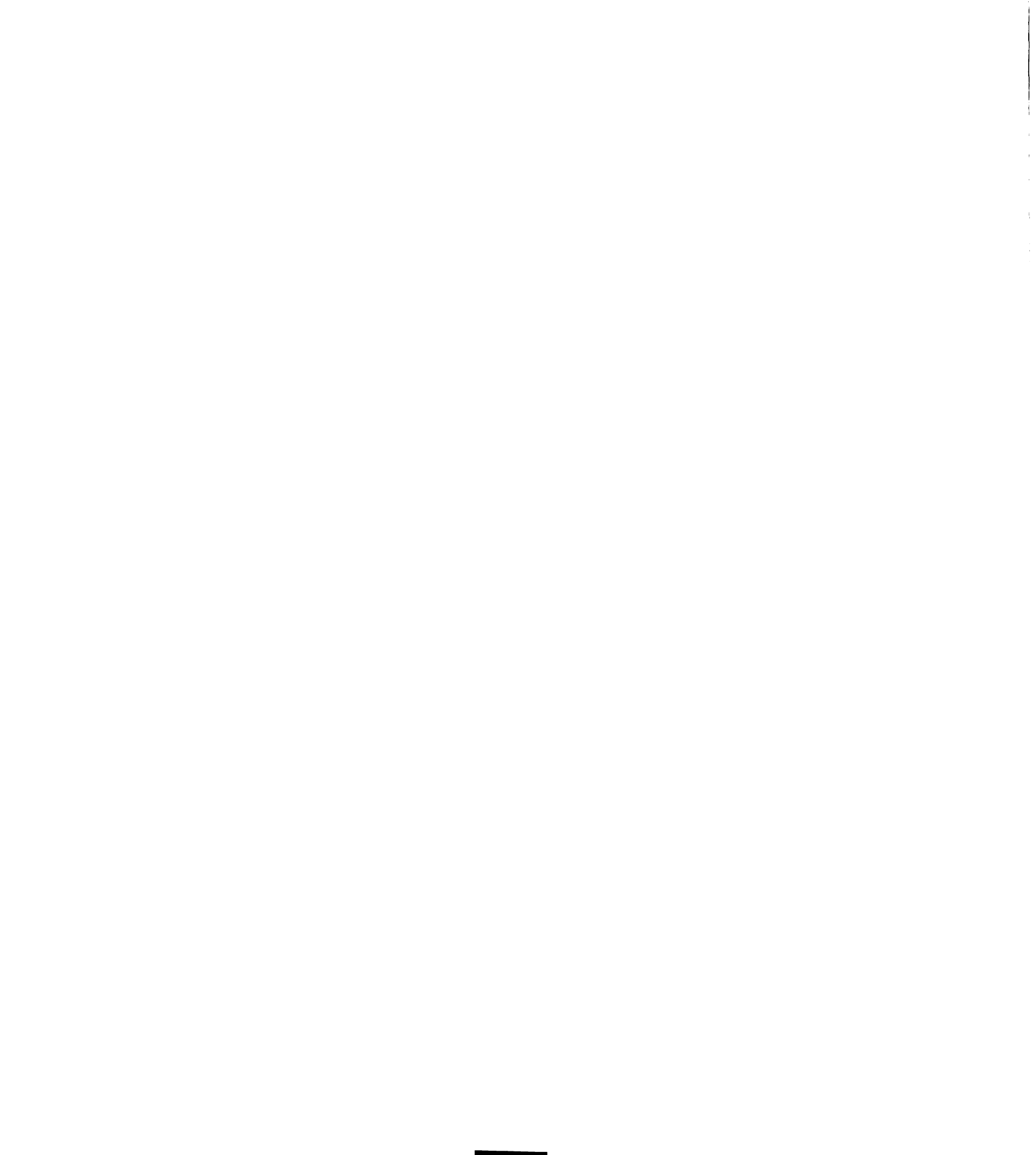
on chloroplast membranes (Adhikari et al., 2009). These ideas cannot be tested with the previously available *gun4* mutants because these mutants contain either null alleles or severe loss-of-function alleles that accumulate barely detectable levels of GUN4 protein. These mutants exhibit severe and pleiotropic phenotypes that are characterized by both severe chlorophyll deficiencies or albinism and abnormal photosynthetic membranes (Vinti et al., 2000; Mochizuki et al., 2001; Larkin et al., 2003; Wilde et al., 2004; Sobotka et al., 2008). Therefore, the analysis of the first set of *gun4* alleles in *Arabidopsis* and *Synechocystis* did not indicate whether the loss of the porphyrin-binding activity or the loss of some other function of GUN4 might be responsible for these extreme phenotypes. Additionally, data collected from a heterologous pea system and reported by Adhikari et al. (2009) did not clearly indicate whether amino acid substitutions that disrupt the porphyrin-binding activity of GUN4 in vitro also disrupt the porphyrin-binding activity of GUN4 in vivo. In this report, we tested whether the porphyrin-binding activity that was previously determined to be important for GUN4 activity in vitro (Adhikari et al., 2009) contributes to the porphyrin-binding activity of GUN4 in vivo and whether this activity is significant in vivo. We expressed *gun4* alleles encoding versions of GUN4 that contain single amino acid substitutions that were previously shown to significantly inhibit the porphyrin-binding activity of GUN4 in vitro (Adhikari et al., 2009) and expressed these porphyrin-binding-deficient versions of GUN4 in stably transformed *gun4* knockout mutant *gun4-2*. We found that not only do these amino acid substitutions inhibit the porphyrin binding activity of GUN4 in vivo, but that transgenic plants expressing only the porphyrin-binding-deficient versions of GUN4 contain lower levels of chlorophyll than wild type, lower levels of GUN4

associated with chloroplast membranes than wild type, and elevated levels of ROS relative to wild type.

**GUN4 helps channel porphyrins into chlorophyll biosynthesis by binding ChlH/GUN5 on chloroplast membranes**

When purified chloroplasts were lysed and fractionated, we observed that F191A and R211A—the porphyrin-binding-deficient versions of GUN4—accumulated to higher levels in soluble fractions and lower levels in membrane-containing pellet fractions than wild-type GUN4. Additionally, we observed that wild-type GUN4 accumulated to elevated levels in soluble fractions and lower levels in membrane-containing pellet fractions derived from chloroplasts that were purified from strong loss-of-function *chlH/gun5* mutants. Based on these data, we conclude that ChlH/GUN5 activity and the porphyrin-binding activity of GUN4 promote interactions between GUN4 and chloroplast membranes. The most parsimonious interpretation of these data is that a significant fraction of GUN4-porphyrin complexes is tethered to chloroplast membranes by binding active ChlH/GUN5.

To test whether the loss of the porphyrin-binding activity or the loss of some other function of F191A and R211A impairs interactions between GUN4 and both ChlH/GUN5 and chloroplast membranes, we fed PPIX to purified chloroplasts. The result was that F191A, R211A, and wild-type GUN4 in the *gun5* and *gun5-101* backgrounds accumulated in the membrane-containing pellet fractions of these chloroplasts. Based on these findings, we conclude that GUN4-porphyrin complexes



bind ChlH/GUN5 and have a higher affinity for ChlH/GUN5 on chloroplast membranes than does free GUN4. This effect of PPIX feeding on the affinity of GUN4 for chloroplast membranes does not occur in *cch*. The P642L substitution encoded by the *cch* allele may cause pleiotropic dysfunction in ChlH/GUN5 that includes an inability to distinguish between free and porphyrin-bound GUN4. Alternatively, *cch* contains significantly less active ChlH/GUN5 than wild type that may already be saturated with GUN4-porphyrin complexes prior to PPIX feeding. Another possible interpretation is that indirect effects that attenuate the activities of GUN4 and ChlH/GUN5 and are promoted by chlorophyll deficiencies may be more robust in *cch* relative to both *gun5* and *gun5-101* because *cch* is more severely chlorophyll deficient than both *gun5* and *gun5-101*.

Porphyrins were previously reported to promote the association of in vitro translated and imported GUN4, pea GUN4, and pea ChlH/GUN5 with pea chloroplast membranes. However, this effect was more robust with in vitro translated GUN4 and pea GUN4 than with pea ChlH/GUN5. One possible interpretation of these data is that ChlH/GUN5 associates with chloroplast membranes by a mechanism that does not entirely depend on GUN4, and that GUN4-porphyrin complexes can nonetheless promote interactions between ChlH/GUN5 and chloroplast membranes (Adhikari et al., 2009). Here, we tested this idea using Arabidopsis mutants and transgenic plants. We expect that the interactions between chloroplast membranes and ChlH/GUN5 are conserved between Arabidopsis and pea. We found that ca. 70% of ChlH/GUN5 was in the membrane-containing pellet fraction when chloroplasts purified from wild-type

Arabidopsis chloroplasts were fractionated. In contrast, pea ChlH/GUN5 was only ca. 50% associated with the membrane-containing pellet fraction when pea chloroplasts were fractionated; a rise in porphyrin levels caused ca. 70% of pea ChlH/GUN5 to associate with the membrane-containing pellet fraction (Adhikari et al., 2009). Thus, we expect that ChlH/GUN5 already maximally associates with chloroplast membranes in the wild-type Arabidopsis system used here, thereby preventing PPIX feeding from further promoting interactions between chloroplast membranes and ChlH/GUN5 in wild type. We found 40 to 50% of ChlH/GUN5 in supernatant fractions and 50 to 60% in the membrane-containing pellet fractions when chloroplasts purified from the transgenic lines, *gun4-1*, and all *chlH/gun5* mutants tested were fractionated. This reduction in the membrane association of ChlH/GUN5 was somewhat muted compared to GUN4. Also, in contrast to GUN4, PPIX feeding had no effect on the interactions between ChlH/GUN5 and chloroplast membranes. These findings indicate that although GUN4 can promote interactions between ChlH/GUN5 and chloroplast membranes, ChlH/GUN5 likely associates with chloroplast membranes using a mechanism that depends relatively less on GUN4 than the mechanism used by GUN4 to associate with chloroplast membranes, which depends relatively more on ChlH/GUN5. Nonetheless, GUN4 can promote interactions between ChlH/GUN5 and chloroplast membranes. The inability of PPIX feeding to promote interactions between ChlH/GUN5 and chloroplast membranes in any of the transgenic lines, *gun4-1*, *gun5*, *cch*, and *gun5-101* provides evidence that porphyrin binding is less important for promoting interactions between chloroplast membranes and ChlH/GUN5 than for promoting interactions between chloroplast membranes and GUN4. Even so, the previous work of Adhikari et al. (2009)

indicates that porphyrins can promote interactions between ChlH/GUN5 and chloroplast membranes, albeit significantly less than for GUN4, consistent with the work reported here.

### **A complex mechanism likely explains the light sensitivities of chlorophyll-deficient mutants**

Similar to other mutants with defects in chlorophyll biosynthesis (Falbel et al., 1996), the transgenic lines expressing F191A and R211A, *gun4-1*, and all of the *chlH/gun5* mutants used in this study exhibited significant chlorophyll deficiencies relative to wild type when they were transferred from 100 to 850  $\mu\text{mol m}^{-2} \text{s}^{-1}$  white light. GUN4 protein levels decreased to very low or undetectable levels in *gun4-1*, F191A, R211A, *gun5-101*, and *cch* but not in *gun5* and *cs* mutants following these fluence rate shifts. These lower levels of GUN4 protein could be caused by an enhanced turnover of GUN4 protein and/or reduced expression of the *GUN4* gene. This striking reduction of GUN4 protein levels was specific to GUN4; similar reductions were not observed for the ChlH/GUN5, ChlI, or ChlD subunits of Mg-chelatase. Consistent with these findings, Peter and Grimm (2009) did not observe a striking reduction in Mg-chelatase subunit levels in *gun4* mutants. Based on previous kinetic analysis of SynGUN4 and *Synechocystis* Mg-chelatase (Larkin et al., 2003; Davison et al., 2005; Verdecia et al., 2005), we expect that this reduction in GUN4 protein levels will significantly attenuate Mg-chelatase activity. It will be interesting to test whether this reduction in GUN4 protein levels is a rapid response that contributes significantly to the down-regulation of chlorophyll biosynthesis when tetrapyrrole metabolism is misregulated.

We also monitored the expression levels of *ZAT10* and *WRKY40*, two ROS-inducible genes, and found evidence that F191A, R211A, and wild type accumulate similar levels of ROS following a fluence rate shift. We found that ROS production increases when wild type and all the mutants tested were transferred from 10 to 850  $\mu\text{mol m}^{-2} \text{s}^{-1}$  white light. Our findings, however, do not support a model in which the enhanced chlorophyll-deficient phenotypes of the F191A- and R211A-expressing lines in bright light are explained by more ROS accumulating in these transgenic lines relative to wild type following fluence-rate shifts from dim to bright light. On the contrary, although we found that the F191A- and R211A-expressing lines, *cch*, and *cs* mutants accumulate more ROS than wild type in 2 to 10  $\mu\text{mol m}^{-2} \text{s}^{-1}$  continuous white light and in 2  $\mu\text{mol m}^{-2} \text{s}^{-1}$  diurnal-dim light, our data indicate that these F191A- and R211A-expressing lines and wild type accumulate similar levels of ROS after a fluence-rate shift from 10  $\mu\text{mol m}^{-2} \text{s}^{-1}$  to 850  $\mu\text{mol m}^{-2} \text{s}^{-1}$ . Therefore, we propose that the enhanced chlorophyll deficiencies of mutants with these defects in chlorophyll biosynthesis may result from a complex mechanism that depends not only on light-induced production of ROS but also other light-regulated processes. (1) Following a fluence-rate shift, the lower rates of chlorophyll biosynthesis that occur in these chlorophyll biosynthesis mutants relative to wild type may be insufficient to compensate for the chlorophyll *a* that is turned over; the rate of chlorophyll *a* turnover can increase in high-intensity light (Beisel et al., 2010). The striking reductions in the levels of GUN4 protein observed in *gun4-1*, F191A, R211A, *gun5-101*, and *cch* reported here is expected to further attenuate rates of chlorophyll biosynthesis, thereby further promoting chlorophyll deficiencies. (2) If

some effect besides lower rates of chlorophyll biosynthesis is responsible for the light sensitivities of these mutants, this effect would not appear to be elevated ROS because *WRKY40* and *ZAT10* expression is not elevated in R211A and F191A following a fluence-rate shift. The data reported here are consistent with these Mg-chelatase-deficient mutants exhibiting an uncoupling of ROS production and some other light-intensity-dependent process such as photoreceptor-based light signaling. The light sensitivities of these chlorophyll-deficient mutants may be explained by effects on photoreceptor-based light signaling if the elevated ROS observed in 2 and 10  $\mu\text{mol m}^{-2} \text{s}^{-1}$  white light reprograms light signaling to promote chlorophyll deficiencies when the mutants are transferred to 850  $\mu\text{mol m}^{-2} \text{s}^{-1}$  light. Consistent with this interpretation, elevated chloroplastic ROS that is derived from the over-accumulation of chlorophyll precursors induces albinism by a mechanism that depends on the blue-light receptor cryptochrome 1 (Danon et al., 2006). Also, plastid dysfunction triggered by inhibitors of chloroplast biogenesis have been reported to convert cryptochrome 1 and other photoreceptors from positive to negative regulators of photosynthesis-related genes (Ruckle et al., 2007). These effects of plastid dysfunction on light signaling were proposed to protect chloroplasts from stress and dysfunction by helping to balance processes that promote and processes that attenuate photooxidative stress within the chloroplast (Ruckle et al., 2007; Larkin and Ruckle, 2008) or in extreme cases promote cell death (Danon et al., 2006; Kim et al., 2008).

The findings that GUN4-porphyrin complexes predominantly associate with ChlH/GUN5 on chloroplast membranes in vivo and that transgenic *Arabidopsis* plants

that express only porphyrin-binding-deficient versions of GUN4 exhibit elevated ROS-inducible gene expression have two major implications. First, these findings support a role for the porphyrin-binding activity of GUN4 in the channeling of PPIX into chlorophyll biosynthesis. Based on previous kinetic analysis of SynGUN4 and *Synechocystis* Mg-chelatase, GUN4-PPIX-ChlH/GUN5 complexes that accumulate on chloroplast membranes are expected to be converted to GUN4-ChlH/GUN5-Mg-PPIX complexes after interacting with the ChlI and ChlD subunits of Mg-chelatase (Larkin et al., 2003; Davison et al., 2005; Verdecia et al., 2005). Second, these findings provide insight into the mechanism by which plants protect themselves from the photooxidative stress derived from the PPIX and Mg-PPIX that accumulate to readily detectable levels during the light-phase of diurnal cycles (Pöpperl et al., 1998; Papenbrock et al., 1999; Mochizuki et al., 2008; Moulin et al., 2008). We tested whether GUN4 or a GUN4-ChlH/GUN5 complex might perform distinct roles (1) in binding pools of PPIX and Mg-PPIX associated with chlorophyll biosynthesis and (2) in binding separate pools of diurnally accumulating PPIX and Mg-PPIX with the purpose of protecting plants from ROS by shielding these porphyrins from collisions with O<sub>2</sub>. The only source of porphyrin-derived ROS in the *cs* mutant is from porphyrins immediately associated with chlorophyll biosynthesis and not from a separate pool of porphyrins that is not associated with the chlorophyll biosynthetic pathway because *cs* mutants have defects in ChlI, which does not bind porphyrins. In contrast, in R211A and *cch*, porphyrin-derived ROS could be derived from either the PPIX and Mg-PPIX associated with the chlorophyll biosynthetic pathway or a separate pool of diurnally accumulating PPIX and Mg-PPIX, because R211A and *cch* have defects in GUN4 and ChlH/GUN5—two

PPIX- and Mg-PPIX-binding proteins. Therefore, if a significant fraction of the diurnally accumulating PPIX and Mg-PPIX forms a pool that is distinct from the PPIX and Mg-PPIX that associates with the chlorophyll biosynthetic pathway, R211A or both R211A and *cch* would accumulate higher levels of ROS than *cs*, and higher levels of mRNAs from *WRKY40* and *ZAT10* than *cs*. Further, R211A would accumulate higher levels of mRNAs transcribed from *WRKY40* and *ZAT10* than *cch* if GUN4 contributed to photooxidative stress tolerance independently of ChlH. The finding that R221A, *cch*, and *cs* express similar amounts of mRNA from *WRKY40* and *ZAT10* is most consistent with the model in which the PPIX and Mg-PPIX that accumulates during the diurnal cycle does not associate with GUN4 or a ChlH/GUN5-GUN4 complex in pools that are distinct from the pools of PPIX and Mg-PPIX that are associated with the chlorophyll biosynthetic pathway. Rather, our findings are most consistent with a model in which the PPIX and Mg-PPIX that builds up during the day associate with the GUN4 and ChlH/GUN5 associated with the chlorophyll biosynthetic pathway. In this model, the PPIX and Mg-PPIX that accumulates to readily detectable levels during the day remains bound to the substrate and product binding sites of chlorophyll biosynthetic enzymes; this association with enzymes of the chlorophyll biosynthetic pathway shields these chlorophyll precursors from collisions with O<sub>2</sub>, thereby protecting plants from the production of ROS that can cause photooxidative damage. We propose that some event such as the accumulation of pigment-binding apoproteins somehow triggers (1) the conversion of these chlorophyll precursors into chlorophyll and (2) the rapid sequestration of chlorophyll into pigment-protein complexes.

## CHAPTER 4

### CONCLUSIONS AND FUTURE PERSPECTIVES

In this thesis, I tested several hypotheses and report several conceptual advances for GUN4. First, I report on a technical advance to porphyrin-binding assays that led to the first demonstration that GUN4 can bind PPIX and Mg-PPIX. Previous quantitative analysis of porphyrin binding utilized cyanobacterial relatives of GUN4 (Larkin et al., 2003; Davison et al., 2005; Verdecia et al., 2005); GUN4 was previously only shown to bind porphyrins in qualitative assays (Larkin et al., 2003). Also, previous quantitative binding assays utilized the unnatural ligands deuteroporphyrin IX (DPIX) and Mg-deuteroporphyrin IX (Mg-DPIX). DPIX and Mg-DPIX lack two vinyl groups found in PPIX and Mg-PPIX and are therefore more water soluble than PPIX and Mg-PPIX. Thus, no data was previously published showing that GUN4 or any GUN4 relative can actually bind PPIX and Mg-PPIX. I modified the previously used porphyrin-binding assay (Karger et al., 2001; Larkin et al., 2003; Davison et al., 2005; Verdecia et al., 2005) by adding 1% dimethyl sulfoxide (DMSO). When 1% DMSO was added to these binding assays, the solubilities of PPIX and Mg-PPIX are increased enough to quantify their binding to GUN4. Additionally, based on results from binding assays that utilized DPIX and Mg-DPIX  $\pm$  1% DMSO, we concluded that 1% DMSO may not affect the affinity of GUN4 for its natural porphyrin ligands. Using this new porphyrin binding assay, the binding constants of GUN4 for protoporphyrin IX, Mg-protoporphyrin IX and a variety of other natural porphyrins were reported for the first time. GUN4 was found to bind Mg-PPIX with a 2-9 fold higher affinity than other natural porphyrins. These findings are consistent with previous findings showing that cyanobacterial

relatives of GUN4 bind Mg-DPIX with higher affinities than other porphyrins. This technical advance may be useful for quantifying the porphyrin binding activity of other proteins or quantifying the binding activity of proteins to other hydrophobic molecules besides porphyrins.

Second, I provide evidence that GUN4 regulates chlorophyll biosynthesis by a novel regulatory mechanism. Previously, cyanobacterial relatives of GUN4 were shown to stimulate Mg-chelatase activity *in vitro*. Based on sequence similarity, the copurification of ChlH with GUN4, and the chlorophyll-deficient phenotype of *gun4* mutants, GUN4 was also proposed to stimulate Mg-chelatase activity in plants. In this thesis, I tested whether porphyrin binding might promote interactions between GUN4 and Mg-chelatase subunits with chloroplast membranes. The first set of experiments followed subchloroplastic distribution of *in vitro* translated and imported GUN4, pea GUN4, and pea Mg-chelatase subunits after inducing a rise in porphyrin levels in purified pea chloroplasts—the site of chlorophyll biosynthesis. I show that porphyrin binding promotes the association of *in vitro* translated and imported GUN4, pea GUN4, pea ChlH with pea chloroplast membranes. These findings are consistent with GUN4 promoting chlorophyll biosynthesis not only by stimulating Mg-chelatase activity but also by channeling porphyrins into chlorophyll biosynthesis. These findings are also consistent with GUN4 stimulating chlorophyll biosynthesis not only by activating Mg-chelatase but also by promoting interactions between ChlH and chloroplast membranes.

Third, I developed a genetic approach to test whether the porphyrin-dependent binding of GUN4 depends on ChlH and vice versa. This genetic approach was also useful for testing whether the porphyrin- and chloroplast-membrane-binding activity of GUN4 helps protect plants from photooxidative stress. Additionally, this genetic approach was useful for resolving an issue from my work with pea chloroplasts. Based on the work with pea, we could not conclude whether residues in GUN4 that were shown to be important for porphyrin-binding activity measured in vitro were also important for porphyrin binding in vivo or whether my inability to demonstrate that these residues are important for binding porphyrins in pea chloroplasts is due to a technical barrier of this system (Chapter 2). I developed transgenic Arabidopsis lines that stably express *gun4* alleles encoding single amino acid substitutions that lower the affinity of GUN4 for porphyrins. I used these lines to show that residues in GUN4 that contribute to porphyrin binding in vitro also contribute to porphyrin binding in vivo. Further I used *chlH/gun5* mutants to show that the interactions between GUN4 and chloroplast membranes depend on ChlH and that these interactions are strengthened by the porphyrin binding activity of GUN4. Also, I found that interactions between ChlH and chloroplast membranes either do not depend on GUN4 or do not depend on GUN4 to the same degree as interactions between GUN4 and chloroplast membranes depend on ChlH. Based on the data reported in Chapter 3, I further conclude that the residues that are important for porphyrin binding in vitro do not appear important for porphyrin binding in the heterologous pea system because of technical limitations of this system. Using the homologous Arabidopsis system, I showed residues that contribute to porphyrin binding in vitro also contribute to porphyrin binding in vivo. Further, based

on the chlorophyll-deficient phenotypes of these transgenic lines, I conclude that the porphyrin-binding activity of GUN4 that was quantified in vitro contributes to its activity in vivo.

Thus, one major conclusion from the work presented in chapters 2 and 3 is that porphyrin binding promotes interactions between GUN4 and ChlH on chloroplast membranes. In chapter 2, I report that increases in these complexes on chloroplast membranes are correlated with increases in Mg-chelatase activity on chloroplast membranes. Therefore, these data strongly support a role for GUN4 in channeling porphyrins into chlorophyll biosynthesis by forming GUN4-PPIX-ChlH complexes on chloroplast membranes.

I used this genetic approach to test whether the porphyrin-binding activity of GUN4 might help protect plants against photooxidative stress as was previously proposed (Larkin et al., 2003; Verdecia et al., 2005). Chloroplastic photooxidative stress can cause necrosis and apoptosis (Kim et al., 2008) and inactivation of ChlH (Willows et al., 2003). Indeed, we found that residues of GUN4 that are important for porphyrin binding are also important for photooxidative stress tolerance in Arabidopsis. For these experiments I used the same transgenic Arabidopsis lines that stably express *gun4* alleles encoding single amino acid substitutions that lower the affinity of GUN4 for porphyrins that I used in my subchloroplastic distribution experiments. I found that these lines and Mg-chelatase subunit gene mutants exhibit enhanced chlorophyll deficiencies when they are transferred to high-intensity light. I also found that these

transgenic lines and mutants exhibit elevated levels of ROS-inducible genes relative to wild type in dim light but not in high intensity light. Based on these data, I conclude that these transgenic lines and mutants contain elevated levels of ROS relative to wild type. After absorbing light, particular electronically excited states of porphyrins can transfer energy to O<sub>2</sub> yielding singlet oxygen that subsequently yields other ROS. Yields of porphyrin-derived ROS increase as fluence rates increase. Therefore, one surprising result was that according to our ROS-inducible gene expression assay, these transgenic lines and mutants exhibit elevated levels of ROS relative to wild type in dim white light (e.g., 2 to 10 μmol m<sup>-2</sup> s<sup>-1</sup> white light) but similar levels of ROS relative to wild type after plants are transferred to high intensity light (e.g., 850 μmol m<sup>-2</sup> s<sup>-1</sup> white light).

Mutants with defects in chlorophyll biosynthesis have long been known to be sensitive to bright light. This light sensitivity has long been proposed to result from (1) enhanced chlorophyll turnover and inefficient chlorophyll biosynthesis in bright light and (2) ROS derived from free porphyrins in bright light. Based on the findings reported here, we conclude that elevated levels of ROS in bright light do not fully explain the light sensitivities of these chlorophyll-deficient mutants because ROS-inducible genes are not elevated in these chlorophyll biosynthesis-deficient transgenic lines and mutants when plants are shifted into intense light. An alternative explanation is that a light signaling that controls chloroplast function is reprogrammed by chloroplastic in dim light and this light signaling network promotes chlorophyll deficiencies when the transgenic lines and mutants are shifted into bright light. Consistent with this proposal,

elevated chloroplastic ROS triggered by misregulated chlorophyll metabolism induces albinism by a mechanism that depends on the blue-light receptor cryptochrome 1 (Danon et al., 2006). Also, plastid dysfunction triggered by inhibitors of chloroplast biogenesis have been reported to convert cryptochrome 1 and phytochrome B from positive to negative regulators of photosynthesis-related genes (Ruckle et al., 2007). These effects of plastid dysfunction on light signaling were proposed to protect chloroplasts from stress and dysfunction by balancing processes that promote and attenuate photooxidative stress within the chloroplast (Larkin and Ruckle, 2008).

The approach that I developed for expressing engineered *gun4* alleles in *gun4-2 sgs3* double mutants resolves a previous major technical barrier; GUN4 expressing transgenes exhibit robust cosuppression (Larkin et al., 2003). This technical advance that will allow researchers to test other hypotheses related to the function of GUN4 in vivo in the future. For example, using this approach, researchers could test whether the recently reported phosphorylation of GUN4 is significant in vivo (Reiland et al., 2009), whether the unusual histidine-rich transit peptide affects GUN4 function in vivo (Larkin et al., 2003), or whether GUN4 might contribute to the negative feedback regulation of chlorophyll biosynthesis as a previously suggested (Peter and Grimm, 2009).

## REFERENCES

- Adhikari N, Orlor R, Chory J, Froehlich J, Larkin R** (2009) Porphyrins Promote the Association of GENOMES UNCOUPLED 4 and a Mg-chelatase Subunit with Chloroplast Membranes. *Journal of Biological Chemistry*: 24783-24796
- Allen KD, Duysen ME, Staehelin LA** (1988) Biogenesis of thylakoid membranes is controlled by light intensity in the conditional chlorophyll b-deficient CD3 mutant of wheat. *Journal of Cell Biology* **107**: 907-919
- Ankele E, Kindgren P, Pesquet E, Strand A** (2007) In vivo visualization of Mg-ProtoporphyrinIX, a coordinator of photosynthetic gene expression in the nucleus and the chloroplast. *In Plant Cell*, pp 1964-1979
- Armstrong G, Runge S, Frick G, Sperling U, Apel K** (1995) Identification of NADPH:protochlorophyllide oxidoreductases A and B: a branched pathway for light-dependent chlorophyll biosynthesis in *Arabidopsis thaliana*. *Plant Physiology* **108**: 1505-1517
- Balmer Y, Koller A, del Val G, Manieri W, Schurmann P, Buchanan BB** (2003) Proteomics gives insight into the regulatory function of chloroplast thioredoxins. *In Proceedings of the National Academy of Sciences of the United States of America*, pp 370-375
- Barthelemy X, Bouvier G, Radunz A, Docquier S, Schmid GH, Franck F** (2000) Localization of NADPH-protochlorophyllide reductase in plastids of barley at different greening stages. *In Photosynthesis Research*, Vol 64, pp 63-76
- Battersby AR, Fookes CJR, Gustafson-Potter KE, Matcham GWJ, McDonald E** (1979) Proof by synthesis that un-rearranged hydroxymethylbilane is the product from deaminase and the substrate for cosynthetase in the biosynthesis of urogen-III. *In Journal of the Chemical Society - Chemical Communications*, pp 1155-1158
- Beale SI** (1999) Enzymes of chlorophyll biosynthesis. *In Photosynthesis Research*, Vol 60, pp 43-73
- Beale SI, Castelfranco PA** (1974) The Biosynthesis of delta-Aminolevulinic Acid in Higher Plants: II. Formation of C-delta-Aminolevulinic Acid from Labeled Precursors in Greening Plant Tissues. *In Plant Physiology*, Vol 53, pp 297-303

- Beale SI, Gough SP, Granick S** (1975) Biosynthesis of delta-aminolevulinic-acid from intact carbon skeleton of glutamic-acid in greening barley. *In* Proceedings of the National Academy of Sciences of the United States of America, pp 2719-2723
- Beator J, Kloppstech K** (1993) The circadian oscillator coordinates the synthesis of apoproteins and their pigments during chloroplast development. *In* Plant Physiology, pp 191-196
- Beisel K, Jahnke S, Hofmann D, Köppchen S, Schurr U, Matsubara S** (2010) Continuous turnover of carotenes and chlorophyll a in mature leaves of Arabidopsis revealed by <sup>14</sup>CO<sub>2</sub> pulse-chase labeling. *Plant Physiology* **152**: 2188-2199
- Bell CJ, Ecker JR** (1994) Assignment of 30 microsatellite loci to the linkage map of Arabidopsis. *Genomics* **19**: 137-144
- Block MA, Tewari AK, Albrieux C, Marechal E, Joyard J** (2002) The plant S-adenosyl-L-methionine : Mg-protoporphyrin IX methyltransferase is located in both envelope and thylakoid chloroplast membranes. *In* European Journal of Biochemistry, Vol 269, pp 240-248
- Bollivar DW** (2006) Recent advances in chlorophyll biosynthesis. *In* Photosynthesis Research, Vol 90, pp 173-194
- Bollivar DW, Beale SI** (1996) The chlorophyll biosynthetic enzyme Mg-protoporphyrin IX monomethyl ester (oxidative) cyclase - Characterization and partial purification from Chlamydomonas reinhardtii and Synechocystis sp PCC 6803. *In* Plant Physiology, Vol 112, pp 105-114
- Bougri O, Grimm B** (1996) Members of a low-copy number gene family encoding glutamyl-tRNA reductase are differentially expressed in barley. *In* Plant Journal, pp 867-878
- Brandis A, Vainstein A, Goldschmidt EE** (1996) Distribution of chlorophyllase among components of chloroplast membranes in Citrus sinensis organs. *In* Plant Physiology and Biochemistry, pp 49-54
- Brown SB, Lantzke IR** (1969) Solution structures of ferrihaem in some dipolar aprotic solvents and their binary aqueous mixtures. *Biochemical Journal* **115**: 279-285

- Bruce BD, Perry S, Froehlich J, Keegstra K** (1994) In vitro import of protein into chloroplasts. *In* SB Gelvin, RB Schilperoort, eds, Plant Molecular Biology Manual, Vol J1. Kluwer Academic Publishers, Boston
- Buchanan BB, Balmer Y** (2005) Redox regulation: A broadening horizon. *In* Annual Review of Plant Biology, pp 187-220
- Butaye KM, Goderis IJ, Wouters PF, Pues JM, Delaure SL, Broekaert WF, Depicker A, Cammue BP, De Bolle MF** (2004) Stable high-level transgene expression in *Arabidopsis thaliana* using gene silencing mutants and matrix attachment regions. *Plant Journal* **39**: 440-449
- Cavaleiro JA, Kenner GW, Smith KM** (1974) Pyrroles and related compounds. XXXII. Biosynthesis of protoporphyrin-IX from coproporphyrinogen-III. *In* Journal of the Chemical Society - Perkin Transactions 1, pp 1188-1194
- Che FS, Watanabe N, Iwano M, Inokuchi H, Takayama S, Yoshida S, Isogai A** (2000) Molecular characterization and subcellular localization of protoporphyrinogen oxidase in spinach chloroplasts. *Plant Physiology* **124**: 59-70
- Cornah JE, Roper JM, Pal Singh D, Smith AG** (2002) Measurement of ferrochelatase activity using a novel assay suggests that plastids are the major site of haem biosynthesis in both photosynthetic and non-photosynthetic cells of pea (*Pisum sativum* L.). *In* Biochemical Journal, Vol 362, pp 423-432
- Cornah JE, Terry MJ, Smith AG** (2003) Green or red: what stops the traffic in the tetrapyrrole pathway? *Trends in Plant Science* **8**: 224-230
- Czechowski T, Stitt M, Altmann T, Udvardi MK, Scheible WR** (2005) Genome-wide identification and testing of superior reference genes for transcript normalization in *Arabidopsis*. *Plant Physiology* **139**: 5-17
- Danon A, Coll NS, Apel K** (2006) Cryptochrome-1-dependent execution of programmed cell death induced by singlet oxygen in *Arabidopsis thaliana*. *Proceedings of the National Academy of Sciences of the United States of America* **103**: 17036-17041

- Davison PA, Schubert HL, Reid JD, Iorg CD, Heroux A, Hill CP, Hunter CN** (2005) Structural and biochemical characterization of Gun4 suggests a mechanism for its role in chlorophyll biosynthesis. *Biochemistry* **44**: 7603-7612
- Eckhardt U, Grimm B, Hortensteiner S** (2004) Recent advances in chlorophyll biosynthesis and breakdown in higher plants. *In Plant Molecular Biology*, Vol 56, pp 1-14
- Eggink LL, LoBrutto R, Brune DC, Brusslan J, Yamasato A, Tanaka A, Hooper JK** (2004) Synthesis of chlorophyll b: localization of chlorophyllide a oxygenase and discovery of a stable radical in the catalytic subunit. *In BMC Plant Biology*, Vol 4, p 5
- Eichwurzel I, Stiel H, Röder B** (2000) Photophysical studies of the pheophorbide a dimer. *Journal of Photochemistry and Photobiology B* **54**: 194-200
- Elmlund H, Lundqvist J, Al-Karadaghi S, Hansson M, Hebert H, Lindahl M** (2008) A new cryo-EM single-particle *ab initio* reconstruction method visualizes secondary structure elements in an ATP-fueled AAA+ motor. *Journal of Molecular Biology* **375**: 934-947
- Espineda CE, Linford AS, Devine D, Brusslan JA** (1999) The AtCAO gene, encoding chlorophyll a oxygenase, is required for chlorophyll b synthesis in *Arabidopsis thaliana*. *Proceedings of the National Academy of Sciences of the United States of America* **96**: 10507-10511
- Falbel TG, Meehl JB, Staehelin LA** (1996) Severity of mutant phenotype in a series of chlorophyll-deficient wheat mutants depends on light intensity and the severity of the block in chlorophyll synthesis. *Plant Physiology* **112**: 821-832
- Falbel TG, Staehelin LA** (1994) Characterization of a family of chlorophyll-deficient wheat (*Triticum*) and barley (*Hordeum vulgare*) mutants with defects in the magnesium-insertion step of chlorophyll biosynthesis. *Plant Physiology* **104**: 639-648
- Fitter DW, Martin DJ, Copley MJ, Scotland RW, Langdale JA** (2002) GLK gene pairs regulate chloroplast development in diverse plant species. *In Plant Journal*, pp 713-727

- Fleischer EB, Stone A, Choi EI, Hambright P** (1964) Porphyrin studies - Kinetics of metalloporphyrin formation. *In Inorganic Chemistry*, pp 1284-&
- Flors C, Fryer MJ, Waring J, Reeder B, Bechtold U, Mullineaux PM, Nonell S, Wilson MT, Baker NR** (2006) Imaging the production of singlet oxygen in vivo using a new fluorescent sensor, Singlet Oxygen Sensor Green. *In Journal of Experimental Botany*, Vol 57, pp 1725-1734
- Fodje MN, Hansson A, Hansson M, Olsen JG, Gough S, Willows RD, Al-Karadaghi S** (2001) Interplay between an AAA module and an integrin I domain may regulate the function of magnesium chelatase. *In Journal of Molecular Biology*, pp 111-122
- Fuesler TP, Wong YS, Castelfranco PA** (1984) Localization of Mg-chelatase and Mg-protoporphyrin-IX monomethyl ester (oxidative) cyclase activities within isolated, developing cucumber chloroplasts. *In Plant Physiology*, Vol 75, pp 662-664
- Fuesler TP, Wright LA, Castelfranco PA** (1981) Properties of Magnesium Chelatase in Greening Etioplasts: Metal ion specificity and effect of substrate concentrations. *Plant Physiology*. **67**: 246-249
- Fufsler TP, Castelfranco PA, Wong YS** (1984) Formation of Mg-Containing Chlorophyll Precursors from Protoporphyrin IX,  $\delta$ -Aminolevulinic Acid, and Glutamate in Isolated, Photosynthetically Competent, Developing Chloroplasts. *Plant Physiology* **74**: 928-933
- Gadjev I, Vanderauwera S, Gechev TS, Laloi C, Minkov IN, Shulaev V, Apel K, Inzé D, Mittler R, Van Breusegem F** (2006) Transcriptomic footprints disclose specificity of reactive oxygen species signaling in Arabidopsis. *Plant Physiology* **141**: 436-445
- Gibson KD, Laver WG, Neuberger A** (1958) Formation of delta-aminolevulinic acid in vitro from succinyl Co-A and glycine. *In Biochemical Journal*, Vol 68, pp P17-P17
- Gibson LC, Marrison JL, Leech RM, Jensen PE, Bassham DC, Gibson M, Hunter CN** (1996) A putative Mg chelatase subunit from *Arabidopsis thaliana* cv C24. Sequence and transcript analysis of the gene, import of the protein into

chloroplasts, and in situ localization of the transcript and protein. *Plant Physiology* **111**: 61-71

**Giraud E, Ho LH, Clifton R, Carroll A, Estavillo G, Tan YF, Howell KA, Ivanova A, Pogson BJ, Millar AH, Whelan J** (2008) The absence of ALTERNATIVE OXIDASE1a in Arabidopsis results in acute sensitivity to combined light and drought stress. *Plant Physiology* **147**: 595-610

**Gomes A, Fernandes E, Lima J** (2005) Fluorescence probes used for detection of reactive oxygen species. *Journal of Biochemical and Biophysical Methods* **65**: 45-80

**Goslings D, Meskauskiene R, Kim C, Lee KP, Nater M, Apel K** (2004) Concurrent interactions of heme and FLU with Glu tRNA reductase (HEMA1), the target of metabolic feedback inhibition of tetrapyrrole biosynthesis, in dark- and light-grown Arabidopsis plants. *In Plant Journal*, Vol 40, pp 957-967

**Gough S** (1972) Defective synthesis of porphyrins in barley plastids caused by mutations in nuclear genes. *Biochimica et Biophysica Acta* **286**: 36-54

**Granick S** (1961) Magnesium protoporphyrin monoester and protoporphyrin monomethyl ester in chlorophyll biosynthesis. *Journal of Biological Chemistry* **236**: 1168-1172

**Guo R, Luo M, Weinstein JD** (1998) Magnesium-chelatase from developing pea leaves. *Plant Physiology* **116**: 605-615

**Halliwell B** (1999) Antioxidant defence mechanisms: from the beginning to the end (of the beginning). *In Free Radical Research*, Vol 31, pp 261-272

**Hambright P** (1975) Dynamic coordination chemistry of metalloporphyrins. In: Smith KM (ed) *Porphyrins and Metalloporphyrins*. Elsevier Scientific Publishing Co., Amsterdam, The Netherlands

**Harlow E, Lane D** (1999) *Using Antibodies: A Laboratory Manual*. Cold Spring Harbor Laboratory Press, Cold Spring Harbor

- Hart GJ, Battersby AR** (1985) Biosynthesis of porphyrins and related macrocycles 26 Purification and properties of uroporphyrinogen-III synthase (co-synthase) from *Euglena gracilis*. *In* *Biochemical Journal*, Vol 232, pp 151-160
- Heazlewood JL, Tonti-Filippini JS, Gout AM, Day DA, Whelan J, Millar AH** (2004) Experimental analysis of the Arabidopsis mitochondrial proteome highlights signaling and regulatory components, provides assessment of targeting prediction programs, and indicates plant-specific mitochondrial proteins. *In* *Plant Cell*, pp 241-256
- Hinchigeri SB, Hundle B, Richards WR** (1997) Demonstration that the BchH protein of *Rhodobacter capsulatus* activates S-adenosyl-L-methionine:magnesium protoporphyrin IX methyltransferase. *FEBS Letters* **407**: 337-342
- Hooper JK, Kahn A, Ash DE, Gough S, Kannangara CG** (1988) Biosynthesis of delta-aminolevulinate in greening barley leaves .9. Structure of the substrate, mode of gabaculine inhibition, and the catalytic mechanism of glutamate 1-semialdehyde aminotransferase. *In* *Carlsberg Research Communications*, Vol 53, pp 11-25
- Horie Y, Ito H, Kusaba M, Tanaka R, Tanaka A** (2009) Participation of Chlorophyll b Reductase in the Initial Step of the Degradation of Light-harvesting Chlorophyll a/b-Protein Complexes in Arabidopsis. *In* *Journal of Biological Chemistry*, pp 17449-17456
- Hortensteiner S** (2006) Chlorophyll degradation during senescence. *In* *Annual Review of Plant Biology*, Vol 57, pp 55-77
- Hortensteiner S, Rodoni S, Schellenberg M, Vicentini F, Nandi OI, Qui YL, Matile P** (2000) Evolution of chlorophyll degradation: The significance of RCC reductase. *In* *Plant Biology*, Vol 2, pp 63-67
- Huang S, Taylor NL, Narsai R, Eubel H, Whelan J, Millar AH** (2009) Experimental Analysis of the Rice Mitochondrial Proteome, Its Biogenesis, and Heterogeneity. *In* *Plant Physiology*, pp 719-734
- Huq E, Al-Sady B, Hudson M, Kim C, Apel K, Quail PH** (2004) Phytochrome-interacting factor 1 is a critical bHLH regulator of chlorophyll biosynthesis. *Science* **305**: 1937-1941

- Ikegami A, Yoshimura N, Motohashi K, Takahashi S, Romano P, Hisabori T, Takamiya K, Masuda T (2007)** The CHL11 subunit of Arabidopsis thaliana magnesium chelatase is a target protein of the chloroplast thioredoxin. *Journal of Biological Chemistry*: 19282-19291
- Ilag LL, Kumar AM, Soll D (1994)** Light regulation of chlorophyll biosynthesis at the level of 5-aminolevulinate formation in Arabidopsis. *In Plant Cell*, pp 265-275
- Ishikawa A, Okamoto H, Iwasaki Y, Asahi T (2001)** A deficiency of coproporphyrinogen III oxidase causes lesion formation in Arabidopsis. *Plant Journal* **27**: 89-99
- Jackson DT, Froehlich JE, Keegstra K (1998)** The hydrophilic domain of Tic110, an inner envelope membrane component of the chloroplastic protein translocation apparatus, faces the stromal compartment. *Journal of Biological Chemistry* **273**: 16583-16588
- Jacob-Wilk D, Holland D, Goldschmidt EE, Riov J, Eyal Y (1999)** Chlorophyll breakdown by chlorophyllase: isolation and functional expression of the Chlase1 gene from ethylene-treated Citrus fruit and its regulation during development. *In Plant Journal*, pp 653-661
- Jacobs JM, Jacobs NJ (1987)** Oxidation of protoporphyrinogen to protoporphyrin, a step in chlorophyll and heme biosynthesis - purification and partial characterization of the enzyme from barley organelles. *In Biochemical Journal*, Vol 244, pp 219-224
- Jander G, Norris SR, Rounsley SD, Bush DF, Levin IM, Last RL (2002)** Arabidopsis map-based cloning in the post-genome era. *Plant Physiology* **129**: 440-450
- Jensen PE, Gibson LC, Shephard F, Smith V, Hunter CN (1999)** Introduction of a new branchpoint in tetrapyrrole biosynthesis in *Escherichia coli* by co-expression of genes encoding the chlorophyll-specific enzymes magnesium chelatase and magnesium protoporphyrin methyltransferase. *FEBS Letters* **455**: 349-354
- Jensen PE, Reid JD, Hunter CN (2000)** Modification of cysteine residues in the ChlI and ChlH subunits of magnesium chelatase results in enzyme inactivation. *In Biochemical Journal*, pp 435-441

- Jez JM, Ferrer JL, Bowman ME, Dixon RA, Noel JP** (2000) Dissection of malonyl-coenzyme A decarboxylation from polyketide formation in the reaction mechanism of a plant polyketide synthase. *Biochemistry* **39**: 890-902
- Johnson ET, Schmidt-Dannert C** (2008) Characterization of three homologs of the large subunit of the magnesium chelatase from *Chlorobaculum tepidum* and interaction with the magnesium protoporphyrin IX methyltransferase. *Journal of Biological Chemistry* **283**: 27776-27784
- Jordan P, Seehra J** (1980) Mechanism of action of 5-aminolevulinic acid dehydratase - stepwise order of addition of the 2 molecules of 5-aminoilevulinic acid in the anzymic-synthesis of porphobilinogen. *Journal of the Chemical Society - Chemical Communications*: 240-242
- Jørgensen K, Rasmussen AV, Morant M, Nielsen AH, Bjarnholt N, Zagrobelny M, Bak S, Møller BL** (2005) Metabolon formation and metabolic channeling in the biosynthesis of plant natural products. *Current Opinion in Plant Biology* **8**: 280-291
- Kannangara CG, Gough SP** (1978) Biosynthesis of delta-aminolevulinate in greening barley leaves - glutamate 1-semialdehyde aminotransferase. *In Carlsberg Research Communications, Vol 43*, pp 185-194
- Kannangara CG, Gough SP, Oliver RP, Rasmussen SK** (1984) Biosynthesis of delta-aminolevulinate in greening barley leaves .6. Activation of glutamate by ligation to RNA. *In Carlsberg Research Communications*, pp 417-437
- Karger GA, Reid JD, Hunter CN** (2001) Characterization of the binding of deuteroporphyrin IX to the magnesium chelatase H subunit and spectroscopic properties of the complex. *Biochemistry* **40**: 9291-9299
- Kauppinen R** (2005) Porphyrins. *In Lancet, Vol 365*, pp 241-252
- Keegstra K, Yousif AE** (1986) Isolation and characterization of chloroplast envelope membranes. *Methods in Enzymology* **118**: 316-325
- Kikuchi G, Kumar A, Talmage P, Shemin D** (1958) Enzymatic synthesis of delta-aminolevulinic acid. *Journal of Biological Chemistry* **233**: 1214-1219



- Kim C, Ham H, Apel K** (2005) Multiplicity of different cell- and organ-specific import routes for the NADPH-protochlorophyllide oxidoreductases A and B in plastids of *Arabidopsis* seedlings. *In* *Plant Journal*, Vol 42, pp 329-340
- Kim CH, Meskauskiene R, Apel K, Laloi C** (2008) No single way to understand singlet oxygen signalling in plants. *In* *EMBO Reports*, pp 435-439
- Kim J, Yi H, Choi G, Shin B, Song P, Choi G** (2003) Functional characterization of phytochrome interacting factor 3 in phytochrome-mediated light signal transduction. *Plant Cell*: 2399-2407
- Klemm DJ, Barton LL** (1987) Purification and properties of protoporphyrinogen oxidase from an anaerobic bacterium, *Desulfovibrio gigas*. *In* *Journal of Bacteriology*, Vol 169, pp 5209-5215
- Kobayashi Y, Kanesaki Y, Tanaka A, Kuroiwa H, Kuroiwa T, Tanaka K** (2009) Tetrapyrrole signal as a cell-cycle coordinator from organelle to nuclear DNA replication in plant cells. *In* *Proceedings of the National Academy of Sciences of the United States of America*, pp 803-807
- Koch M, Breithaupt C, Kiefersauer R, Freigang J, Huber R, Messerschmidt A** (2004) Crystal structure of protoporphyrinogen IX oxidase: a key enzyme in haem and chlorophyll biosynthesis. *EMBO Journal* **23**: 1720-1728
- Kohchi T, Mukougawa K, Frankenberg N, Masuda M, Yokota A, Lagarias JC** (2001) The *Arabidopsis* HY2 gene encodes phytochromobilin synthase, a ferredoxin-dependent biliverdin reductase. *In* *Plant Cell*, Vol 13, pp 425-436
- Koncz C, Mayerhofer R, Koncz-Kalman Z, Nawrath C, Reiss B, Redei GP, Schell J** (1990) Isolation of a gene encoding a novel chloroplast protein by T-DNA tagging in *Arabidopsis thaliana*. *EMBO Journal* **9**: 1337-1346
- Konieczny A, Ausubel FM** (1993) A procedure for mapping *Arabidopsis* mutations using co-dominant ecotype-specific PCR-based markers. *Plant Journal* **4**: 403-410
- Koussevitzky S, Nott A, Mockler TC, Hong F, Sachetto-Martins G, Surpin M, Lim IJ, Mittler R, Chory J** (2007) Signals from chloroplasts converge to regulate nuclear gene expression. *In* *Science*, pp 715-719

- Krautler B** (2008) Chlorophyll breakdown and chlorophyll catabolites in leaves and fruit. *In* Photochemical and Photobiological Sciences, Vol 7, pp 1114-1120
- Krieger-Liszkay A** (2005) Singlet oxygen production in photosynthesis. *In* Journal of Experimental Botany, pp 337-346
- Kruse E, Grimm B, Beator J, Kloppstech K** (1997) Developmental and circadian control of the capacity for delta-aminolevulinic acid synthesis in green barley. *Planta*: 235-241
- Kuzmic P** (1996) Program DYNAFIT for the analysis of enzyme kinetic data: application to HIV proteinase. *Analytical Biochemistry* **237**: 260-273
- Köhler RH, Schwille P, Webb WW, Hanson MR** (2000) Active protein transport through plastid tubules: velocity quantified by fluorescence correlation spectroscopy. *Journal of Cell Science* **113**: 3921-3930
- Larkin RM, Alonso JM, Ecker JR, Chory J** (2003) GUN4, a regulator of chlorophyll synthesis and intracellular signaling. *In* Science, Vol 299, pp 902-906
- Larkin RM, Ruckle ME** (2008) Integration of light and plastid signals. *In* Current Opinion in Plant Biology, pp 593-599
- Lecerof D, Fodje M, Hansson A, Hansson M, Al-Karadaghi S** (2000) Structural and mechanistic basis of porphyrin metallation by ferrochelatase. *In* Journal of Molecular Biology, pp 221-232
- Legnaioli T, Cuevas J, Mas P** (2009) TOC1 functions as a molecular switch connecting the circadian clock with plant responses to drought. *In* EMBO Journal, pp 3745-3757
- Lermontova I, Kruse E, Mock HP, Grimm B** (1997) Cloning and characterization of a plastidal and a mitochondrial isoform of tobacco protoporphyrinogen IX oxidase. *Proceedings of the National Academy of Sciences of the United States of America* **94**: 8895-8900
- Leustek T, Smith M, Murillo M, Singh DP, Smith AG, Woodcock SC, Awan SJ, Warren MJ** (1997) Siroheme biosynthesis in higher plants - Analysis of an S-

adenosyl-L-methionine-dependent uroporphyrinogen III methyltransferase from *Arabidopsis thaliana*. *In Journal of Biological Chemistry*, pp 2744-2752

- Li Z, Wakao S, Fischer BB, Niyogi KK** (2009) Sensing and responding to excess light. *Annual Review of Plant Biology* **60**: 239-260
- Loeb MR** (1995) Ferrochelatase activity and protoporphyrin-IX utilization in *Haemophilus influenzae*. *In Journal of Bacteriology*, Vol 177, pp 3613-3615
- Luo J, Lim CK** (1993) Order of uroporphyrinogen-III decarboxylation on incubation of porphobilinogen and uroporphyrinogen-III with erythrocyte uroporphyrinogen decarboxylase. *In Biochemical Journal*, Vol 289, pp 529-532
- Luo M, Weinstein JD, Walker CJ** (1999) Magnesium chelatase subunit D from pea: characterization of the cDNA, heterologous expression of an enzymatically active protein and immunoassay of the native protein. *Plant Molecular Biology*. **41**: 721-731
- Mach JM, Castillo AR, Hoogstraten R, Greenberg JT** (2001) The *Arabidopsis*-accelerated cell death gene *ACD2* encodes red chlorophyll catabolite reductase and suppresses the spread of disease symptoms. *In Proceedings of the National Academy of Sciences of the United States of America*, Vol 98, pp 771-776
- Masuda T** (2008) Recent overview of the Mg branch of the tetrapyrrole biosynthesis leading to chlorophylls. *Photosynthesis Research* **96**: 121-143
- Masuda T, Fujita Y** (2008) Regulation and evolution of chlorophyll metabolism. *Photochemical and Photobiological Sciences*: 1131-1149
- Masuda T, Fusada N, Oosawa N, Takamatsu K, Yamamoto Y, Ohto M, Nakamura K, Goto K, Shibata D, Shirano Y, Hayashi H, Kato T, Tabata S, Shimada H, Takamiya K** (2003) Functional analysis of isoforms of NADPH : protochlorophyllide oxidoreductase (POR), PORB and PORC, in *Arabidopsis thaliana*. *Plant and Cell Physiology* **44**: 963-974
- Masuda T, Suzuki T, Shimada H, Ohta H, Takamiya K** (2003) Subcellular localization of two types of ferrochelatase in cucumber. *Planta* **217**: 602-609

- Matile P, Hortensteiner S, Thomas H** (1999) Chlorophyll degradation. *In Annual Review of Plant Physiology and Plant Molecular Biology*, Vol 50, pp 67-95
- Matile P, Schellenberg M** (1996) The cleavage of phaeophorbide a is located in the envelope of barley gerontoplasts. *Plant Physiology and Biochemistry* **34**: 55-59
- Matile P, Schellenberg M, Vicentini F** (1997) Localization of chlorophyllase in the chloroplast envelope. *Planta* **201**: 96-99
- Matsumoto F, Obayashi T, Sasaki-Sekimoto Y, Ohta H, Takamiya K, Masuda T** (2004) Gene expression profiling of the tetrapyrrole metabolic pathway in *Arabidopsis* with a mini-array system. *In Plant Physiology*, pp 2379-2391
- Meller E, Belkin S, Harel E** (1975) Biosynthesis of delta-aminolevulinic-acid in greening maize leaves. *In Phytochemistry*, pp 2399-2402
- Meskauskiene R, Nater M, Goslings D, Kessler F, op den Camp R, Apel K** (2001) FLU: a negative regulator of chlorophyll biosynthesis in *Arabidopsis thaliana*. *Proceedings of the National Academy of Sciences of the United States of America* **98**: 12826-12831
- Mochizuki N, Brusslan JA, Larkin R, Nagatani A, Chory J** (2001) *Arabidopsis* genomes uncoupled 5 (GUN5) mutant reveals the involvement of Mg-chelatase H subunit in plastid-to-nucleus signal transduction. *Proceedings of the National Academy of Sciences of the United States of America* **98**: 2053-2058
- Mochizuki N, Tanaka R, Tanaka A, Masuda T, Nagatani A** (2008) The steady-state level of Mg-protoporphyrin IX is not a determinant of plastid-to-nucleus signaling in *Arabidopsis*. *Proceedings of the National Academy of Sciences of the United States of America* **105**: 15184-15189
- Mock HP, Grimm B** (1997) Reduction of uroporphyrinogen decarboxylase by antisense RNA expression affects activities of other enzymes involved in tetrapyrrole biosynthesis and leads to light-dependent necrosis. *Plant Physiology* **113**: 1101-1112
- Mock HP, Heller W, Molina A, Neubohn B, Sandermann HJ, Grimm B** (1999) Expression of uroporphyrinogen decarboxylase or coproporphyrinogen oxidase antisense RNA in tobacco induces pathogen defense responses conferring

increased resistance to tobacco mosaic virus. *Journal of Biological Chemistry* **274**: 4231-4238

**Mohapatra A, Tripathy BC** (2007) Differential distribution of chlorophyll biosynthetic intermediates in stroma, envelope and thylakoid membranes in *Beta vulgaris*. *Photosynthesis Research* **94**: 401-410

**Monte E, Tepperman JM, Al-Sady B, Kaczorowski KA, Alonso JM, Ecker JR, Li X, Zhang Y, Quail PH** (2004) The phytochrome-interacting transcription factor, PIF3, acts early, selectively and positively in light-induced chloroplast development. *Proceedings of the National Academy of Sciences of the United States of America* **101**: 16091-16098

**Moulin M, McCormac AC, Terry MJ, Smith AG** (2008) Tetrapyrrole profiling in *Arabidopsis* seedlings reveals that retrograde plastid nuclear signaling is not due to Mg-protoporphyrin IX accumulation. *Proceedings of the National Academy of Sciences of the United States of America* **105**: 15178-15183

**Nagane T, Tanaka A, Tanaka R** (2010) Involvement of AtNAP1 in the regulation of chlorophyll degradation in *Arabidopsis thaliana*. *Planta*: 939-949

**Nagata N, Tanaka R, Satoh S, Tanaka A** (2005) Identification of a vinyl reductase gene for chlorophyll synthesis in *Arabidopsis thaliana* and implications for the evolution of *Prochlorococcus* species. *Plant Cell* **17**: 233-240

**Nakanishi H, Nozue H, Suzuki K, Kaneko Y, Taguchi G, Hayashida N** (2005) Characterization of the *Arabidopsis thaliana* mutant *pcb2* which accumulates divinyl chlorophylls. *In Plant and Cell Physiology*, Vol 46, pp 467-473

**Nakayama M, Masuda T, Bando T, Yamagata H, Ohta H, Takamiya K** (1998) Cloning and expression of the soybean *chlH* gene encoding a subunit of Mg-chelatase and localization of the Mg<sup>2+</sup> concentration-dependent ChlH protein within the chloroplast. *In Plant and Cell Physiology*, Vol 39, pp 275-284

**Niyogi KK** (1999) Genetic and Molecular Approaches. *Annual Review of Plant Physiology and Plant Molecular Biology* **50**: 333-359

**Nott A, Jung HS, Koussevitzky S, Chory J** (2006) Plastid-to-nucleus retrograde signaling. *In Annual Review of Plant Biology*, Vol 57, pp 739-759

- Olsen LJ, Keegstra K** (1992) The binding of precursor proteins to chloroplasts requires nucleoside triphosphates in the intermembrane space. *Journal of Biological Chemistry* **267**: 433-439
- Oster U, Tanaka R, Tanaka A, Rudiger W** (2000) Cloning and functional expression of the gene encoding the key enzyme for chlorophyll b biosynthesis (CAO) from *Arabidopsis thaliana*. *In Plant Journal*, Vol 21, pp 305-310
- Papenbrock J, Mochk H-P, Kruse E, Grimm B** (1999) Expression studies in tetrapyrrole biosynthesis: inverse maxima of magnesium chelatase and ferrochelatase activity during cyclic photoperiods. *Planta* **208**: 264-273
- Park SY, Yu JW, Park JS, Li J, Yoo SC, Lee NY, Lee SK, Jeong SW, Seo HS, Koh HJ, Jeon JS, Park YI, Paek NC** (2007) The senescence-induced staygreen protein regulates chlorophyll degradation. *Plant Cell* **19**: 1649-1664
- Peter E, Grimm B** (2009) GUN4 Is Required for Posttranslational Control of Plant Tetrapyrrole Biosynthesis. *Molecular Plant*: 1198-1210
- Pontoppidan B, Kannangara CG** (1994) Purification and partial characterization of barley glutamyl-tRNA reductase, the enzyme that directs glutamate to chlorophyll biosynthesis. *In European Journal of Biochemistry*, pp 529-537
- Pruzinska A, Tanner G, Anders I, Roca M, Hortensteiner S** (2003) Chlorophyll breakdown: pheophorbide a oxygenase is a Rieske-type iron-sulfur protein, encoded by the accelerated cell death 1 gene. *In Proceedings of the National Academy of Sciences of the United States of America*, Vol 100, pp 15259-15264
- Pruzinská A, Tanner G, Aubry S, Anders I, Moser S, Müller T, Ongania KH, Kräutler B, Youn JY, Liljegren SJ, Hörtensteiner S** (2005) Chlorophyll breakdown in senescent *Arabidopsis* leaves. Characterization of chlorophyll catabolites and of chlorophyll catabolic enzymes involved in the degreening reaction. *Plant Physiology* **139**: 52-63
- Puy H, Gouya L, Deybach J** (2010) Porphyrrias. *Lancet* **375**: 924-937
- Pöpperl G, Oster U, Rüdiger W** (1998) Light-dependent increase in chlorophyll precursors during the day-night cycle in tobacco and barley seedlings. *Journal of Plant Physiology* **153**: 40-45

- Raux-Deery E, Leech HK, Nakrieko KA, McLean KJ, Munro AW, Heathcote P, Rigby SEJ, Smith AG, Warren MJ** (2005) Identification and characterization of the terminal enzyme of siroheme biosynthesis from *Arabidopsis thaliana* - A plastid-located sirohydrochlorin ferrochelatase containing a 2Fe-2S center. *In Journal of Biological Chemistry*, pp 4713-4721
- Rebeiz CA** (2002) Analysis of intermediates and end products of the chlorophyll biosynthetic pathway. *In* AG Smith, M Witty, eds, Heme, Chlorophyll, and Bilins. Humana Press, Inc., Totowa, pp 111-155
- Reid JD, Hunter CN** (2004) Magnesium-dependent ATPase activity and cooperativity of magnesium chelatase from *Synechocystis* sp PCC6803. *In Journal of Biological Chemistry*, pp 26893-26899
- Reiland S, Messerli G, Baerenfaller K, Gerrits B, Endler A, Grossmann J, Gruissem W, Baginsky S** (2009) Large-Scale *Arabidopsis* Phosphoproteome Profiling Reveals Novel Chloroplast Kinase Substrates and Phosphorylation Networks. *In Plant Physiology*, pp 889-903
- Reinbothe S, Reinbothe C, Apel K, N. L** (1996) Evolution of Chlorophyll Biosynthesis—The Challenge to Survive Photooxidation. *Cell* **86**: 703-705
- Reinbothe S, Runge S, Reinbothe C, Vancleve B, Apel K** (1995) Substrate-dependent transport of the NADPH-protochlorophyllide oxidoreductase into isolated plastids. *In Plant Cell*, Vol 7, pp 161-172
- Riechmann JL, Heard J, Martin G, Reuber L, Jiang CZ, Keddie J, Adam L, Pineda O, Ratcliffe OJ, Samaha RR, Creelman R, Pilgrim M, Broun P, Zhang JZ, Ghandehari D, Sherman BK, Yu CL** (2000) *Arabidopsis* transcription factors: Genome-wide comparative analysis among eukaryotes. *In Science*, pp 2105-2110
- Rimington C** (1960) Spectral-absorption coefficients of some porphyrins in the Soret-band region. *Biochemical Journal* **75**: 620-623
- Rodermel S, Park S** (2003) Pathways of intracellular communication: tetrapyrroles and plastid-to-nucleus signaling. *In Bioessays*, Vol 25, pp 631-636
- Rodoni S, Muhlecker W, Anderl M, Krautler B, Moser D, Thomas H, Matile P, Hortensteiner S** (1997) Chlorophyll breakdown in senescent chloroplasts -

Cleavage of pheophorbide a in two enzymic steps. *Plant Physiology* **115**: 669-676

**Rossini L, Cribb L, Martin DJ, Langdale JA** (2001) The maize Golden2 gene defines a novel class of transcriptional regulators in plants. *In Plant Cell*, pp 1231-1244

**Ruckle ME, DeMarco SM, Larkin RM** (2007) Plastid signals remodel light signaling networks and are essential for efficient chloroplast biogenesis in *Arabidopsis*. *Plant Cell* **19**: 3944-3960

**Sambrook J, Russell DW** (2001) *Molecular cloning: a laboratory manual*, Ed 3rd. Cold Spring Harbor Laboratory Press, Cold Spring Harbor

**Sato Y, Morita R, Katsuma S, Nishimura M, Tanaka A, Kusaba M** (2009) Two short-chain dehydrogenase/reductases, NON-YELLOW COLORING 1 and NYC1-LIKE, are required for chlorophyll b and light-harvesting complex II degradation during senescence in rice. *Plant Journal*: 120-131

**Schelbert S, Aubry S, Burla B, Agne B, Kessler F, Krupinska K, Hörtensteiner S** (2009) Pheophytin Pheophorbide Hydrolase (Pheophytinase) Is Involved in Chlorophyll Breakdown during Leaf Senescence in *Arabidopsis*. *Plant Cell* **21**: 767-785

**Schenk N, Schelbert S, Kanwischer M, Goldschmidt EE, Dormann P, Hortensteiner S** (2007) The chlorophyllases AtCLH1 and AtCLH2 are not essential for senescence-related chlorophyll breakdown in *Arabidopsis thaliana*. *In FEBS Letters*, Vol 581, pp 5517-5525

**Scheumann V, Ito H, Tanaka A, Schoch S, Rudiger W** (1996) Substrate specificity of chlorophyll(ide) b reductase in etioplasts of barley (*Hordeum vulgare* L). *In European Journal of Biochemistry*, pp 163-170

**Severance S, Hamza I** (2009) Trafficking of Heme and Porphyrins in Metazoa. *Chemical Reviews* **109**: 4596-4616

**Shepherd M, McLean S, Hunter CN** (2005) Kinetic basis for linking the first two enzymes of chlorophyll biosynthesis. *FEBS Journal* **272**: 4532-4539

- Sigfridsson E, Ryde U** (2003) The importance of porphyrin distortions for the ferrochelatase reaction. *Journal of Biological Inorganic Chemistry*: 273-282
- Sobotka R, Dühring U, Komenda J, Peter E, Gardian Z, Tichy M, Grimm B, Wilde A** (2008) Importance of the cyanobacterial Gun4 protein for chlorophyll metabolism and assembly of photosynthetic complexes. *Journal of Biological Chemistry* **283**: 25794-25802
- Stephenson P, Fankhauser C, Terry M** (2009) PIF3 is a repressor of chloroplast development. *Proceedings of the National Academy of Sciences of the United States of America* **106**: 7654-7659
- Stephenson P, Terry M** (2008) Light signalling pathways regulating the Mg-chelatase branchpoint of chlorophyll synthesis during de-etiolation in *Arabidopsis thaliana*. *Photochemical and Photobiological Sciences*: 1243-1252
- Stephenson PG, Terry MJ** (2008) Light signalling pathways regulating the Mg-chelatase branchpoint of chlorophyll synthesis during de-etiolation in *Arabidopsis thaliana*. *Photochemical and Photobiological Sciences* **7**: 1243-1252
- Strand Å, Asami T, Alonso J, Ecker JR, Chory J** (2003) Chloroplast to nucleus communication triggered by accumulation of Mg-protoporphyrinIX. *Nature* **421**: 79-83
- Susek RE, Ausubel FM, Chory J** (1993) Signal transduction mutants of *Arabidopsis* uncouple nuclear *CAB* and *RBCS* gene expression from chloroplast development. *Cell* **74**: 787-799
- Susek RE, J C** (1992) A tale of 2 genomes - role of a chloroplast signal in coordinating nuclear and plastid genome expression. *In Australian Journal of Plant Physiology*, pp 387-399
- Suzuki T, Kunieda T, Murai F, Morioka S, Shioi Y** (2005) Mg-dechelation activity in radish cotyledons with artificial and native substrates, Mg-chlorophyllin a and chlorophyllide a. *Plant Physiology and Biochemistry*: 459-464
- Suzuki T, Kunieda T, Murai F, Shioi Y** (2005) Properties of low molecular substances and proteins that function in Mg-dechelating reaction in chlorophyll degradation pathway. *Plant and Cell physiology*: S236-S236

- Suzuki T, Masuda T, Singh DP, Tan FC, Tsuchiya T, Shimada H, Ohta H, Smith AG, Takamiya K** (2002) Two types of ferrochelatase in photosynthetic and nonphotosynthetic tissues of cucumber: their difference in phylogeny, gene expression, and localization. *Journal of Biological Chemistry* **277**: 4731-4737
- Tanaka A, Tanaka R** (2006) Chlorophyll metabolism. *Current Opinion in Plant Biology* **9**: 248-255
- Tanaka R, Tanaka A** (2005) Effects of chlorophyllide a oxygenase overexpression on light acclimation in *Arabidopsis thaliana*. *Photosynthesis Research* **85**: 327-340
- Tanaka R, Tanaka A** (2007) Tetrapyrrole biosynthesis in higher plants. *Annual Review of Plant Biology* **58**: 321-346
- Tanaka R, Yoshida K, Nakayashiki T, Masuda T, Tsuji H, Inokuchi H, Tanaka A** (1996) Differential expression of two hemA mRNAs encoding glutamyl-tRNA reductase proteins in greening cucumber seedlings. *Plant Physiology*: 1223-1230
- Terry M, McDowell M, Lagarias J** (1995) (3Z)-Phytochromobilin and (3E)-Phytochromobilin are intermediates in the biosynthesis of the phytochrome chromophore. *Journal of Biological Chemistry*: 11111-11118
- Terry M, Wahleithner J, Lagarias J** (1993) Biosynthesis of the plant photoreceptor phytohormone. *Archives of Biochemistry and Biophysics*: 1-15
- Terry MJ, Linley PJ, Kohchi T** (2002) Making light of it: the role of plant haem oxygenases in phytochrome chromophore synthesis. *In Biochemical Society Transactions*, Vol 30, pp 604-609
- Thomas J, Weinstein JD** (1990) Measurement of heme efflux and heme content in isolated developing cotyledons. *Plant Physiology* **94**: 1414-1423
- Tottey S, Block MA, Allen M, Westergren T, Albrieux C, Scheller HV, Merchant S, Jensen PE** (2003) *Arabidopsis* CHL27, located in both envelope and thylakoid membranes, is required for the synthesis of protochlorophyllide. *In Proceedings of the National Academy of Sciences of the United States of America*, Vol 100, pp 16119-16124

- Tripp J, Inoue K, Keegstra K, Froehlich JE** (2007) A novel serine/proline-rich domain in combination with a transmembrane domain is required for the insertion of AtTic40 into the inner envelope membrane of chloroplasts. *Plant Journal* **52**: 824-838
- Tsai SF, Bishop DF, Desnick RJ** (1987) Purification and properties of uroporphyrinogen-III synthase from human erythrocytes. *In* *Journal of Biological Chemistry*, Vol 262, pp 1268-1273
- Tsuchiya T, Ohta H, Okawa K, Iwamatsu A, Shimada H, Masuda T, Takamiya K** (1999) Cloning of chlorophyllase, the key enzyme in chlorophyll degradation: Finding of a lipase motif and the induction by methyl jasmonate. *In* *Proceedings of the National Academy of Sciences of the United States of America*, pp 15362-15367
- Umesono K, Murakami KK, Thompson CC, Evans RM** (1991) Direct repeats as selective response elements for the thyroid hormone, retinoic acid and vitamin D3 receptors. *Cell* **65**: 1255–1266
- van Lis R, Atteia A, Nogaj LA, Beale SI** (2005) Subcellular localization and light-regulated expression of protoporphyrinogen IX oxidase and ferrochelatase in *Chlamydomonas reinhardtii*. *Plant Physiology* **139**: 1946-1958
- Verdecia MA, Larkin RM, Ferrer JL, Riek R, Chory J, Noel JP** (2005) Structure of the Mg-chelatase cofactor GUN4 reveals a novel hand-shaped fold for porphyrin binding. *In* *PLoS Biology*, pp 777-789
- Vinti G, Hills A, Campbell S, Bowyer JR, Mochizuki N, Chory J, López-Juez E** (2000) Interactions between *hyl* and *gun* mutants of *Arabidopsis*, and their implications for plastid/nuclear signalling. *Plant Journal* **24**: 883-894
- Voigt C, Oster U, Börnke F, Jahns P, Dietz K, Leister D, Kleine T** (2009) In-depth analysis of the distinctive effects of norflurazon implies that tetrapyrrole biosynthesis, organellar gene expression and ABA cooperate in the GUN-type of plastid signalling. *Physiologia Plantarum*
- Vothknecht U, Kannangara C, von Wettstein D** (1996) Expression of catalytically active barley glutamyl tRNA(Glu) reductase in *Escherichia coli* as a fusion protein with glutathione S-transferase. *Proceedings of the National Academy of Sciences of the United States of America*: 9287-9291

- Walker CJ, Weinstein JD** (1991) Further characterization of the magnesium chelatase in isolated developing cucumber chloroplasts : substrate specificity, regulation, intactness, and ATP requirements. *Plant Physiology* **95**: 1189-1196
- Walker CJ, Weinstein JD** (1991) *In vitro* assay of the chlorophyll biosynthetic enzyme Mg-chelatase: resolution of the activity into soluble and membrane-bound fractions. *Proceedings of the National Academy of Sciences of the United States of America* **88**: 5789-5793
- Walley JW, Coughlan S, Hudson ME, Covington MF, Kaspi R, Banu G, Harmer SL, Dehesh K** (2007) Mechanical stress induces biotic and abiotic stress responses via a novel *cis*-element. *PLoS Genetics* **3**: 1800-1812
- Watanabe N, Che FS, Iwano M, Takayama S, Yoshida S, Isogai A** (2001) Dual targeting of spinach protoporphyrinogen oxidase II to mitochondria and chloroplasts by alternative use of two in-frame initiation codons. *In Journal of Biological Chemistry*, Vol 276, pp 20474-20481
- Waters M, Wang P, Korkaric M, Capper R, Saunders N, Langdale J** (2009) GLK Transcription Factors Coordinate Expression of the Photosynthetic Apparatus in Arabidopsis. *Plant Cell*: 1109-1128
- Waters MT, Moylan EC, Langdale JA** (2008) GLK transcription factors regulate chloroplast development in a cell-autonomous manner. *In Plant Journal*, pp 432-444
- Weigel D, Glazebrook J** (2002) *Arabidopsis: A Laboratory Manual*. Cold Spring Harbor Laboratory Press, Cold Spring Harbor
- Wilde A, Mikolajczyk S, Alawady A, Lokstein H, Grimm B** (2004) The *gun4* gene is essential for cyanobacterial porphyrin metabolism. *FEBS Letters* **571**: 119-123
- Willows R** (2003) Biosynthesis of chlorophylls from protoporphyrin IX. *Natural Product Reports* **20**: 327-341
- Willows RD, Hansson A, Birch D, Al-Karadaghi S, Hansson M** (2004) EM single particle analysis of the ATP-dependent Bchl complex of magnesium chelatase: an AAA(+) hexamer. *In Journal of Structural Biology*, pp 227-233

- Willows RD, Lake V, Roberts TH, Beale SI** (2003) Inactivation of Mg chelatase during transition from anaerobic to aerobic growth in *Rhodobacter capsulatus*. *Journal of Bacteriology* **185**: 3249-3258
- Winkel BS** (2004) Metabolic channeling in plants. *Annual Review of Plant Biology* **55**: 85-107
- Witkowski D, Halling B** (1988) Accumulation of photodynamic tetrapyrroles induced by Acifluorfen-methyl. *Plant physiology*: 632-637
- Witkowski D, Halling B** (1989) Inhibition of plant protoporphyrinogen oxidase by the herbicide Acifluorfen-methyl. *Plant Physiology*: 1239-1242
- Woodson JD, Chory J** (2008) Coordination of gene expression between organellar and nuclear genomes. *Nature Reviews Genetics* **9**: 383-395
- Wuthrich K, Bovet L, Hunziker P, Donnison I, Hortensteiner S** (2000) Molecular cloning, functional expression and characterisation of RCC reductase involved in chlorophyll catabolism. *Plant Journal*: 189-198
- Yao N, Greenberg JT** (2006) Arabidopsis ACCELERATED CELL DEATH2 modulates programmed cell death. *In Plant Cell*, Vol 18, pp 397-411
- Yasumura Y, Moylan EC, Langdale JA** (2005) A conserved transcription factor mediates nuclear control of organelle biogenesis in anciently diverged land plants. *In Plant Cell*, pp 1894-1907
- Yee WC, Eglsaer SJ, Wr R** (1989) Confirmation of a ping-pong mechanism for S-adenosyl-L-methionine-magnesium protoporphyrin methyltransferase of etiolated wheat by an exchange reaction. *In Biochemical and Biophysical Research Communications*, Vol 162, pp 483-490

MICHIGAN STATE UNIVERSITY LIBRARIES



3 1293 03063 6421